Power Quality Analysis for High Pressure Sodium Lamps in Low Voltage Networks

Delft University of Technology

MASTER OF SCIENCE THESIS

G.A. Mier

Faculty of Electrical Engineering, Mathematics and Computer Science

TU Delft Delft University of Technology

STEDIN.NET

Challenge the future

Power Quality Analysis for High Pressure Sodium Lamps

by

Guillermo Andres Mier

Intelligent Electrical Power Grids - EWI

Thesis committee:

Prof. Dr. Peter Palensky

Dr. Ir. Marjan Popov

Dr. Ir. Armando Rodrigo

Ir. Anne van der Molen

Abstract

Unaware connection of high pressure sodium lamps to the grid, represent a relevant problem for the grid operators. They have several negative effects in the network, they can overload the circuits and affect the quality of the energy delivered to customers by the injection of harmonics.

This thesis aims to answer the question: Can the high pressure sodium lamps connected to the grid be detected through measurements at a centralized location such as a substation? The hypothesis that the lamps have specific electrical characteristics which can be used for its detection, was stablished and validated.

Current harmonics and power characteristics of several high pressure sodium lamps were measured. The measured values were used for simulations of the harmonic flow in a low voltage network, and to emulate aggregated measurements combining the lamps with several loads. These calculations were compared with field tests done with high pressure lamps in a low voltage network. The results prove that within certain limitations, in a combination of several loads, the high pressure sodium lamps characteristics can be enhanced in order to be detected and identified from the aggregated data.

Acknowledgements

First of all, I would like to thank the company Stedin for supporting this project. To Anne van der Molen and Peter van't End for their help and supervision. I would also like to thank all the staff from Stedin that helped me during the process of this project.

I want to give my gratitude to Dr. ir Marjan Popov for his guidance and encouragement throughout the research. Thank you for all your advices.

I would like to thank my parents for always being there for me, and for helping me become who I am now. I would like to thank my girlfriend for helping me whenever I need it. At last, I would like to thank all my friends that I met during the master, for all the good moments we shared together.

Contents

Glossary

AC	Alternating Current
ALM	Appliance Load Monitoring
CS	Current Source
DC	Direct Current
DSO	Distribution System Operator
EV	Electric Vehicle
HP	Heat pumps
HPS	High pressure sodium
HV	High Voltage
Hz	Hertz
ILM	Intrusive Load Monitoring
LV	Low Voltage
MV	Medium Voltage
NILM	Non-Intrusive Load Monitoring
PCC	Point of common coupling
PF	Power factor
POC	Point of connection
PQ	Power Quality
PV	Photovoltaic systems
RMS	Root Mean Square
THD	Total Harmonic Distortion
VS	Voltage Source

Chapter 1

1. Introduction

The use of different technologies and user behavior represents a challenge for the grid operators. Grid overloads, power quality problems, technical and non-technical losses may arise with the penetration of distributed generation, electric vehicles, different lighting devices.

Grid operators, such as Stedin, need to design and operate their networks so the delivered power to its users comply with the voltage quality standards EN50160 and the National grid code, while keeping loses at minimum. Power quality is influenced by the topology of the network and the type of loads that are connected to it. This makes the information of user behavior and tendencies of high relevance.

The development of methods to identify relevant appliances and technologies that the user connects to the grid, can help the grid operators plan and take actions accordingly. In order to know in which technology to focus for this study, a brief overview of electric vehicle chargers (EV), grid connected solar panels (PV), heat pumps (HP), and high pressure sodium (HPS) lamps took place.

Based on this overview, it was decided to focus on HPS lamps. Unaware connection of HPS lamps to the network have several negative effects, they can overload the circuits and affect the quality of the energy delivered to customers by the injection of harmonics.

This thesis aims to solve the research question: Can the HPS lamps connected to the grid be detected through measurements in a centralized location such as a substation? As a first step it is established the hypothesis that the lamps have specific electrical characteristics which can be used to distinguish from the rest of the loads in order to detect them. At the end of the report it can be seen that this hypothesis was validated, within certain limitations.

The objective is to analyze the possibility of detecting the existence of HPS lamps by means of power quality measurements. The power quality characteristics which were taken into account are the harmonic distortion, power factor and voltage levels. The thesis focuses on the electrical characteristics of the HPS lamps with electromagnetic ballast. Machine learning techniques are out of the scope for this study, nevertheless there are recommended as a next step to complement this work. The results of this

thesis might be applied to different devices beside the HPS lamps, however it is out of the scope of this study.

The thesis consists of the following sections: Chapter 1 begins with a discussion and a solution proposal. Afterwards there is a brief description of Stedin's main activities (company involved in the thesis). Chapter 2 consists of the theory behind the detection. The first section introduces the harmonics, which is one of the electrical characteristics that would be used for the detection of the HPS lamps. Afterwards, different identification methods are presented, which describes existing work in load monitoring and detection. Chapter 3 explains the laboratory measurements that were done to several HPS lamp in order to determine the electrical characteristics that can be used for their detection. In Chapter 4, calculations to predict the aggregated date in a meter are explained, and later compared to field tests in chapter 6. Chapter 5 explains the simulations done with DIgSILENT Power Factory software. The objective of this chapter is to calculate and observe how the harmonics would flow through the LV grid and how distorted the original waveform of the HPS lamps would reach the meter at different locations. In Chapter 6, it is described the field tests that were done at a LV grid in order to observe the behavior of the HPS lamps in the aggregated data in a real congested grid. Finally, chapter 7 gives a conclusion to the report, and recommendations for future work.

1.1 Stedin

Stedin, which makes part of the Eneco group, is a regional grid operator responsible for reliable and safe transportation of gas and electricity. Stedin operates in the provinces of South Holland, Utrecht and parts of Amstelland Kennemerland, North Friesland and Weert. It is the second largest grid operator in the Netherlands. It services over 2 million customers ranging from small consumers to large industry. Stedin owns around 23180 km of gas pipes and 45171 km of electric wires. [2]

Stedin fulfills a task for the Dutch government. It is the only licensed grid operator in its geographical region and is authorized to request yearly transportation fees and rent for the meters, it is a regulated monopolist.

Stedin continuously invest in modernization, replacement, expansion and maintenance of the terminals, networks and stations. Stedin not only facilitates sustainable energy transport, it is also legally responsible for the maintenance and installation of energy meters for their small business customers. Together with partners they fight and prevent energy theft.

Stedin spends roughly 250 million euros per year to expand and replace assets, representing 2/3rd and 1/3rd of the total, respectively. Proper maintenance routines for these assets is critical for the stability of the grid. Most of the assets of the company are in the planning for replacement over the next 15 years, which is not unusual for a grid operator.

Figure 1. Stedin's electricity network. [2]

Figure 2. Stedin's gas network. [2]

Chapter 2

2. Background Theory

2.1 Harmonics

As previously explained, the electrical characteristics of the HPS lamps are going to be used to explore the possibility of detection. One of this characteristics are the harmonic components of the current wave form. In this subchapter, a brief introduction to harmonics, how to calculate them, and its effects on the network are going to be presented.

A linear load has a constant resistance. If connected to the grid, it draws current which is proportional to the applied voltage. When the load is connected to an AC grid with a 50 Hz sinusoidal voltage, it will draw a sinusoidal current at the same frequency as the voltage (not necessarily in phase).

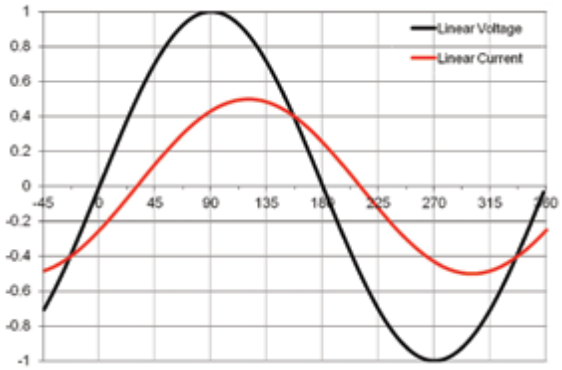

Figure 3. A current from a linear load. [3]

In the case of non-linear loads, the resistance is not constant and changes during each cycle of the voltage. Due to this changing impedance, the current drawn from a sinusoidal voltage results in a distorted non-sinusoidal current. Examples of nonlinear loads are electric arc furnaces, static power converters, discharge lamps.

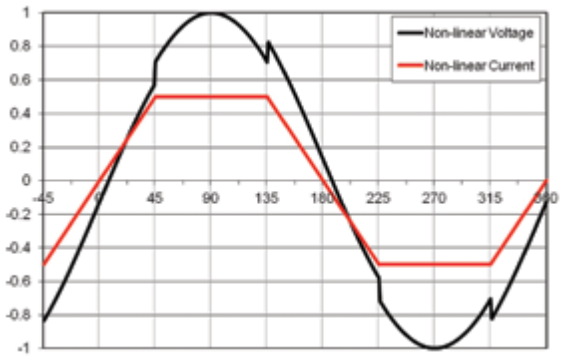

Figure 4. Current from a non-linear load. [3]

Harmonics can be mathematically represented with the Fourier theorem which expresses that periodic non-sinusoidal waveforms can be separated into sinusoidal components. The term harmonic refers to a component of a waveform that occurs at the integer multiple of the fundamental frequency. The Fourier series can be expressed as follows:

$$f(t) = F_o + \sum_{h=1}^{\infty} F_h \sqrt{2} \sin(h\omega t - \varphi_h)$$

Where:

$\boldsymbol{f(t)}$ Time domain function.

$\boldsymbol{h}$ Harmonic number.

$\boldsymbol{F_o}$ Value of the DC component.

$\boldsymbol{F_h}$ Rms value of the h^{th} harmonic.

$\boldsymbol{\omega}$ Angular frequency of the fundamental frequency.

$\boldsymbol{\varphi_h}$ Displacement of the harmonic component at t=0.

A periodic distorted signal is the sum of the fundamental and a number of superimposed harmonics. Figure 5 shows an example of a current wave affected by harmonic distortion.

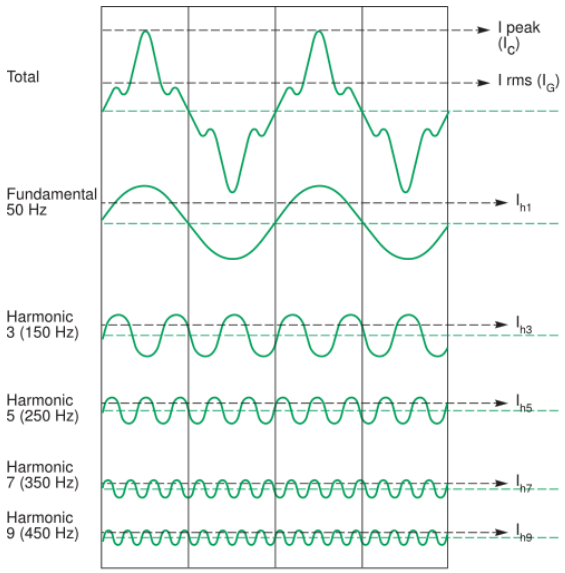

Figure 5. A distorted current and its expansion by harmonic orders. [4]

One of the most common ways to represent the harmonics contained in a periodic signal is the harmonic spectrum also known as frequency spectrum. Each bar of Figure 6 represents the magnitude of each harmonic (absolute magnitude or as percentage of the fundamental). The presence of harmonics and its relevance can be easily analyzed in this type of representation.

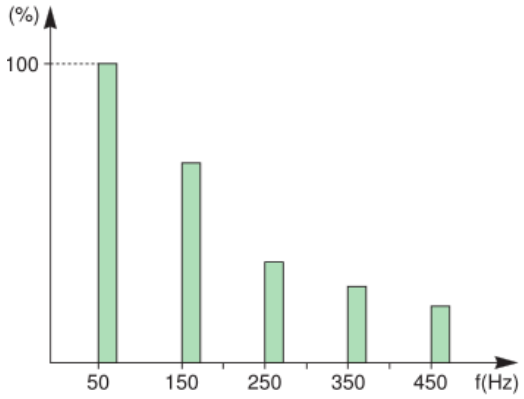

Figure 6. Harmonic spectrum of Figure 5. [4]

The amount of distortion in the voltage or current waveform is quantified by the index called the total harmonic distortion (THD). According to IEEE 519-1992, it is defined as:

$$\%THD = \frac{\sqrt{\sum_{=2}^{\infty} {F_h}^2}}{F_1} 100$$

Where:

$\boldsymbol{F_h}$ Magnitude of individual harmonic components.

$\boldsymbol{h}$ Harmonic order.

$\boldsymbol{F_1}$ Magnitude of fundamental.

2.2.1 Effects of harmonics

When the nonlinear loads draw non-sinusoidal current across the distribution system, the current goes through all the impedance connected to that load. The fundamental and harmonics components of this current causes voltage drops for each frequency based on Ohm's law. The vector sum of each voltage harmonic results in a distorted voltage waveform.

The impedance's magnitude and angle change as a function of the current frequency flowing through it. Each h-order harmonic current has its specific impedance in the supply circuit.

$$\Delta V_h = I_h Z_h$$

Where:

$\Delta \boldsymbol{V_h}$ Harmonic voltage drop at h^{th} harmonic.

$\boldsymbol{I_h}$ Harmonic current at h^{th} harmonic.

$\boldsymbol{Z_h}$ Impedance at frequency of h^{th} harmonic.

This voltage drop causes distorted voltage. Harmonics in the current and in the voltage have negative impact on the electrical equipment such as:

Transformers: The increase of ohmic losses because of the increased current due to the harmonic components in the current. The increase of eddy current losses which can be divided in two parts: The ones occurring in the iron core of the windings normally called ''eddy current loss'', these losses are proportional to the square of the load current and the square of frequency. The portion outside the windings is called ''other stray loss'', their losses are proportional to the square of the load current as well but with exponent factor of approximately 0.8 or less for the frequency [5]. All this effects have an impact in reducing the operating life in the insulator of the transformer. [6] [7]

Cables: The increase of ohmic losses because of the increased current due to the harmonic component. The AC conductor resistance changes due to skin and proximity effects which depends of frequency, conductor size, cable construction and spacing. [6]

Induction and synchronous machines: The existence of extra losses. The negative sequence harmonics (5^{th}, 11^{th}, 17^{th},…) produce rotating magnetic fields in the opposite direction of the fundamental magnetic field which may cause not only reduced torque and overheating but mechanical oscillations in the motor-load system. [8]

Capacitors: The capacitive reactance is directly proportional to the frequency. In a power system with harmonic currents, capacitors become a low impedance path for the harmonics which may overload them. Another effect is the generation of harmonic resonance, where high amplitudes of the harmonic in resonance can result in considerable damage of the capacitor banks or other electrical equipment in the system. [6] [8]

2.2.2 Harmonic Resonance

Harmonic resonance greatly affects the system harmonic levels as it can greatly magnify a load generated harmonic. Resonant conditions arise when the produced harmonic frequency closely coincides with the power system natural frequency. There are two types of resonance: parallel and series. In the formula below, $f_{\propto}$ represents the frequency of resonance.

$$2\pi f_{\propto} = \frac{1}{\sqrt{LC}}$$

The parallel resonance is reached if the shunt capacitances which are in parallel with the system inductances have the same impedance at a certain point of the system. In this parallel circuit, the impedance is high at resonance frequency. This produces high harmonic voltages and high harmonic currents flowing between the capacitors and system inductance.

In the series resonance, the series combination of inductance and capacitance presents a very low impedance for the harmonic frequency in resonance. The voltage across the inductance and the capacitance are equal in magnitude but opposite in sign. The generated voltages can get high values, many times the initial voltage at that harmonic leading to harmful values.

2.3 Detection Methods

This subchapter describes existing work in load monitoring and detection, which would be used as a first step for the detection of the HPS lamps. The concept of Appliance Load Monitoring (ALM) is not a new concept, but nowadays it has seen a growth of interest because of the parallel improvements in sensing technology, data communication and networks, artificial intelligence and machine learning methods [9]. There are two major approaches for ALM: Intrusive Load Monitoring (ILM) and Non-Intrusive Load Monitoring (NILM).

ILM, also called distributed sensing point, requires one or more sensors per appliance to perform the monitoring. Having a sensor per appliance, make this method more accurate in means of specific data per appliance compared with NILM. Nevertheless the high costs of the quantity of sensors required, complexity of installation and multiple sensors configuration are important disadvantages [9] [10], especially in large scale deployments which is the case of a DSO such as Stedin.

NILM, also called single point sensing method, can determine the operating schedule in target circuits from a centralized location which could be a MV/LV substation. NILM reduces costs by using fewer sensors that in the attempt of using an intrusive method [11]. The major disadvantage is in the difficulty of disaggregation of the measured data in order to identify individual loads from the combination of many loads.

NILM method was chosen for the thesis, because Stedin cannot have access to the installation inside the customer's property. In the following subchapters there is a brief introduction to NILM and some load disaggregation techniques.

2.3.1 Non-Intrusive Load Monitoring (NILM)

As mentioned before, disaggregation of measurements is one of the main challenges of NILM. According to literature [9], there are three main methods of disaggregation which can be used separately or complementing each other: Steady state methods, transient-state methods and non-traditional appliance features.

Steady State Analysis

As the name suggests, these methods use the steady state characteristics of the appliances. To track the On/Off operations. The most simple disaggregation method are the power based. Power based methods utilize the real power feature of the appliance, and make use of distinctive power consumption characteristic among appliances. Nevertheless, the existence of appliances with similar power consumption or simultaneous state transitions of different appliances leads to erroneous results [9] [12]. To address the problem of appliances with similar power consumption, the use of the power factor can discriminate between loads of resistive, inductive or capacitive characteristics. Current harmonics can also characterize non-linear loads with non-sinusoidal currents wave shapes [13]. The combination of harmonics, real and reactive power features improve the detection, however harmonic metering requires high rate sampling of the waveforms.

In the power meters, the sampling rate determines the amount of information than can be extracted from the electric signals. The harmonic order that the meter can capture from the original waveforms depends on the sampling rate fulfilling the Nyquist-Shannon sampling criteria. It states that the sampling rate must be at least 2 times or more the higher frequency of interest. For example if we want to measure till the 9^{th} harmonic, a sampling rate of 1080Hz is required.

Transient State Analysis

The transient methods make use of the state transitions by extracting its waveform characteristics such as shape, size, duration and harmonics. The disaggregation methods can make use of the transient characteristics to differentiate between overlapping steady state characteristics of different loads. The transient behavior between different appliances is related to the task the equipment performs, giving each type of load a specific electrical signature during the transient waveform.

One of the limitations is the high sampling rate required in the meters to capture the transients. The waveforms must be sampled in the range of 10 to 100 MHz [9], making the equipment expensive.

Non-traditional appliances features

Besides steady state and transient analysis, other non-traditional features can be used for the disaggregation of data. This features take into account non electrical characteristics related with the time behavior of the appliance such as starting time, peak time, peak values, ending time, on and off durations, frequency of the appliance usage. The combination of this features with steady states and/or transient state analysis can improve the disaggregation algorithms.

Chapter 2

3. Laboratory measurements of the lamps

Voltage and current readings took place in order to learn the electric characteristics of the HPS lamps. The measurement methodology is explained in Appendix A. Several lamps were measured for each of the following models:

- Philips model SON-T 400W. Ballast values: λ=0.45, tw=120, Δt=70; with 45±10% μF capacitor.
- Philips model SON-T 600W. Ballast values: λ=0.50, tw=130, Δt=80; with 60±10% μF capacitor.
- Philips model SON-T 1000W. Ballast values: λ=0.45, tw=130, Δt=80; with 40±10% μF capacitor.

The input voltage and the current for each lamp were obtained using an oscilloscope Yokogawa DLM2034 at a rate of 2.5 MHz. Afterwards, the current waveform was decomposed using fast Fourier transform in MatLab software environment.

During the measurements, it was observed that for each lamp model, the same current waveform repeated at every test. Being more specific, the displacement power factor and the current harmonics till the 15^{th} order repeated at every test for each lamp model. The harmonics of order higher than 15^{th} never reached steady state, nevertheless their magnitudes are less significant.

The displacement power factor and the current waveform have a transition from the initial values when the lamp is switched on till the final values at steady state (around 6-7 minutes). During the initial stage the lamps have a very poor displacement power factor. This process repeats with the same values at every test.

The measurement results for each lamp can be observed in the following figures:

HPS lamp SON-T 400W: Figure 7 to Figure 14.

HPS lamp SON-T 600W: Figure 15 to Figure 22.

HPS lamp SON-T 1000W: Figure 23 to Figure 30.

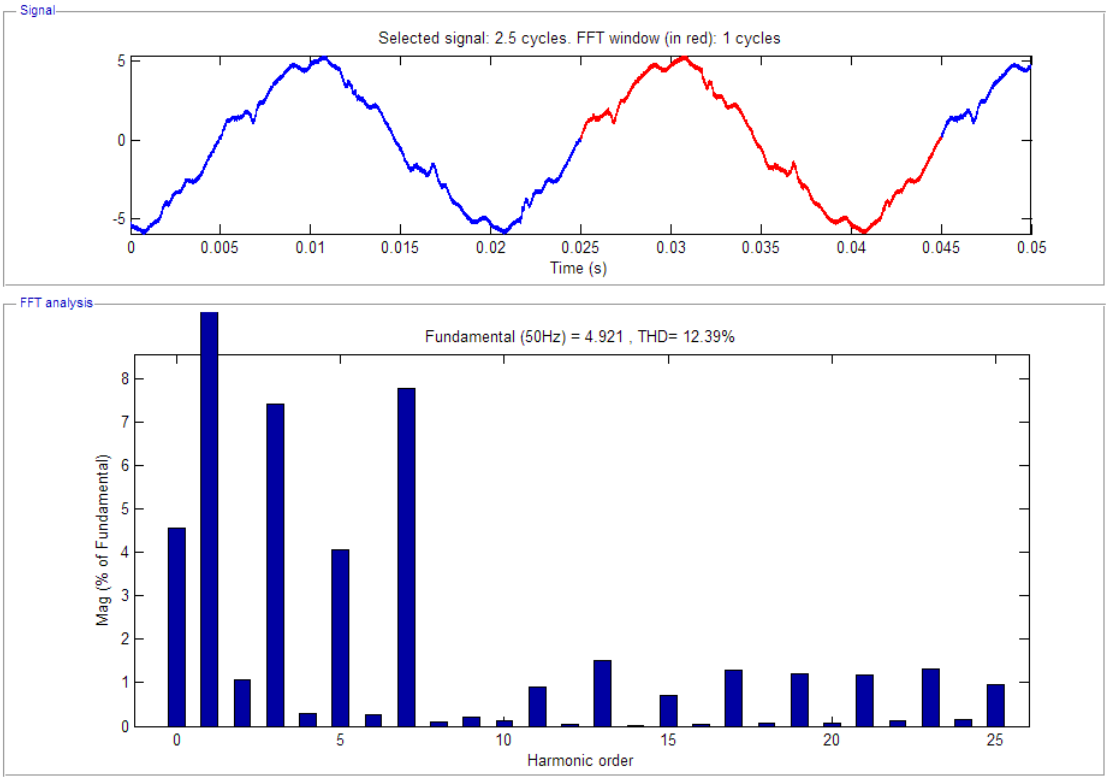

Figure 7. 400W HPS lamp, initial current.

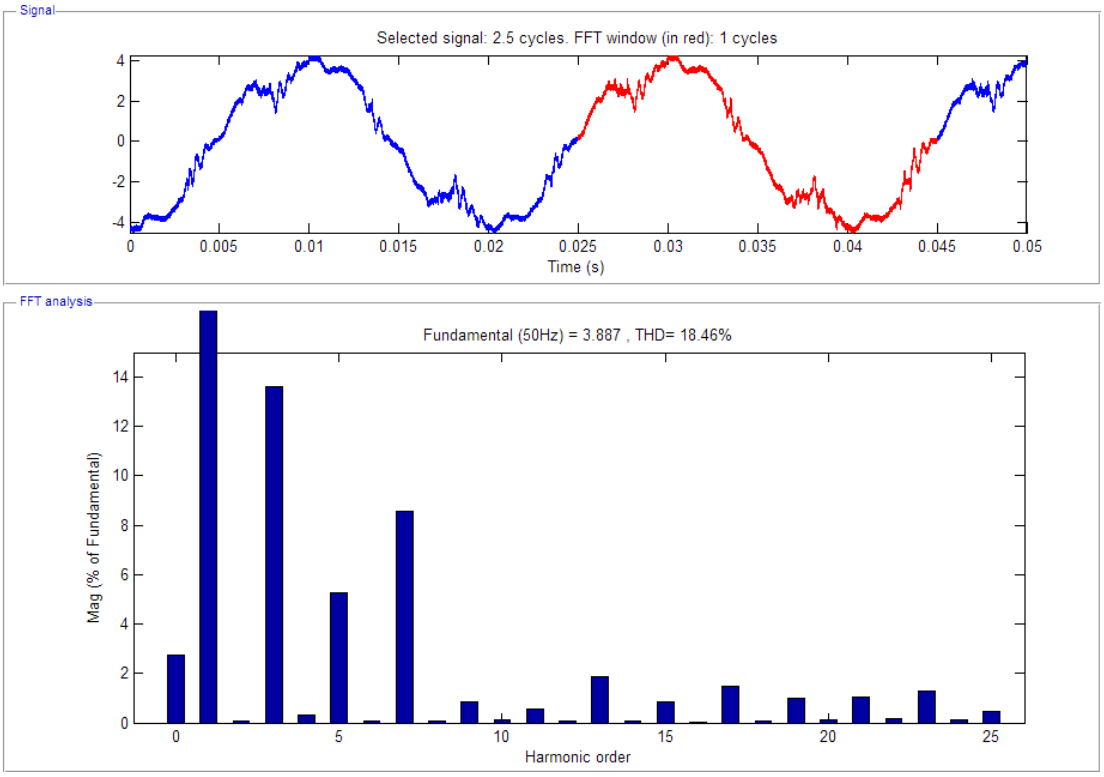

Figure 8. 400W HPS lamp, after 7 minutes (steady state)

Change of characteristics though time, first minutes after being switch on (lamp SON-T 400W):

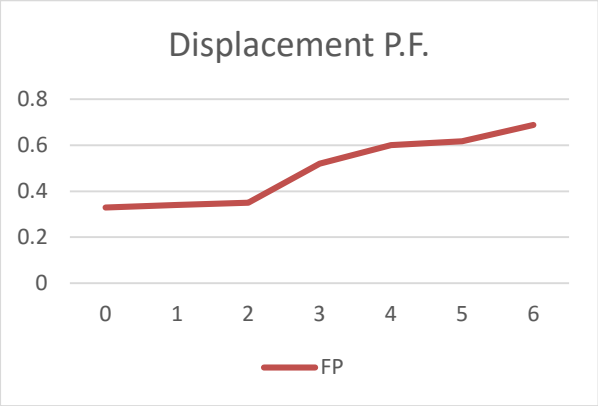

Figure 9. 400W HPS lamp, PF vs time (min).

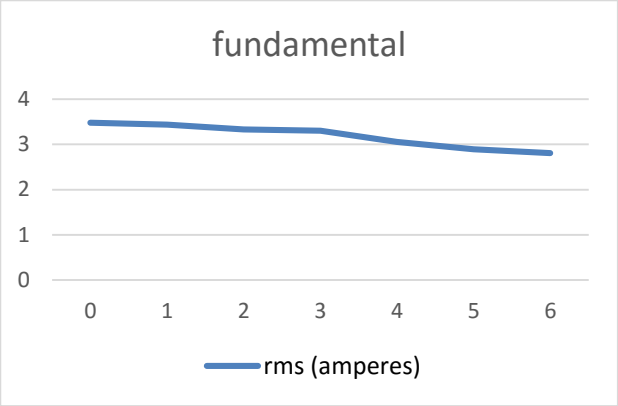

Figure 10. 400W HPS lamp, fundamental vs time (min).

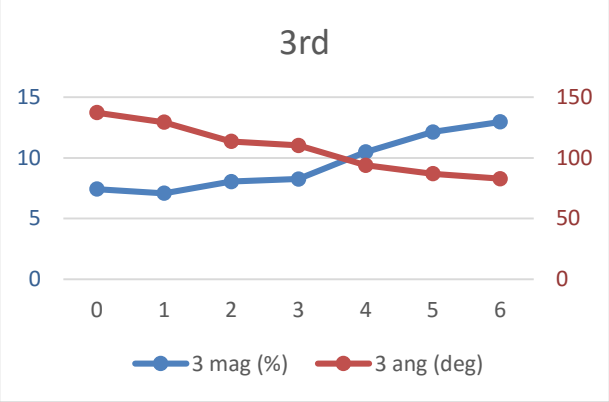

Figure 11. . 400W HPS lamp, 3rd harmonic vs time (min).

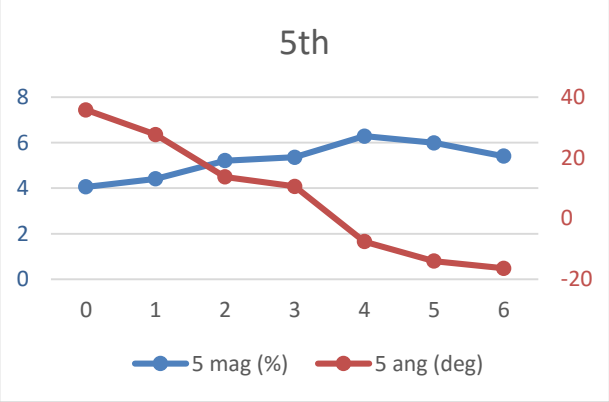

Figure 12. 400W HPS lamp, 5th harmonic vs time (min).

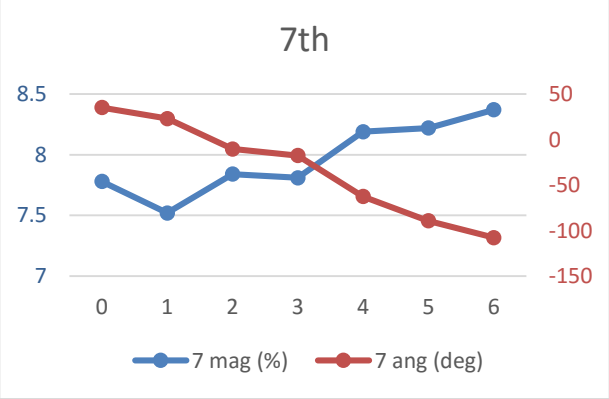

Figure 13. 400W HPS lamp, 7th harmonic vs time (min).

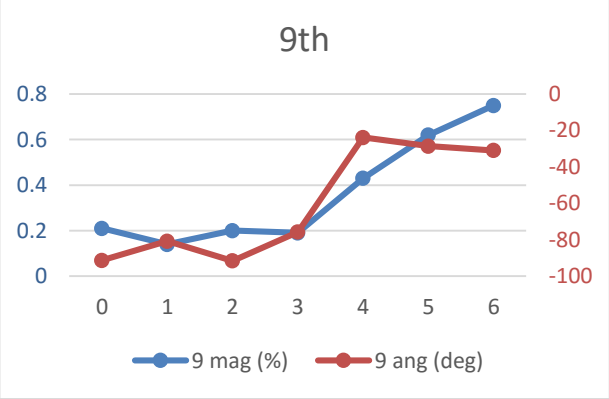

Figure 14. 400W HPS lamp, 9th harmonic vs time (min).

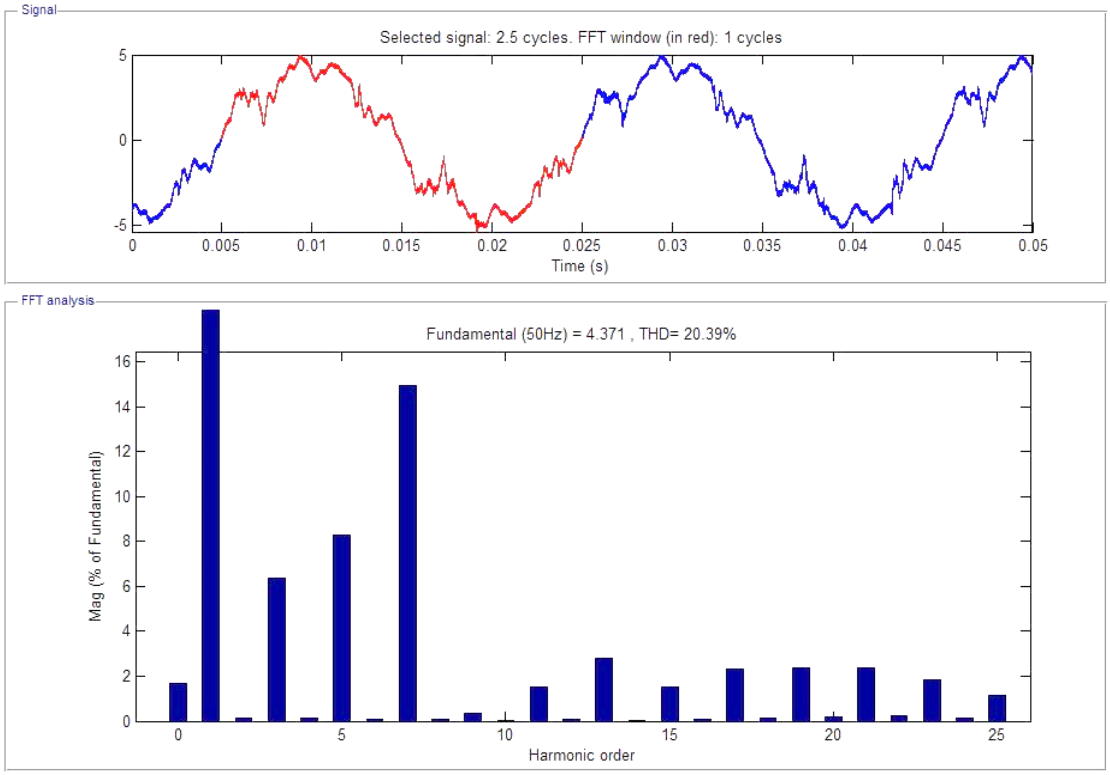

Figure 15. 600W HPS lamp, initial current.

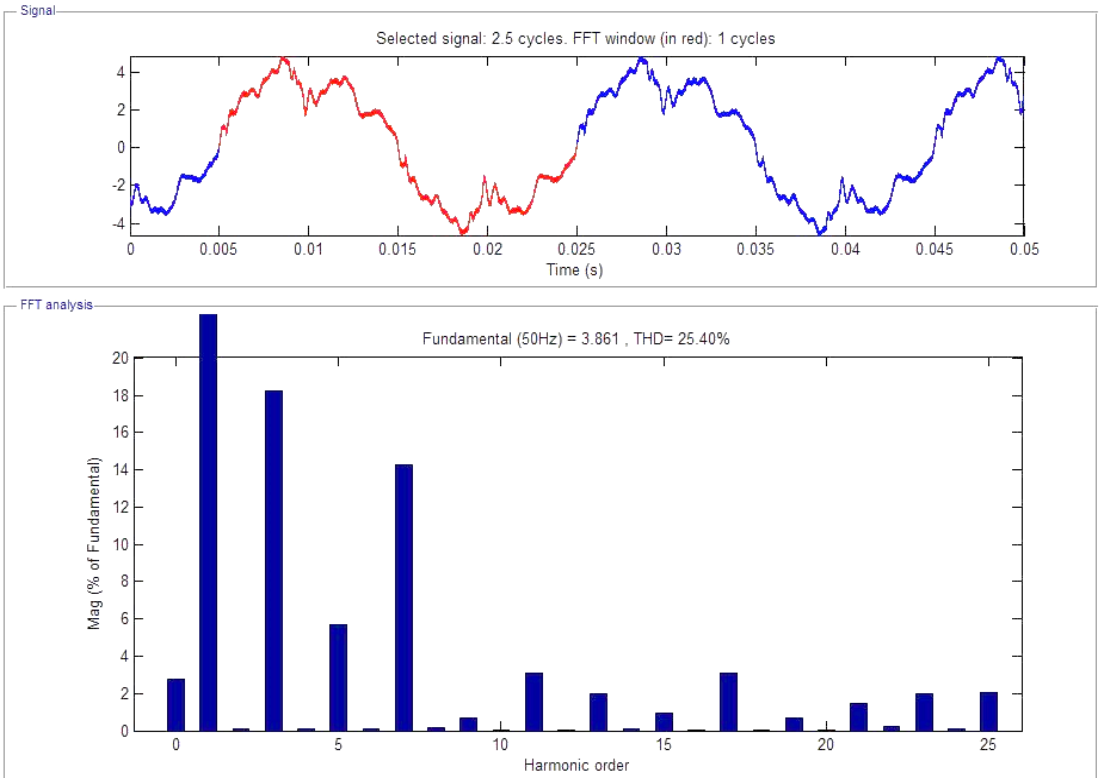

Figure 16. 600W HPS lamp, after 7 min (steady state).

Change of characteristics through time, first minutes after being switch on (lamp SON-T 600W)

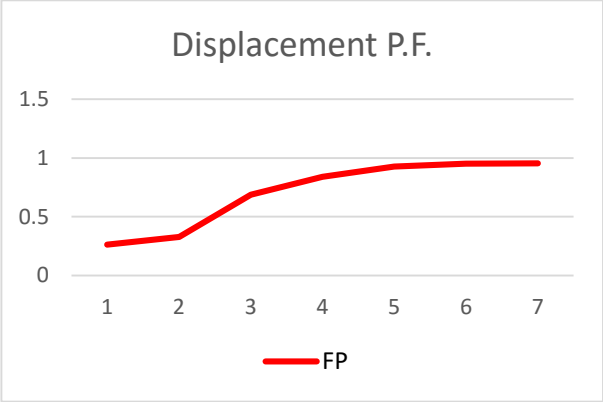

Figure 17. 600W HPS lamp, PF vs time (min).

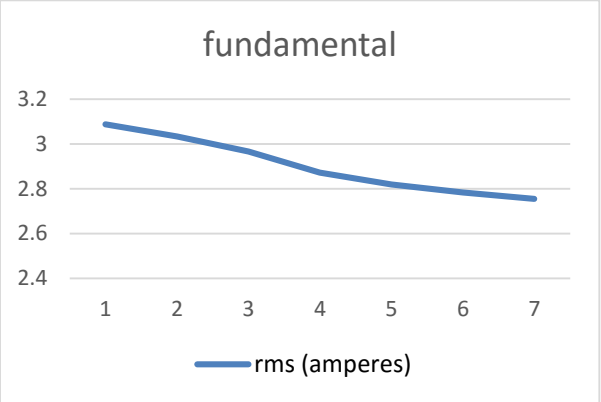

Figure 18. 600W HPS lamp, fundamental vs time (min).

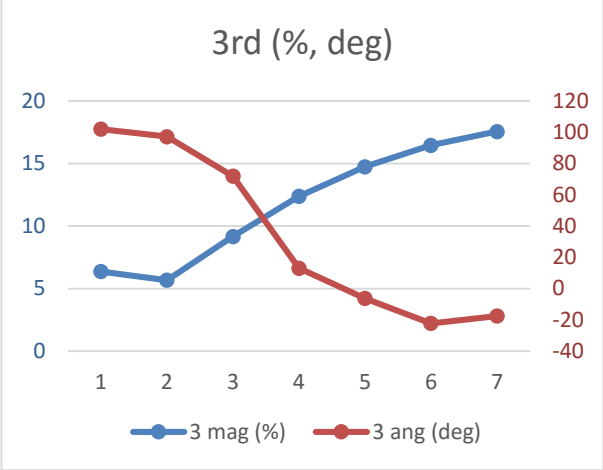

Figure 19. 600W HPS lamp, 3rd harmonic vs time (min).

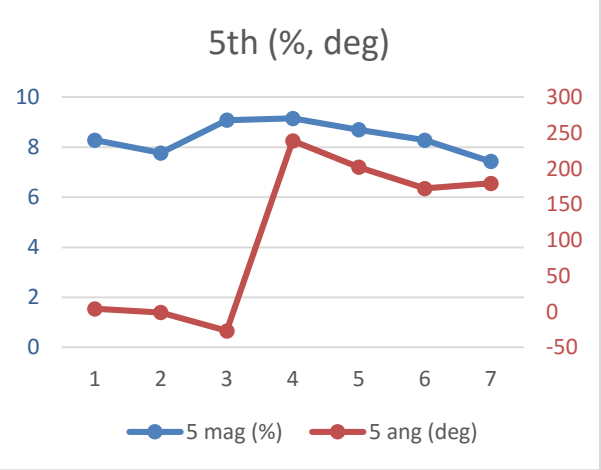

Figure 20. 600W HPS lamp, 5th harmonic vs time (min).

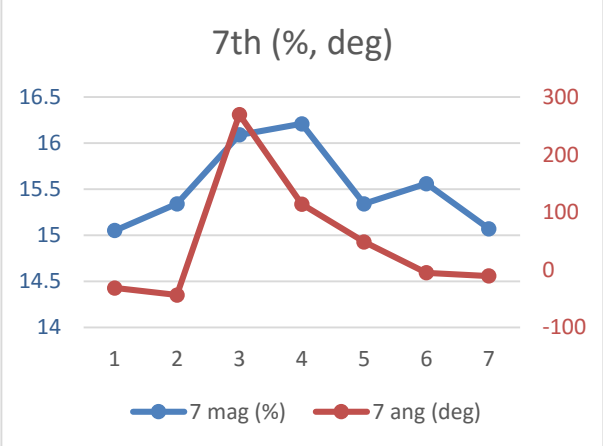

Figure 21. 600W lamp, 7th harmonic vs time (min).

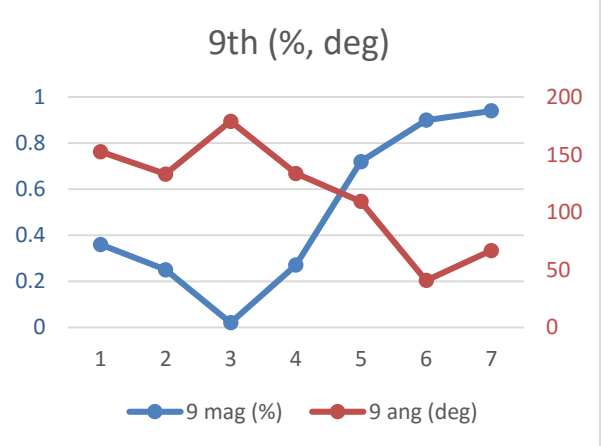

Figure 22. 600W lamp, 9th harmonic vs time (min).

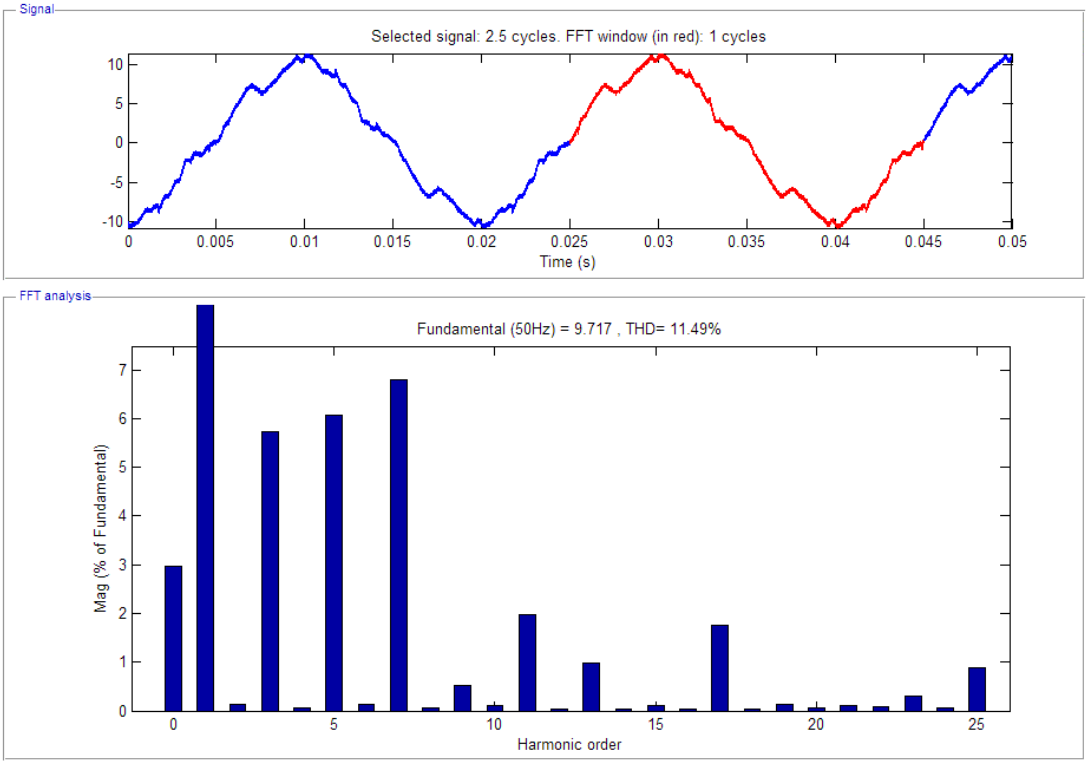

Figure 23. 1000W HPS lamp, initial current.

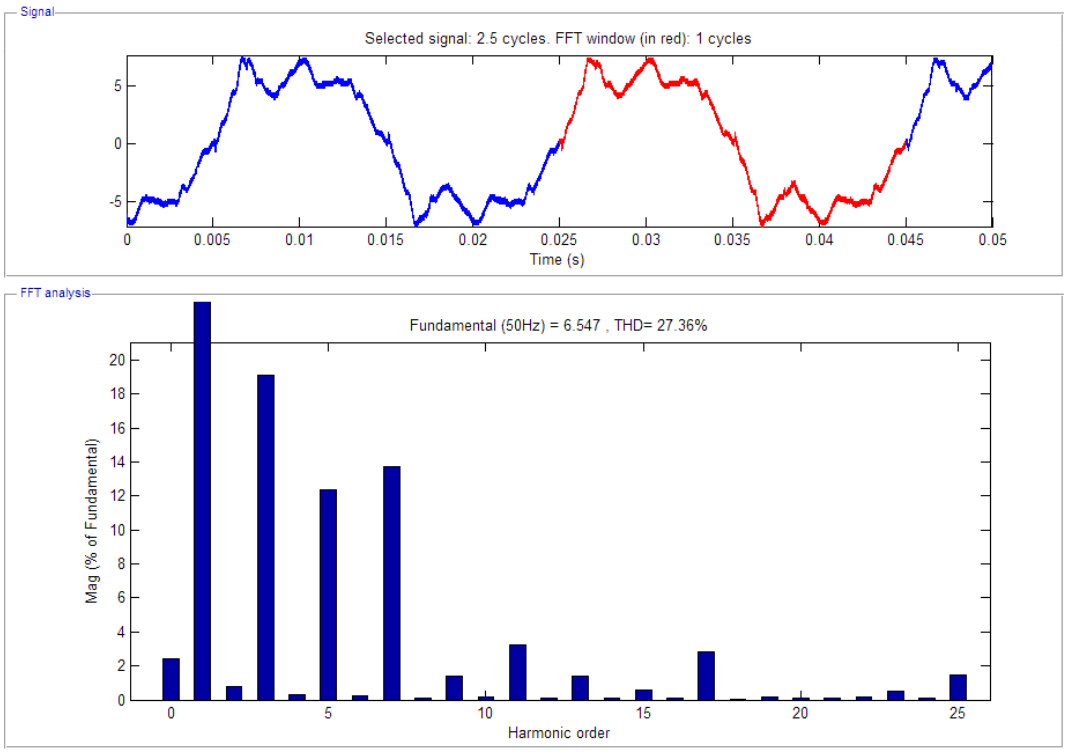

Figure 24. 1000W HPS lamp, after 7 min (steady state).

Change of characteristics trough time, first minutes after being switch on (lamp SON-T 1000W):

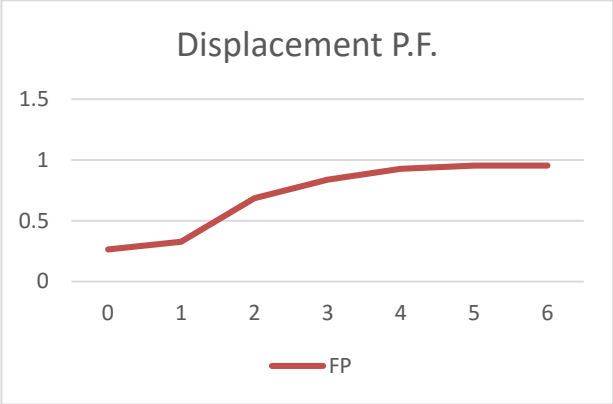

Figure 25. 1000W HPS lamp, PF vs time (min).

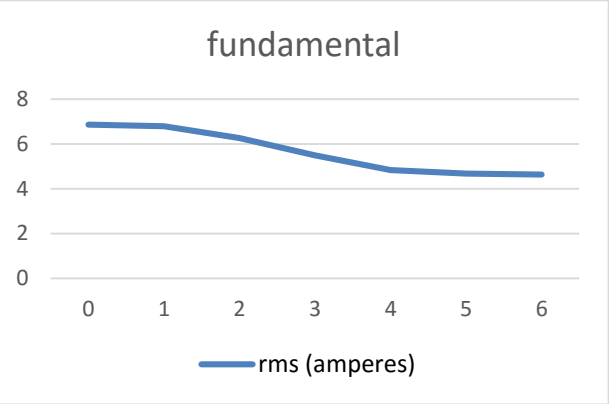

Figure 26. 1000W HPS lamp, fundamental vs time (min).

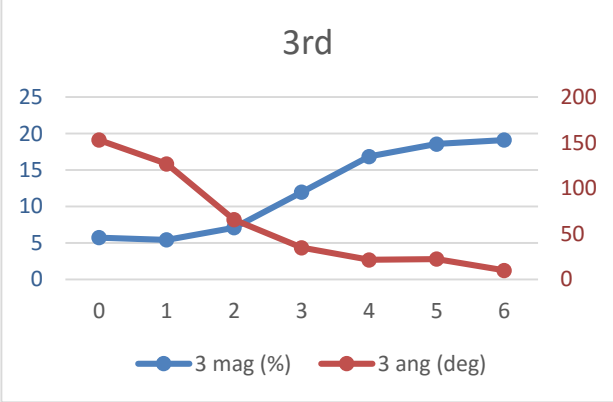

Figure 27. 1000W HPS lamp, 3rd harmonic vs time (min).

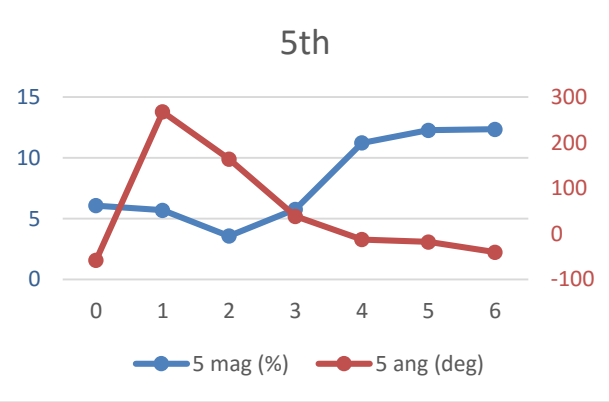

Figure 28. 1000W HPS lamp, 5th harmonic vs time (min).

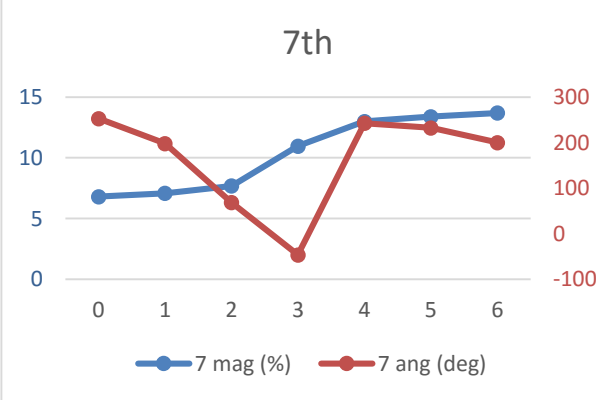

Figure 29. 1000W HPS lamp, 7th harmonic vs time (min).

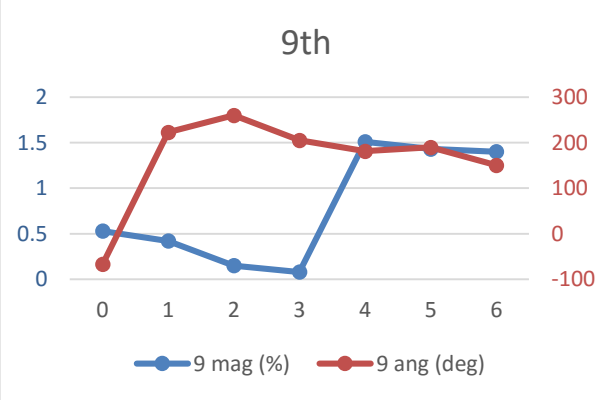

Figure 30. 1000W HPS lamp, 7th harmonic vs time (min).

Chapter 4

4. Calculation of aggregated data

After obtaining the electrical characteristics of the HPS lamps, the identification in aggregated data was explored. For the experiment, real measurement data from a LV substation was modified in order to emulate having HPS lamps combined with it. The real data was measured using a Locamation AIM meter with voltage and current harmonic capabilities, which was installed in every circuit feeder of the substation. Afterwards, the data was selected to emulate a worst case scenario because of its high amount of harmonics, current magnitudes, and variations of reactive and active power. To this data, the current characteristics of the 600W lamp in chapter 3, were added to simulate a measurement of a circuit feeding the lamps. For a complete explanation of the calculation methodology refer to Appendix B. Two scenarios were simulated.

Scenario 1

Considerations:

- The circuit consist of 10 lamps SON-T 600W with the current characteristics that were shown previously.
- The 10 lamps cycle is 12 hours on and 12 off.
- The measurement are the average of the measured values for a time interval of 5 minutes.
- The simulations were performed for a duration of 2 days.
- The influence of the voltage is neglected.
- Any distortion of the current waveform of the lamps by the impedance between the lamps and the measuring point is considered negligible.
- The change of the current waveform by every minute is taken into account in the simulation.
- The time interval are period of 5 minutes, 288 intervals equal a day (minute=5*time interval). The lamps are turned on and off at:

Interval	**State**	
1 to 107	off	
108 to 252	on	(at minute 541, 541/5≈108 interval)
253 to 395	off	
396 to 540	on	(at minute 1981, 541/5≈396 interval)
541 to 576	off	

1 room waveforms

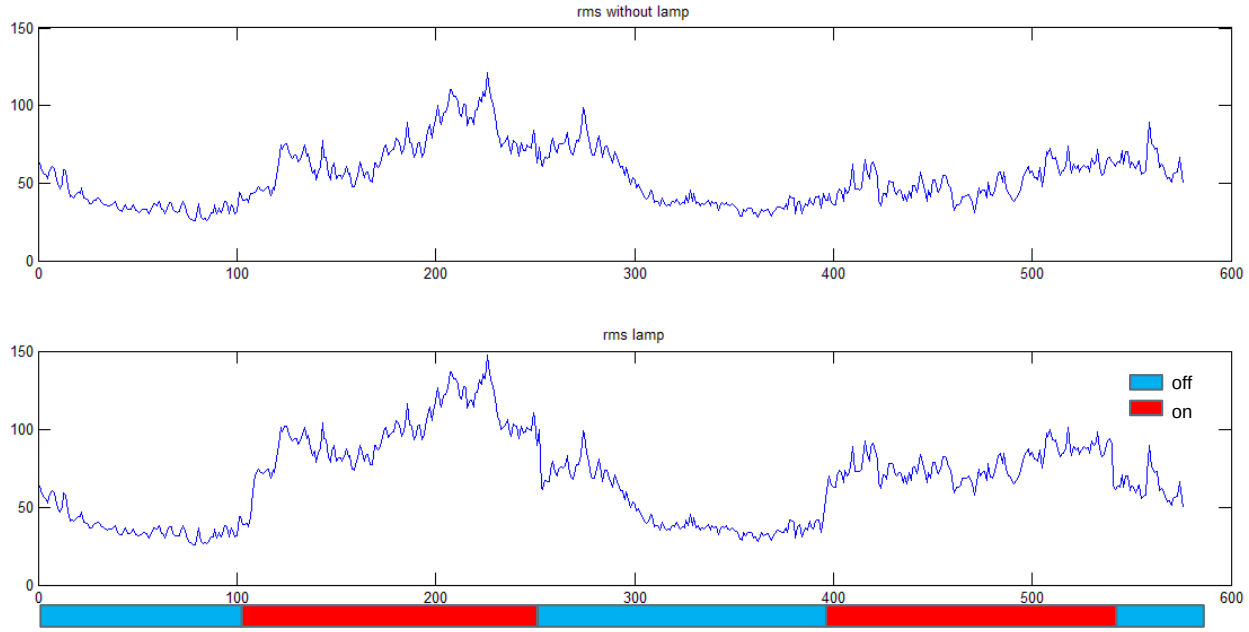

Figure 31. Scenario 1, current rms (Amperes vs time). The time axis is 5 minutes periods.

As it can be observed in Figure 31, there is an abrupt change in current magnitude during each switch on and off of the HPS lamps. This is a good insight that a big load is being switch on periodically. In more crowded measurements this behavior may become difficult to visualize. Also it may be confused with normal behavior of working schedule, so more electric characteristics need to be taken into account.

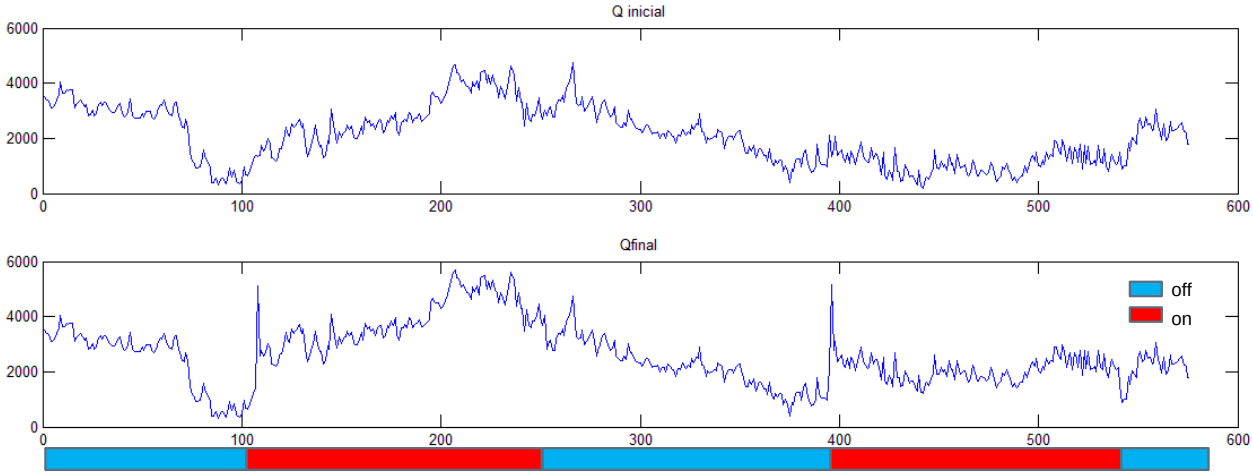

Figure 32. Scenario 1, Reactive power (VAR vs time). The time axis is 5 minutes periods.

In chapter 3 it is mentioned that the HPS lamps have a low power factor between the instant they "switch on" and the moment they reach steady state. This characteristic can be a powerful tool to recognize the "switch on" event. Figure 32 shows this characteristic, where the low power factor is observed as spikes in a VAR versus time graph. Attention should be paid to the fact that in the calculations, the "switch on" instant happens at the second minute of the 5 minute period. In practice the switch on instant may change slightly, increasing or decreasing (according to the case) this spike.

As can be observed from Figure 33 to Figure 35, the harmonics magnitude is affected with the insertion of the lamps. The change can be reflected as an increase or decrease (depending on the angles) as the harmonics are vectors and not scalars. Another remark is that the harmonics have a transition in magnitude and angle from the instant the lamps switch on, to the steady state. This can be reflected as small spikes or sags (depending on the angles) at the switch on event.

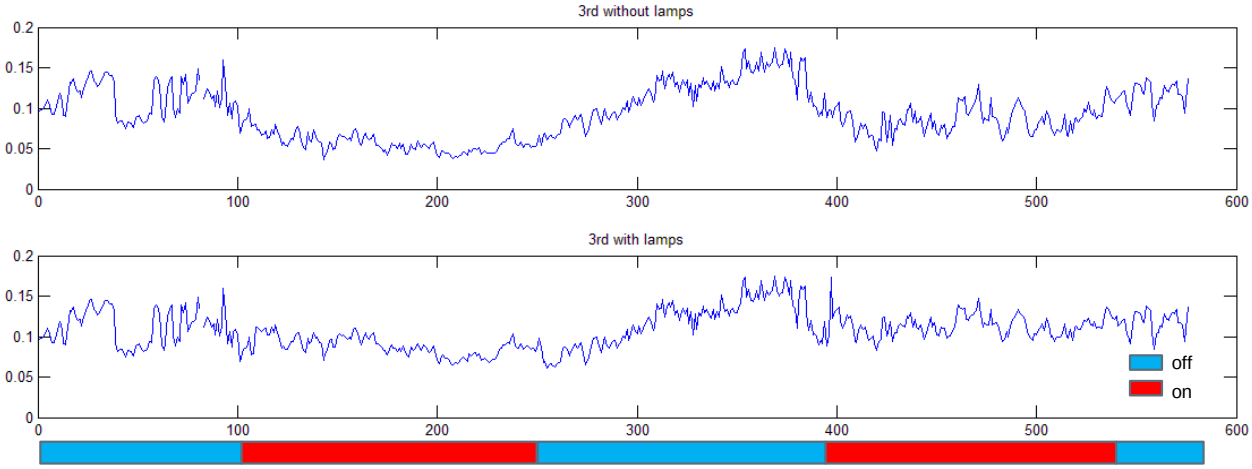

Figure 33. Scenario 1, 3rd harmonic (0.10=10% vs time). The time axis is 5 minutes periods.

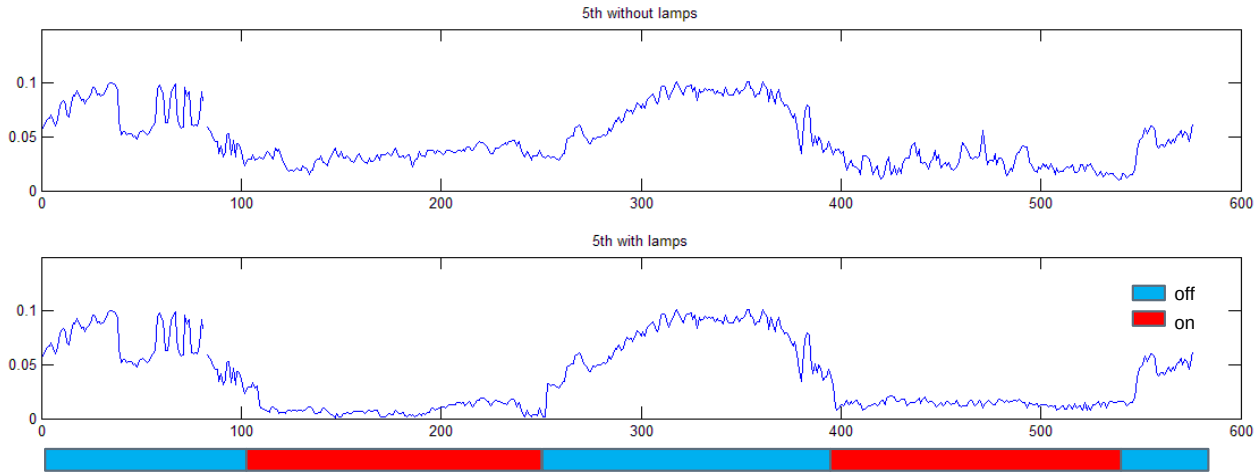

Figure 34. Scenario 1, 5th harmonic (0.10=10% vs 5 time). The time axis is 5 minutes periods.

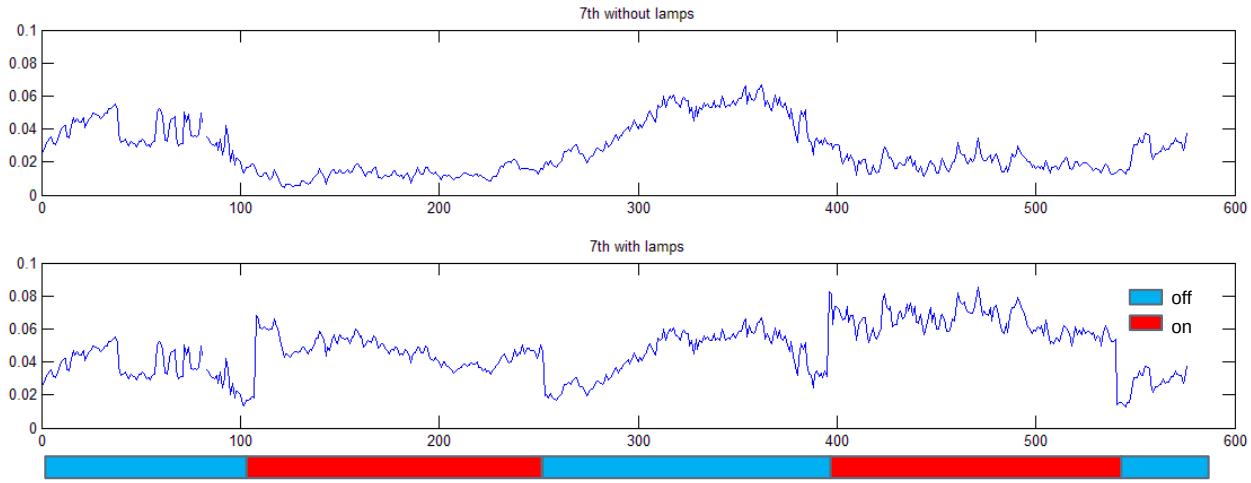

Figure 35. Scenario 1, 7th harmonic (0.10=10% vs time). The time axis is 5 minutes periods.

Scenario 2

Considerations:

- 5 lamps work at a time. Every 12 hours 5 are turned off and other 5 are turned on simultaneously (transient values of the lamps are present because the switch on instant).
- The circuit consist of lamps SON-T 600W with the characteristics that shown at chapter 3.
- The simulations were performed for a duration of 2 days.
- The influence of the voltage is neglected.
- Any distortion of the current waveform of the lamps by the impedance between the lamps and the measuring point is considered negligible.
- Change of the lamps current waveform by every minute is taken into account in the simulation.
- The time axis is every five minutes, each transition (5 lamps off, 5 lamps on) is at:

Interval	**State**
1 to 107	on
108	5 lamps turn off and other 5 turn on
109 to 252	on
253	5 lamps turn off and other 5 turn on
254 to 395	on
396	5 lamps turn off and other 5 turn on
397 to 540	on
541	5 lamps turn off and other 5 turn on
542 to 576	on

Scenario 2 waveforms

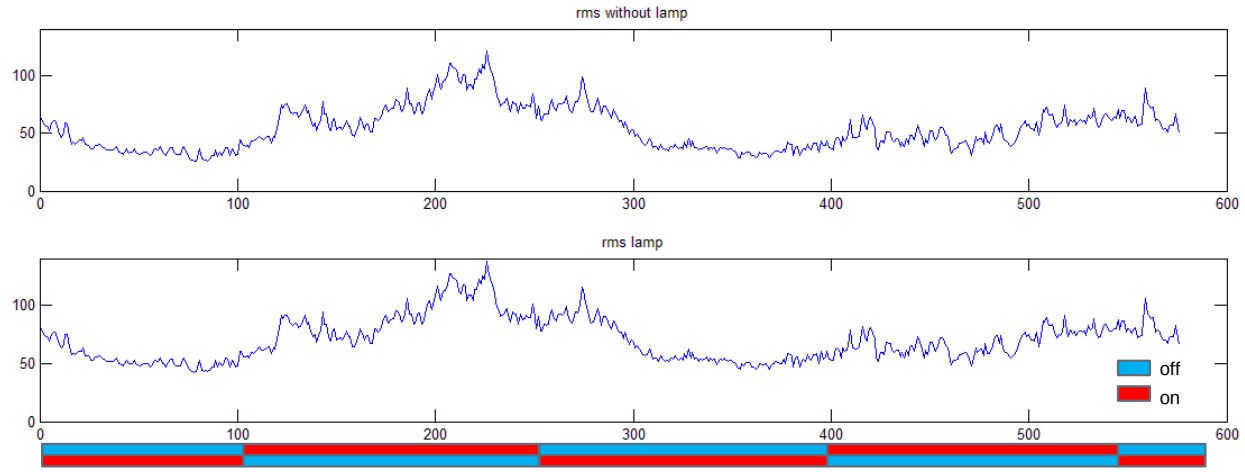

Figure 36. Scenario 2, current rms (Amperes vs time).

As can be observed in Figure 36, in this scenario the current does not have a visible patron every 12 hours. In Figure 37, the reactive power spikes at every "switch on" of the lamps can be observed. In this case the number of lamps at a time was chosen to be 5 to make the event less noticeable. There is one spike every 12 hours corresponding to each switch on event, but due to the small number of lamps, the "switch on" spikes of the lamps can get confused with the spikes produced by the other loads. As a countermeasure, the rate of change of the reactive power is plotted and compared between both days. Because the switching of the lamps occur every 12 hours, the ones that occur at the same time each day are the ones corresponding to the lamps (Figure 37). Just 2 days were simulated, in practice the more days compared, the more noticeable it becomes.

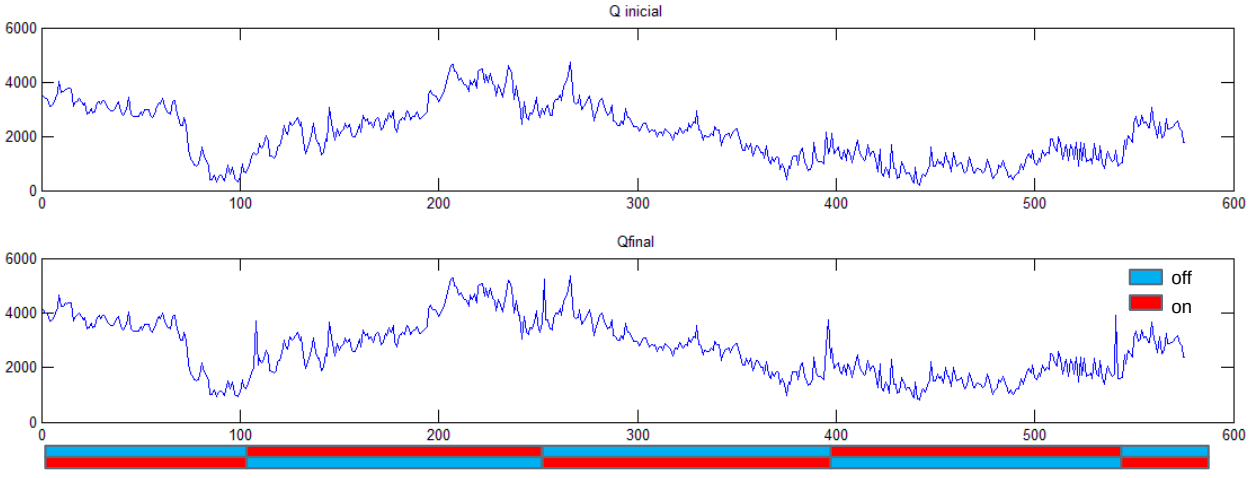

Figure 37. Scenario 2, Reactive power (VAR vs time).

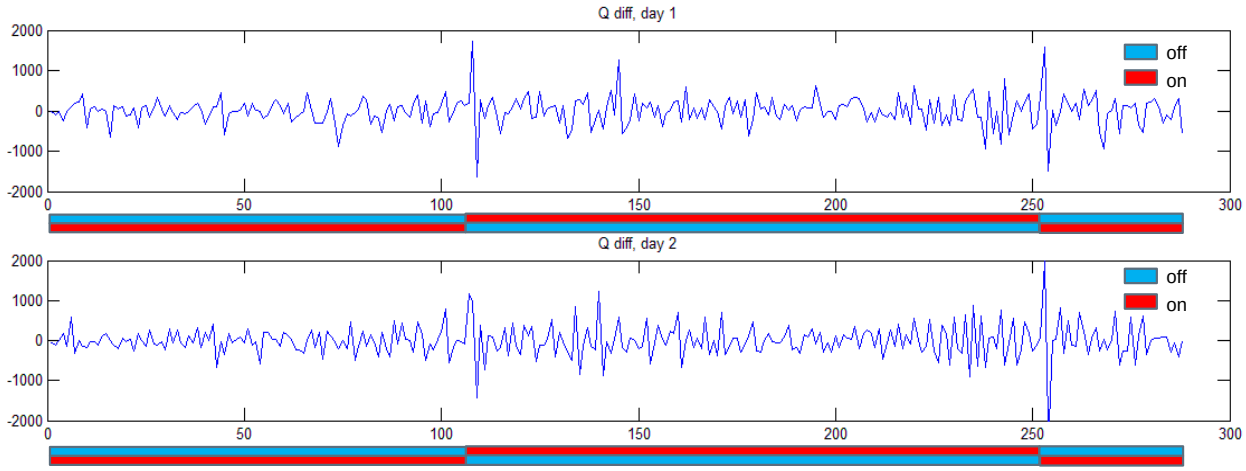

Figure 38. Scenario 2, rate of change of reactive power (VAR diff vs time).

The same situation is be observed in the harmonics. Every 12 hours at the switch on instant, sudden change in the harmonics is observed because of the harmonic transition before reaching steady state. The same procedure as with the reactive power can be done, and the rate of change of the reactive power is plotted and compared between both days. As mentioned before, in practice, the more days are compared, the more distinguishable. From Figure 39 to Figure 44, the harmonics percentage and its rate of change are plotted.

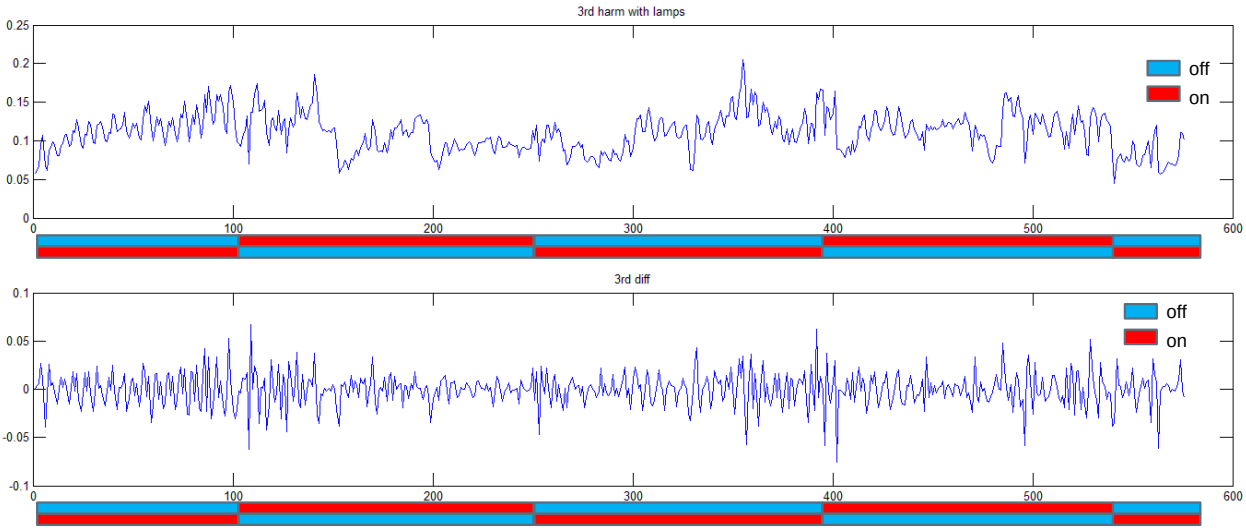

Figure 39. Scenario 2, 3rd harmonic (.10=10% vs time) and rate of change (VAR diff vs time).

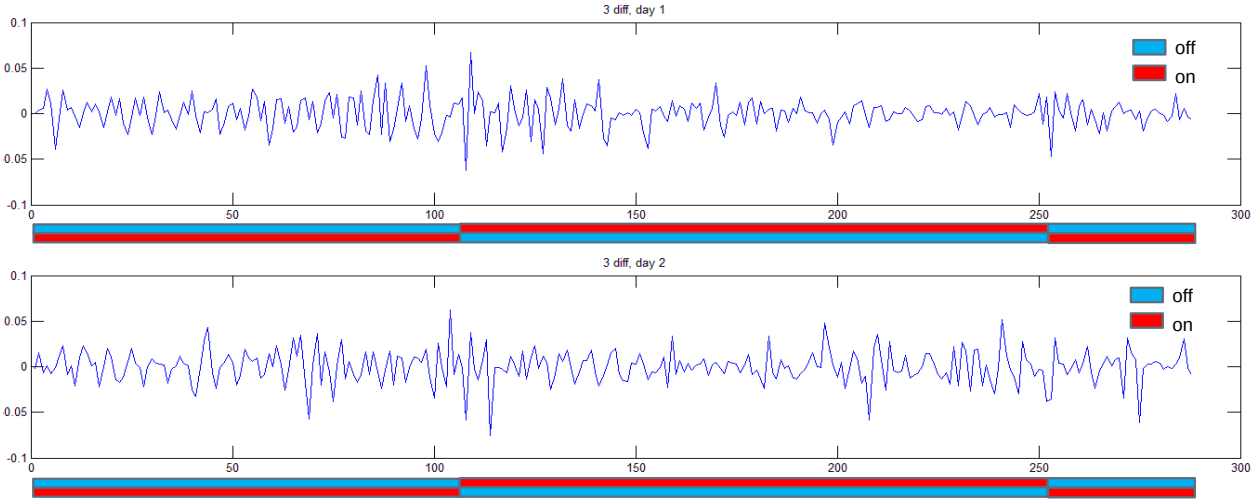

Figure 40. Scenario 2, 3rd rate of change (VAR diff vs time).

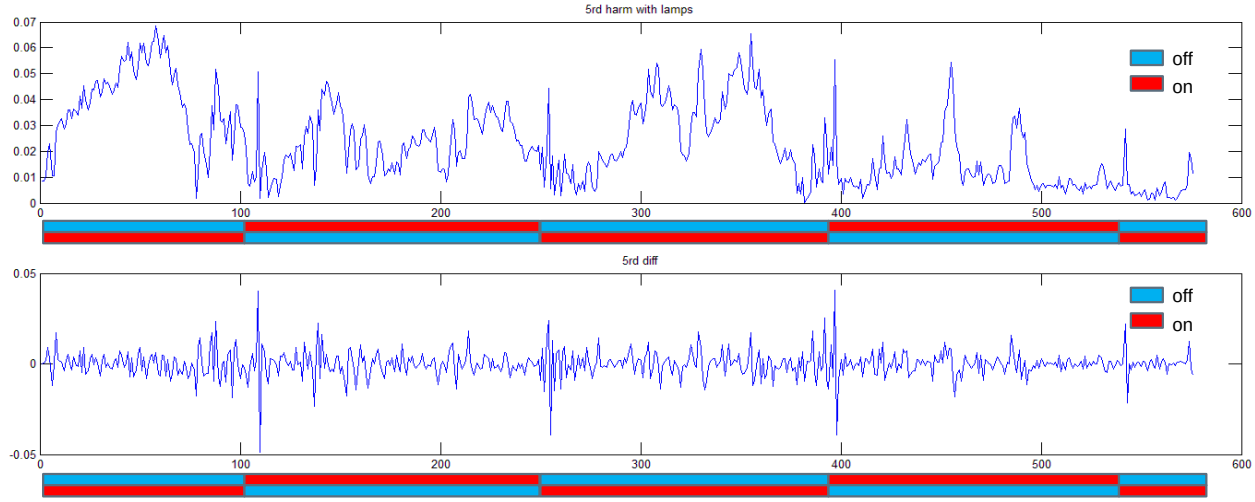

Figure 41. Scenario 2, 5th harmonic (.10=10% vs time) and rate of change (VAR diff vs time).

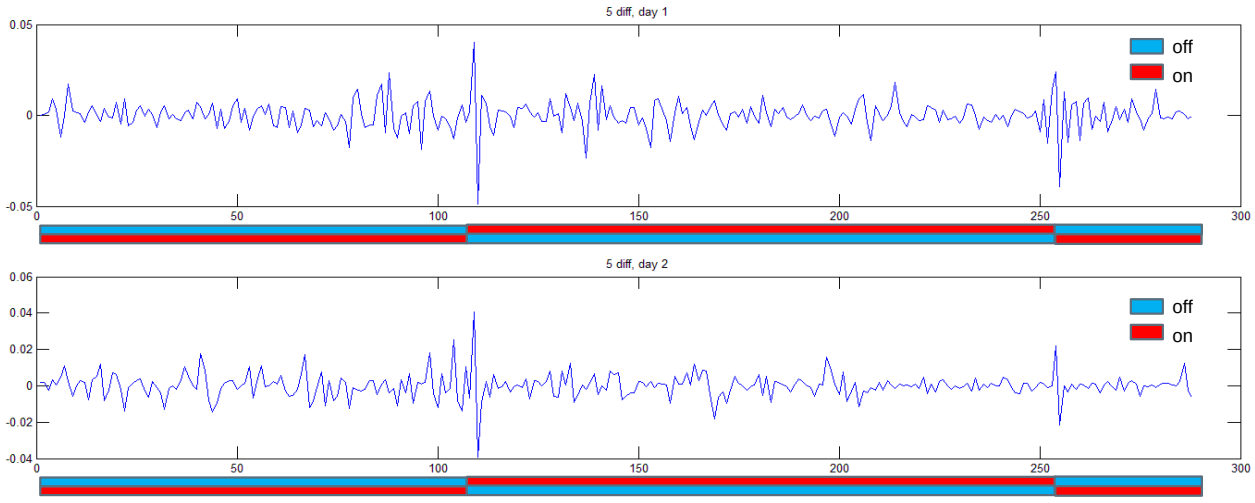

Figure 42. Scenario 2, 5th rate of change (VAR diff vs time).

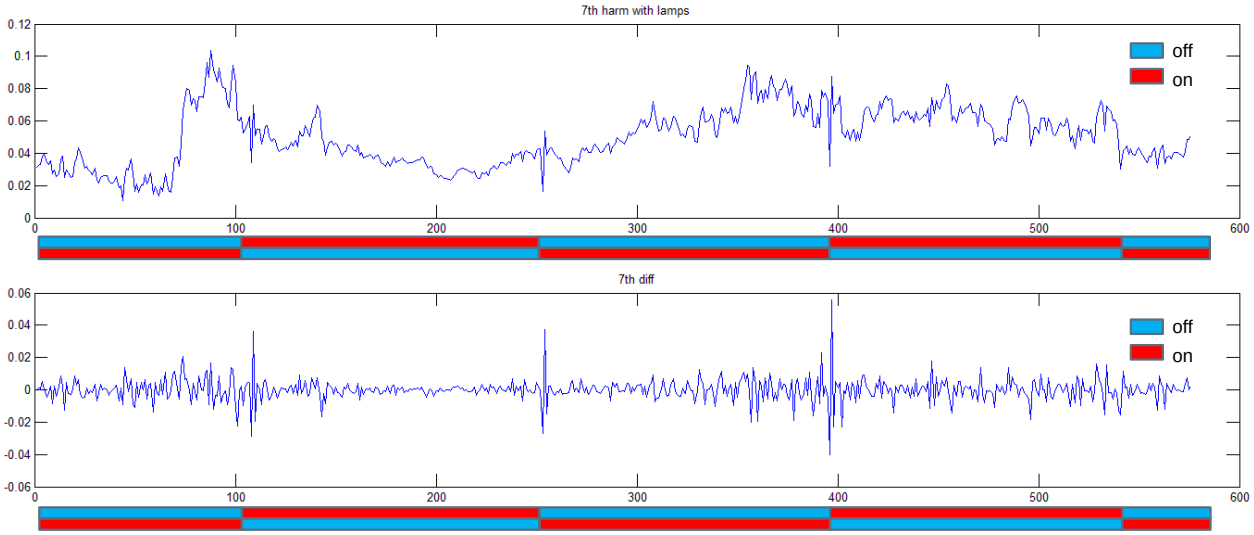

Figure 43. Scenario 2, 7th harmonic (.10=10% vs time) and rate of change (VAR diff vs time).

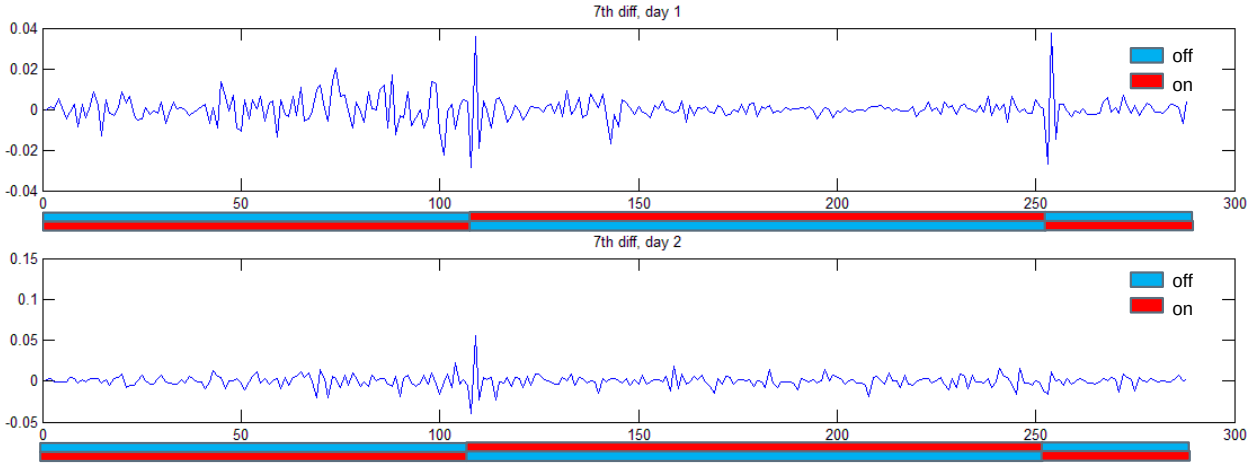

Figure 44. Scenario 2, 7th rate of change (VAR diff vs time).

Form this results we can observe that using the electrical characteristics of the HPS lamps, we can distinguish the switching on/off from the aggregated data by the use of the spikes of the reactive power at the instant of switching on, as well as the changes in the harmonics. In this calculation, the HPS lamp's waveform were considered undistorted from the waveform measured at chapter 3. The current characteristics of the HPS lamps used for the calculations were considered undamped between the point of connection of the lamps, and the emulated meter. In chapter 5 we can observe that the harmonic values of a load that reach the centralized meter, are slightly modified or damped across the network. To compare the calculations, real field test were performed and its results are presented in chapter 6.

Chapter 5

5. Power flow simulation

In order to see the expected current and voltage harmonic values of the HPS lamps at different points of the low voltage network, a simulation was done with DIgSILENT PowerFactory software. The main parameters of interest are the voltage drop, current magnitudes, voltage and current harmonics at different points in the low voltage network.

To model the HPS lamps in the frequency domain, the Norton equivalent model was used. It consists of a current source in parallel with an impedance. The ideal current source with an infinite parallel impedance, represents the emission of the device when supplied by an ideal voltage. The impedance part (Z_h) interacts with the voltage at the device terminals (U_h) representing the influence of the voltage in the device. The total current (I_{tot}) is the sum of the two parts [14].

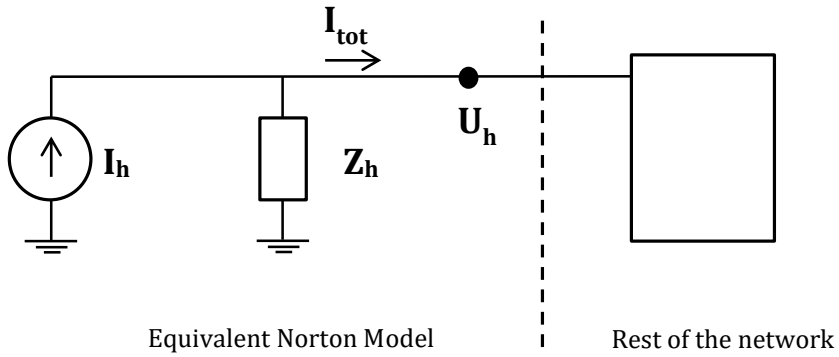

Figure 45. Norton equivalent model.

5.1 Modeling of the HPS lamps:

The lamps were modeled with a Norton equivalent model. The measured values shown in chapter 3 were used. The lamps were modeled with a Norton equivalent, an ideal current source with the parallel impedances set to infinite. The reason is that the measured values were taken with a reasonable undistorted voltage coming from the grid, the voltage dependence was not measured as it needs at least two different measurements with different distorted voltage [14].

The validation of considering negligible the voltage dependence for the low harmonic order is the following: Two Norton models with the measured harmonic spectrum were modeled. One as an ideal current source and the second with a parallel capacitance of 40μF as depicted in [14]. It is in good agreement with the size of the capacitor of the lamp ballasts, which has a name plate value of 40 μF ±10%.

Four cases were analyzed:

Case 1: Norton model of ideal CS connected to an undistorted VS.

Case 2: Norton model with parallel capacitance of 40μF connected to an undistorted VS.

Case 3: Norton model of ideal CS connected to a VS distorted with the harmonic limits of the standard EN 50160.

Case 4: Norton model with parallel capacitance of 40μF connected to a VS distorted with the harmonic limits of the standard EN 50160.

The output current of the lamp's Norton model for each case can be seen at Table 1. The limits for the odd voltage harmonics till 9th of the standard EN 50160 can be seen at the second column of the table.

Harmonics f_h/f_1	EN 50160 LV and MV Limits in %	Case 1 Current in % of fund.	Case 2 Current in % of fund.	Case 3 Current in % of fund.	Case 4 Current in % of fund.	Difference % of CS at EN50160 VS
3	5	19.13	19.50	19.13	20.6	1.47
5	6	12.36	12.60	12.36	12.59	0.23
7	5	13.69	13.95	13.69	14.87	1.18
9	1.5	1.4	1.42	1.4	1.99	0.59

Table 1. HPS lamp Norton model cases comparison.

In the last column of Table 1, the change in percentage between case 3 and 4 is shown. Being the maximum difference 2%, and with the lack of measurements with different distorted voltages for the lamps; the Norton model subsequently used for the calculations was the ideal CS with zero parallel admittance. This is considered reasonable, as in the actual detection method, the existence of other kind of loads in parallel, as well as the difference between HPS lamp brands, would make a bigger difference in the current harmonic spectrum of the lamps, than the voltage dependence.

As mentioned in chapter 3, HPS lamps have two different states, the dynamic state (the moment they are switch on, till they reach thermal equilibrium) and the steady state after they reach thermal equilibrium. During the dynamic state of the lamps, the fundamental, its harmonics and the power factor are changing. The dynamic state of the lamp last around 6 minutes. As the time step for the 24 hours simulation is 1 minute, 7 different values for the HPS lamp CS were modeled. Each CS value injects the current characteristics of the lamps (current magnitude, harmonic spectrum, power factor) for minute 0 of being switched on, until minute 6 which represents the steady state of the lamp, and this value stays for 12 hours before the process repeats.

Table 2 contains the characteristics of the CS for every minute. The harmonics are in percentage of the fundamental and the angle is in reference with the angle of the fundamental.

Name	I at 50Hz	P.F.	3rd harm %	5th harm %	7th harm %	9th harm %
CS-0	6.87	0.264	5.73∟153	6.07∟-57.9	6.81∟252	0.53∟201.3
CS-1	6.794	0.328	5.43∟126.9	5.69∟267.8	7.08∟198.1	0.42∟222.5
CS-2	6.266	0.6865	7.1∟65.3	3.57∟164.3	7.69∟68.28	0.15∟259.8
CS-3	5.489	0.839	11.96∟34.8°	5.77∟38.5°	10.9∟-46.4°	0.08∟205.2°
CS-4	4.842	0.928	16.87∟21.5°	11.24∟-12.5°	12.99∟242.5°	1.51∟181.2°
CS-5	4.674	0.953	18.58∟22.3°	12.28∟-17.6°	13.39∟232.5°	1.43∟189.5°
CS-6	4.629	0.954	19.13∟9.8°	12.36∟-40.3°	13.69∟200.1°	1.4∟150.3°

Table 2. 1000W HPS lamp characteristics used for the simulation.

5.2 Network Modeling:

Cables

The low voltage grid of Stedin consists mainly of cables. The capacitance effect of the cables have a significant influence on the impedance. The cables were represented by its π equivalent using the lumped impedance model. The π model was considered sufficient as the low voltage lines are relatively

short in comparison to the highest frequency of interest [14], which in this case is the 11th. Skin effect was not taken into account.

Transformer

The transformer was modeled as a series RL circuit. As the frequencies of interest are below 7 kHz [14], the capacitances for the model were neglected as their impact is considered insignificant in comparison to the capacitance of the cables.

Modeling of households:

The households were modeled as parallel RC loads. Each house was considered to consume 900W. The capacitance represents the aggregated capacitance of all power electronics devices. The value for the capacitance used ranged from 0.6µF to 6µF [15].

Modeling of MV grid:

The medium voltage grid which feeds the MV/LV transformer was modeled as an ideal voltage source in series with an impedance. The impedance represents the short circuit impedance of the MV grid and the short circuit X/R relation.

LV grid model

The LV grid chosen for the simulation is situated at Lombok. It consists of a 315kVA delta-star transformer connected to a 10.75kV voltage. The transformer feeds a 400V bus with 10 feeders. These feeders connect the households to the grid. There are 318 households in total.

5.3 Simulations

Power Flow

The Norton equivalent model of 5 lamps were positioned at the middle point of one of the feeders. A power flow analysis was calculated with the households at 900 Watts consumption and the lamps at the steady state. With this calculation, a voltage drop across the line was calculated. Figure 46 shows the voltage across the feeder. As it can be appreciated in Figure 46, the voltage drop rate is higher

before reaching the lamps point, where it gets an inflection. It can also be seen a change of voltage drop due to a change in the cable cross sectional area which has a direct impact in the voltage drop.

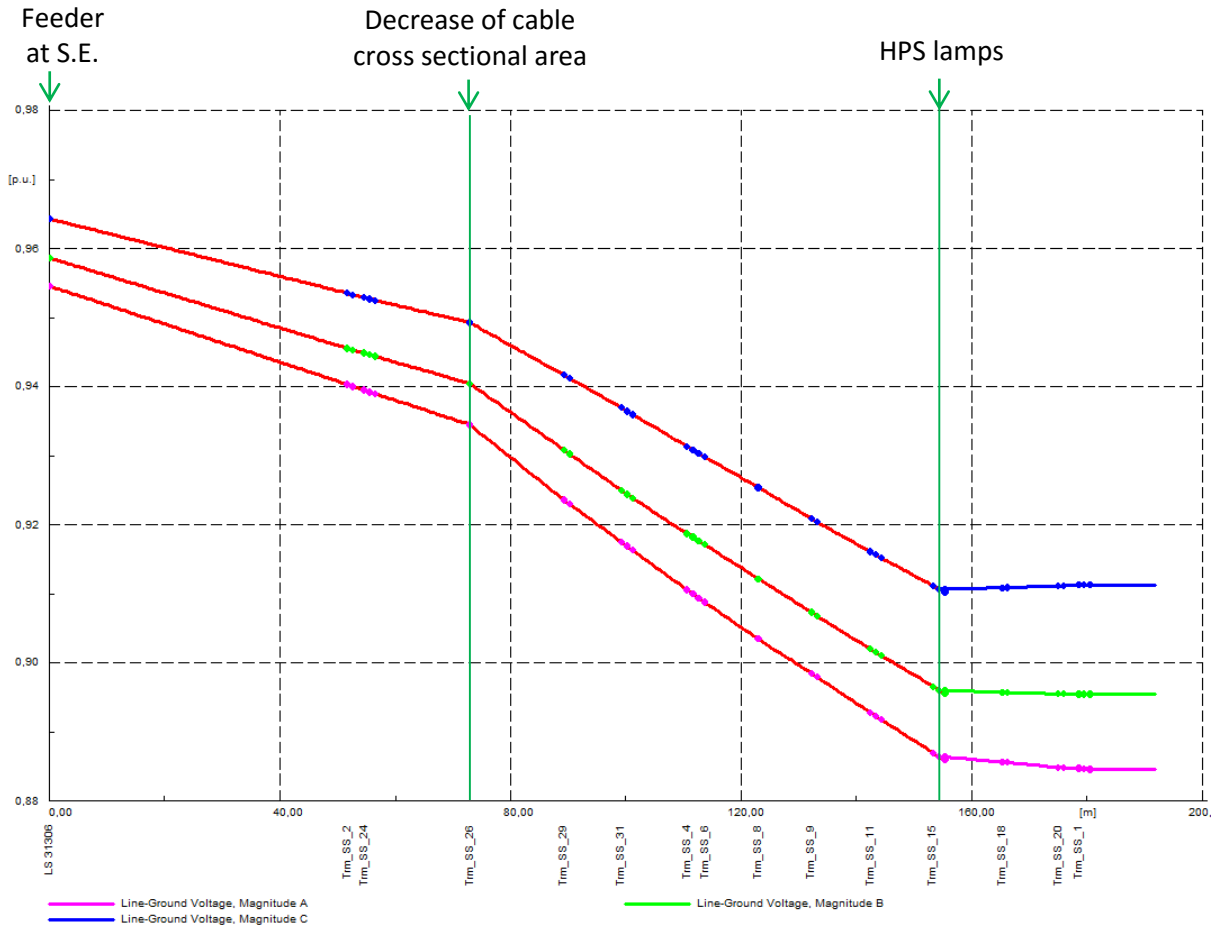

Figure 46. Voltage drop across the circuit feeding the HPS lamps.

Harmonic Power Flow

With the same load configuration as the power flow, a harmonic power flow was carried out from the fundamental harmonic till the 11th. It is important to mention that the only harmonic source in the calculations are the lamps, in real systems this is not completely true as any electronic device in the households injects harmonic currents into the grid. Nevertheless, the harmonics injected by these loads are generally several times smaller than those injected by the lamps (in the case of several of these loads, they can become significant). The main purpose was to see how the harmonic currents produced from

the lamps flow across the network and to see how damped is the measurement at different metering points. Figure 47 shows a representation of the feeder with the measuring points and the model of the lamps are shown. Figure 48 illustrates the harmonic flow of the current at the POC of the lamps, at the feeder and at the low voltage side of the transformer, the harmonic spectrum is slightly different at different measuring points. This is mainly caused by two reasons: The capacitance across the cable act as an extra path for the harmonics. The linear loads consume a distorted current according to the distorted voltage following ohms law for every harmonic.

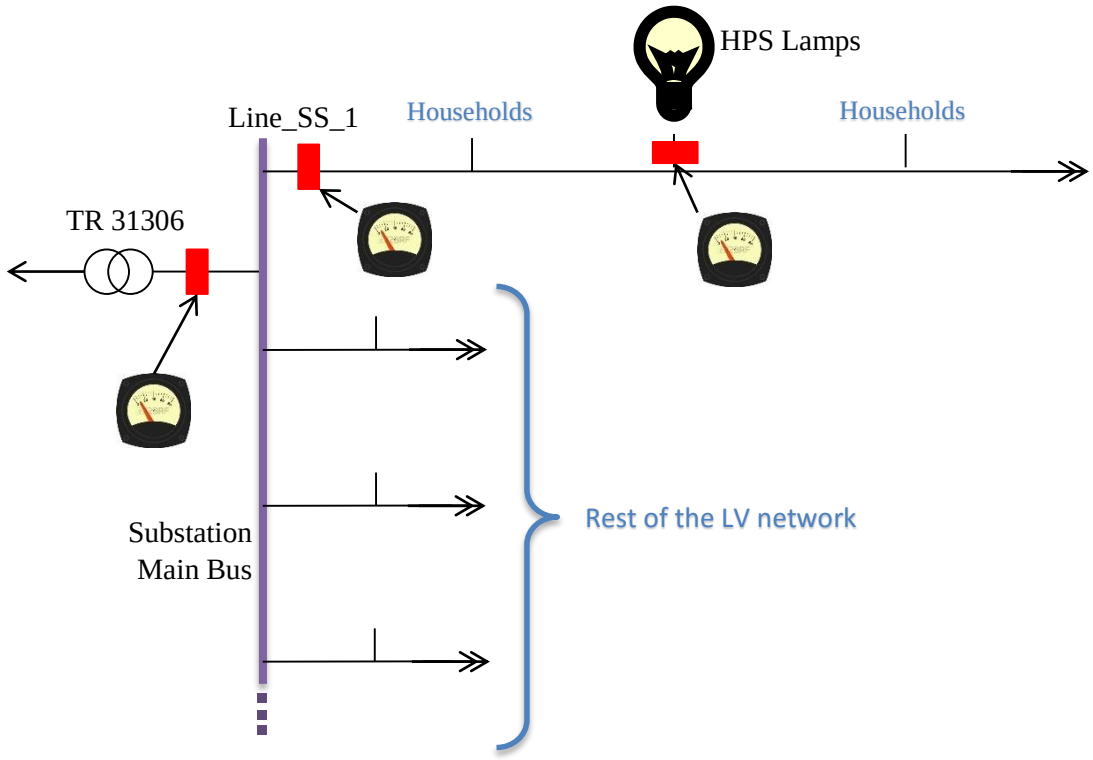

Figure 47. Simplified representation of the metering points and the lamps used at the simulation.

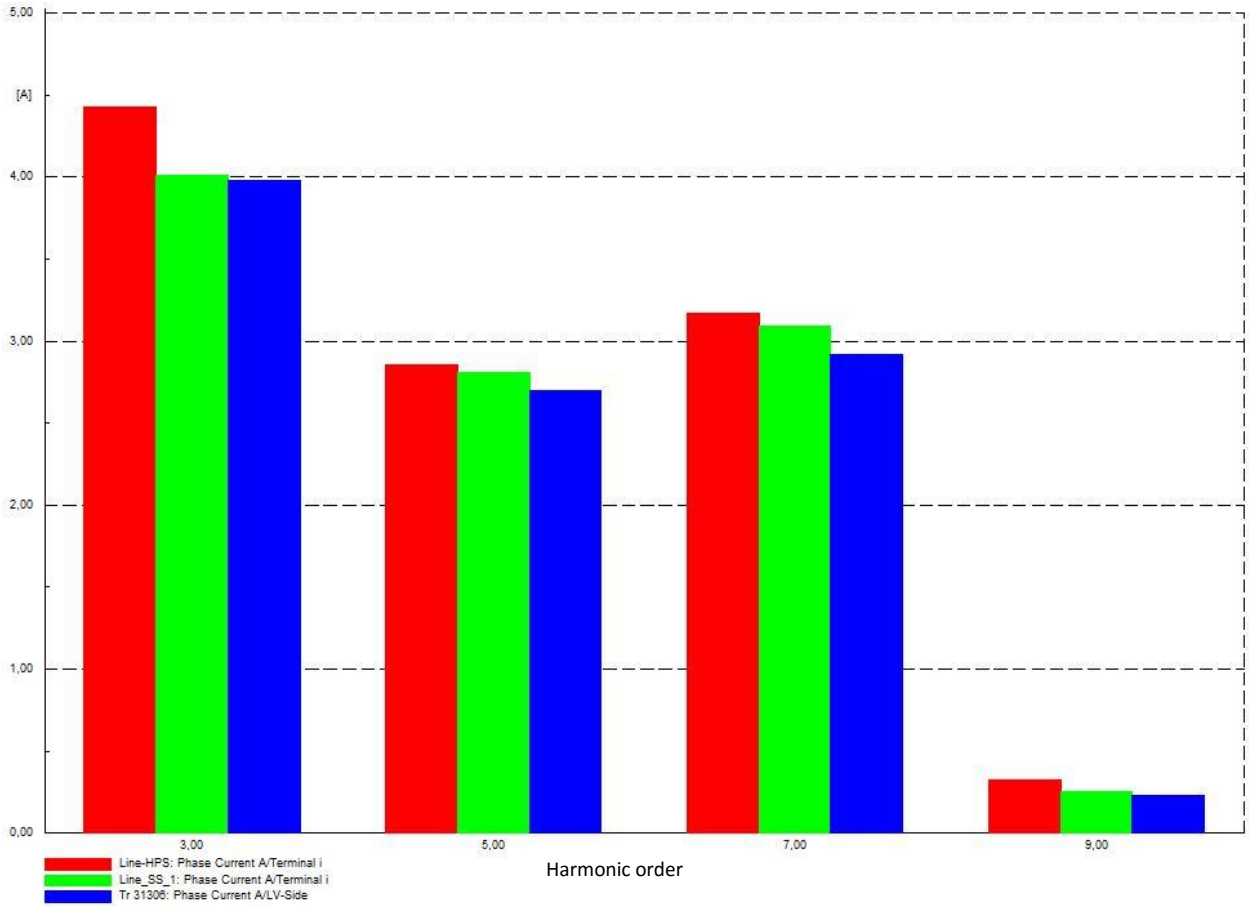

Figure 48. Magnitude of harmonic currents in Amperes at the POC of the lamps (Line-HPS), the feeder of the circuit at the substation (Line_SS_1), and at the transformer (Tr31306).

As it can be appreciated in Figure 48, the current magnitudes change depending on the harmonic value, as well as the metering position. For example in the 3rd harmonic from the position "Line-HPS" to the position "Line_SS_1" the magnitude changed 9.3%, while from "Line_SS_1" to "Tr 31306" the percentage decreased to 0.7%. In contrast, for the 5th harmonic from the position "Line-HPS" to the position "Line_SS_1" the magnitude changed 1.9%, while from "Line_SS_1" to "Tr 31306" the percentage increased to 3.8%. All this values are summarized in Table 3.

	"Line-HPS" to "Line_SS_1"	"Line_SS_1" to "Tr 31306"
3rd harmonic difference: $\frac{i_0-i_f}{i_0}$	9.3%	0.7%
5th harmonic difference: $\frac{i_0-i_f}{i_0}$	1.9%	3.8%
7th harmonic difference: $\frac{i_0-i_f}{i_0}$	2.3%	5.8%
9th harmonic difference: $\frac{i_0-i_f}{i_0}$	23.1%	6.8%

Table 3. Difference of current magnitude at different measuring points.

These values show that the damping of the harmonic current values is not only proportional to the distance or impedance of the conductor from the metering point to the harmonic source (in this case the HPS lamps). The damping is related to the interaction of the total impedance between the source and the metering point, and not only the one of the cable. Meaning that the impedance of the households have a relevant role.

A harmonic sweep calculation is a calculation of the equivalent Norton impedance for a specific point in the grid. Therefore, a calculation was done along a range of frequencies of interest, in order to see the frequency dependence. Looking at the "Substation Main bus" of Figure 47, the harmonic current coming from "Line_SS_1" splits between the parallel impedance of the transformer and the rest of the LV grid following the current division formula. As a remark, the values should be vectors and not only the magnitude.

$$I_{x,h} = \frac{I_{tot,h} Z_x}{Z_x + Z_y}$$

The equivalent Norton impedances were calculated for different points in the grid to observe the frequency dependence, the calculation was done along a range of frequencies of interest. The equivalent impedance calculated were the following:

- The transformer in series with the MV grid.
- The LV network excluding the feeder with the HPS Lamps.
- The complete network from the POC of the lamps.

Figure 49, shows the part of the LV network used to calculate equivalent impedances. The results can be seen in Figure 50, Figure 51 and Figure 52.

With these results it can be concluded that the damping of the harmonics from the source till the measuring point, not only depends on the location, but in the actual load of each household, giving a high level of unpredictability in the distortion of harmonics. Nevertheless, as it can be seen in Table 3, the damping of the harmonics does not surpass the 10% except for the 9th harmonic, whose magnitude is small compared to the lower harmonics. This 10% is smaller than the actual variations produced by the aggregated data as a consequence of having other parallel nonsinusoidal loads.

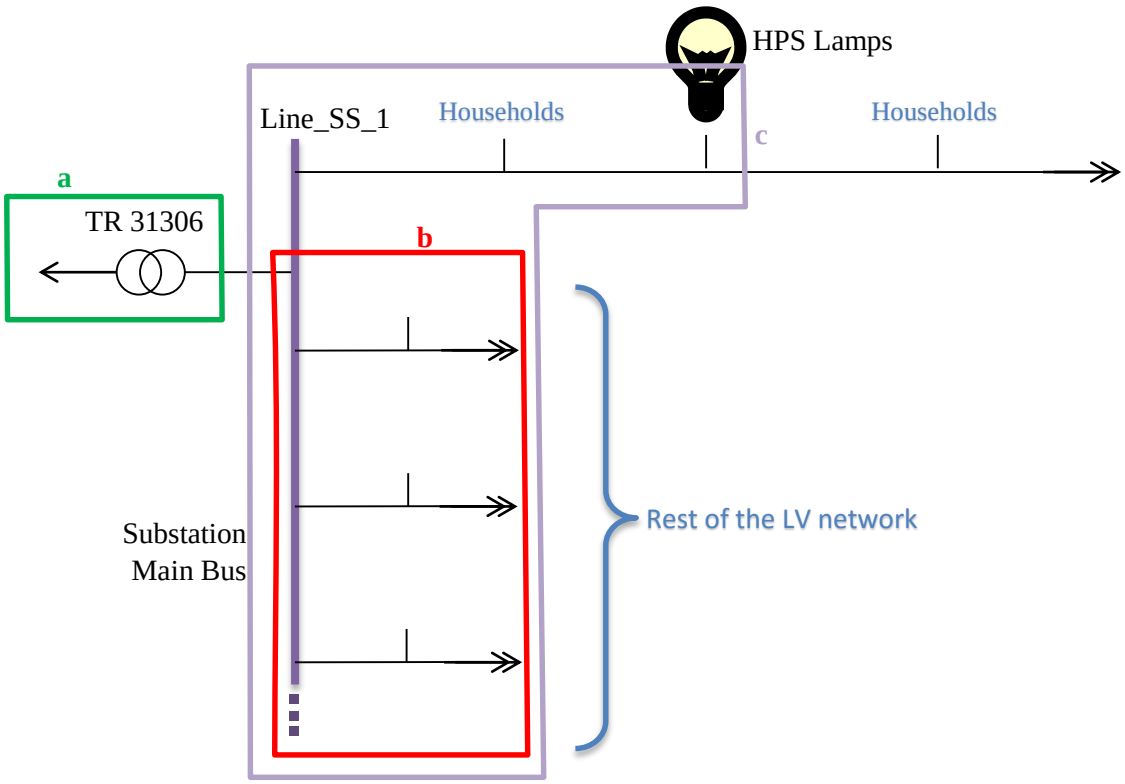

Figure 49. Impedances calculated. a) Transformer in series with the MV grid. b) LV network excluding the feeder with the HPS lamps. c) LV network from the POC of the lamps.

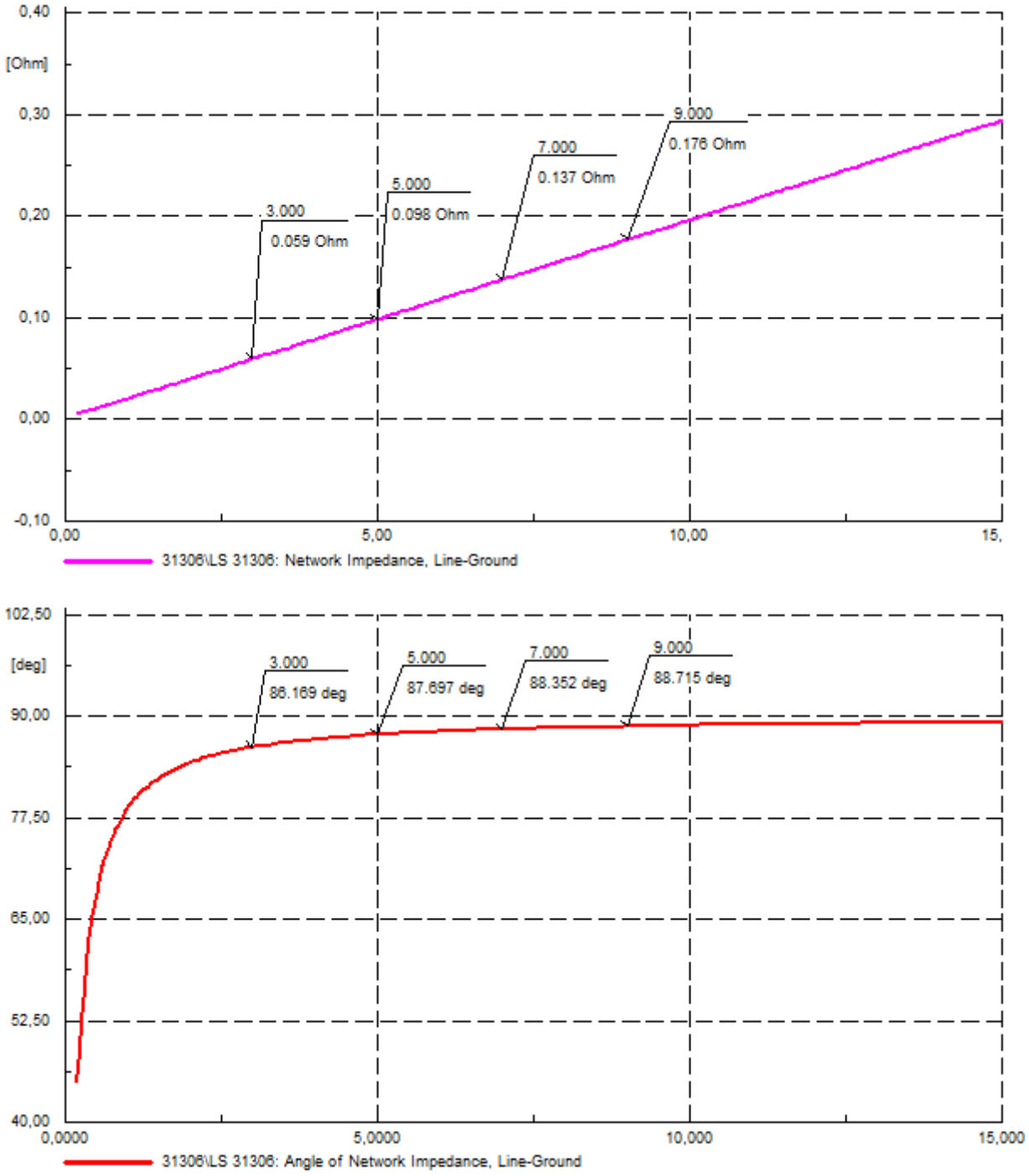

Figure 50. Transformer and MV grid equivalent impedance for different harmonics.

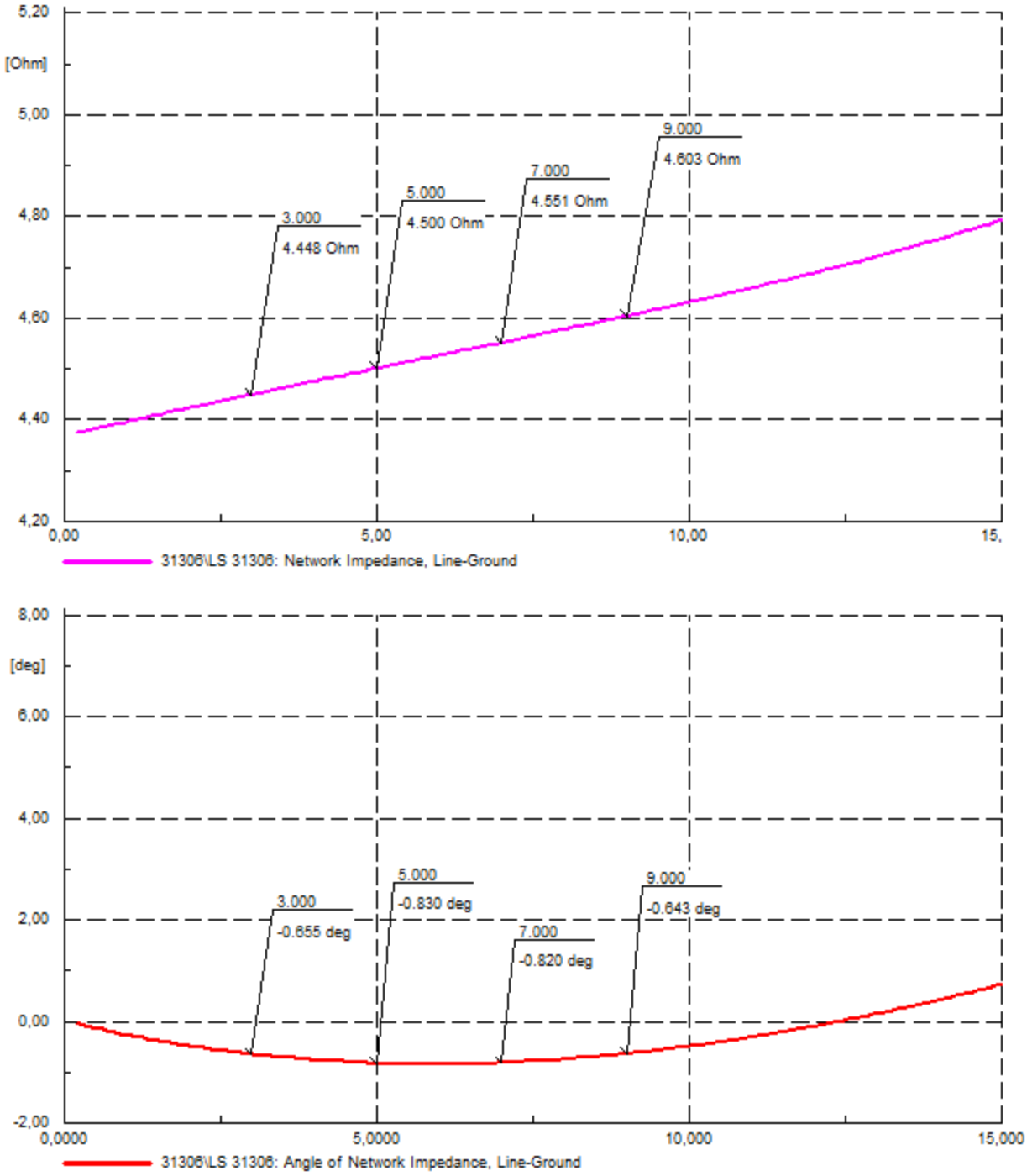

Figure 51. Lamps' feeder equivalent impedance for different harmonics.

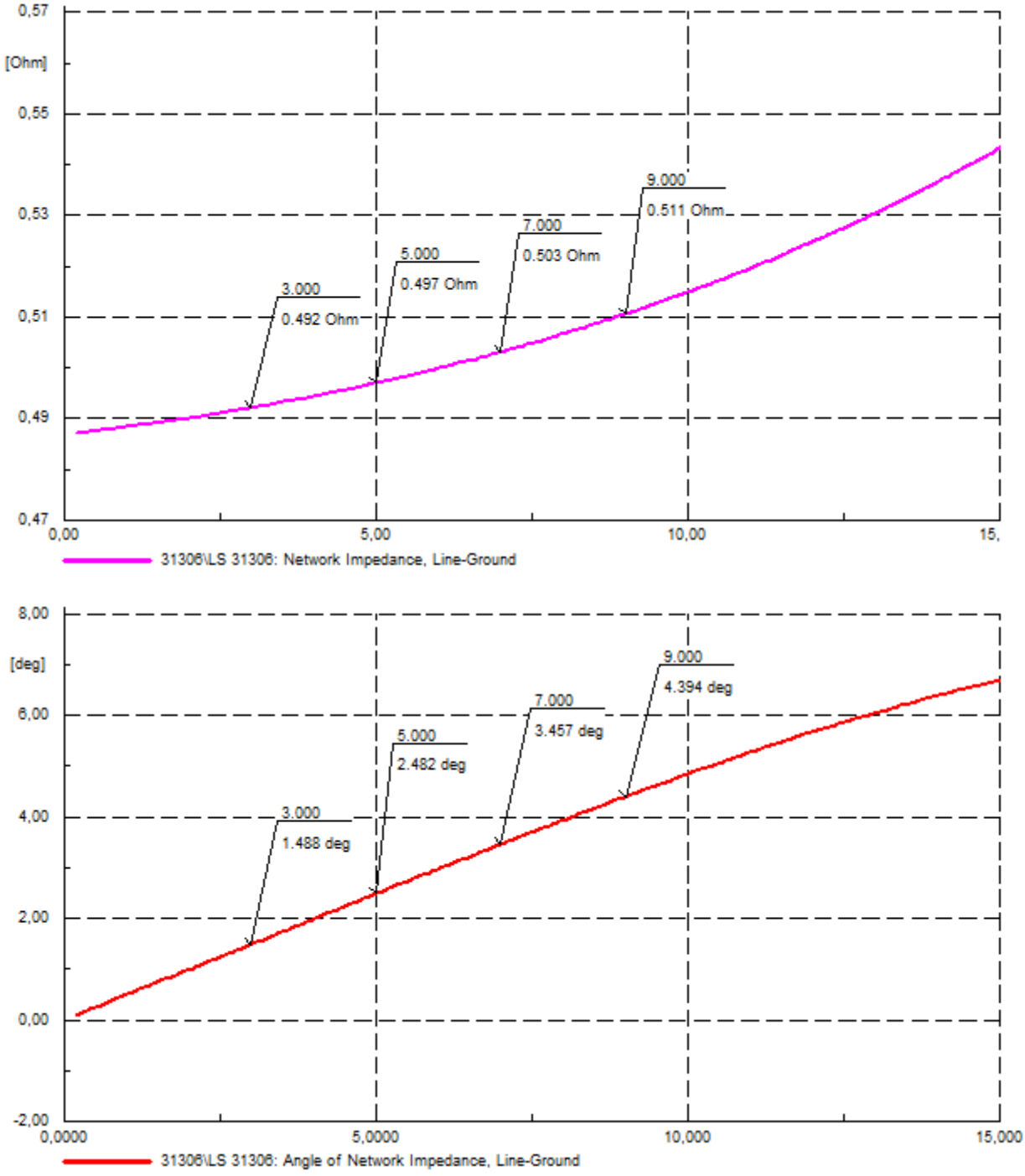

Figure 52. LV grid except Lamps' feeder equivalent impedance for different harmonics.

Chapter 6

6. Field Testing

The previous section gave an insight of how the harmonics would flow through the network. Afterwards, field tests were conducted in order to see how the harmonics of the HPS lamps interact with the rest of the loads in the LV grid selected. The results would be used to discuss how the electric characteristics of the HPS lamps can be observed in the aggregated data measured at a central point which in this case is the MV/LV Substation.

For the test, a low voltage grid with a high implementation of smart meters was selected. The low voltage grid is fed by a 15/0.4 kV, 400 kVA transformer. The transformer feeds a main LV bus in the substation which has 7 derived circuits. This LV grid have a smart meter at the transformer as well as in several households. 9 HPS lamps were connected in one of the 7 derived circuits. The lamps were split in the following way: 3 lamps in phase L1, 2 lamps in phase L2 and 4 lamps in phase L3. For the test, a combination of two the HPS lamp models were used for the field testing:

- 600 Watts Phillips Son-T lamp, 600 Watts Phillips ballast with three capacitors in parallel with a total of 65µF ±10%.
- 600 Watts Phillips Son-T lamp, 600 Watts Mari-1/A HQ300 NG 600 ZT with a 60µF ±10% capacitor.

The duty cycle of the HPS lamps is 14 hours Off and 10 hours On. The schedule is the following:

Interval	**State**
00:00 am to 08:29 am	Off
08:30 am to 06:29 pm	On
06:30 pm to 11:59 pm	Off

To avoid repetition, only phase L3 results are shown in this chapter. From Figure 54 to Figure 58, the measured values for a duty cycle of the HPS lamps at the POC to the network are presented. These values are compared with the measured aggregated data at different point of the LV substation, in order to observe if the electric characteristics of the lamps are still visible in the aggregated data.

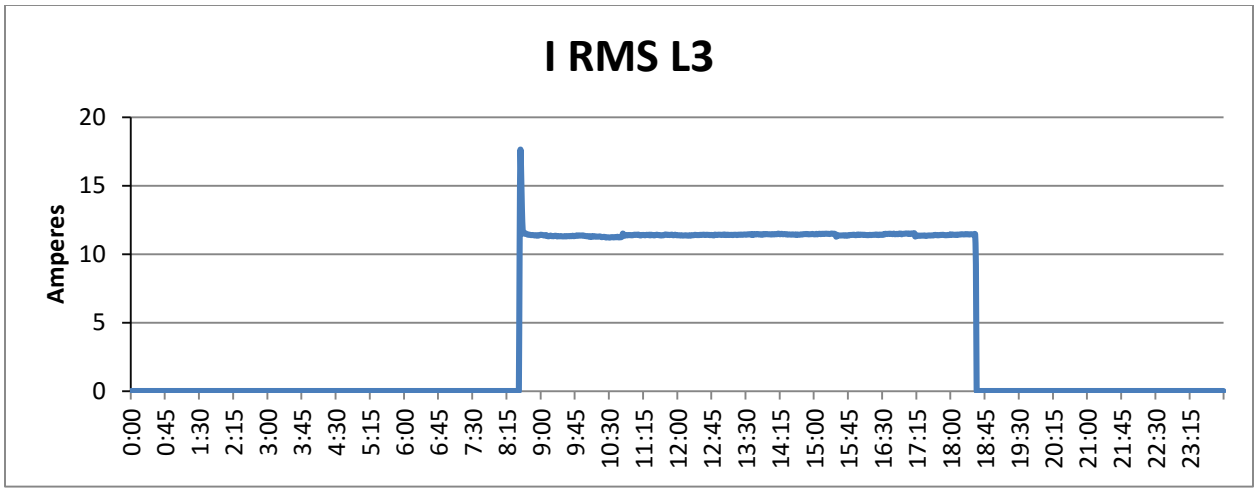

Figure 53. I in Amperes RMS for 4 HPS lamps in L3.

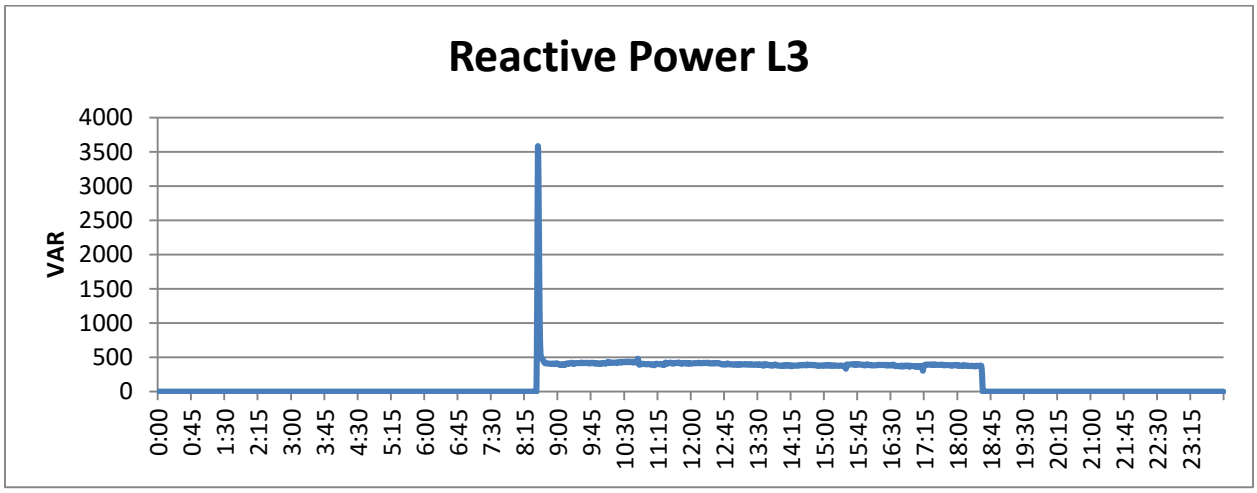

Figure 54. Reactive Power in VAR for 4 HPS lamps in L3.

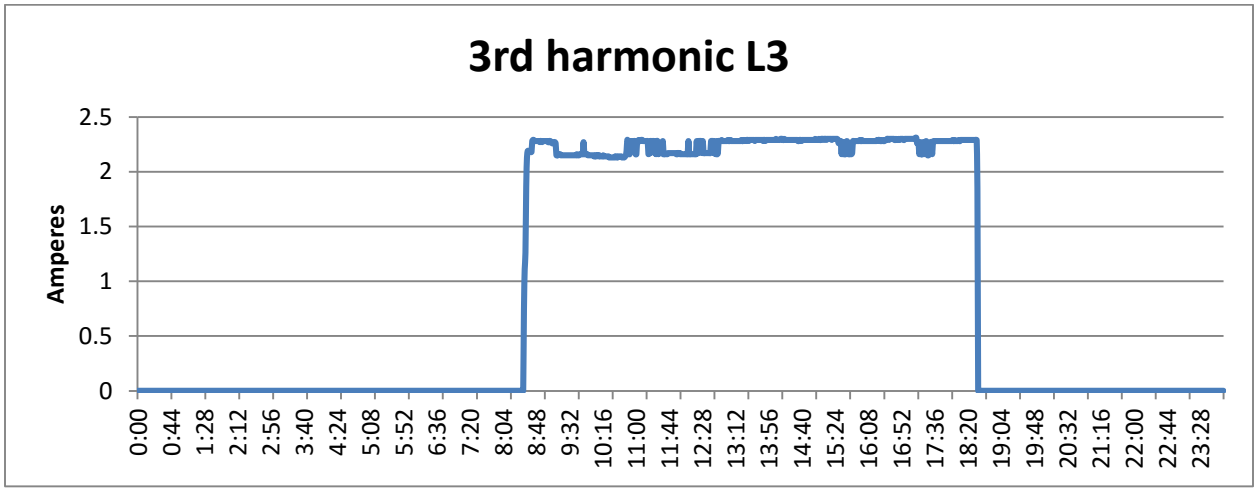

Figure 55. 3rd harmonic RMS in Amperes for 4 HPS lamps in L3.

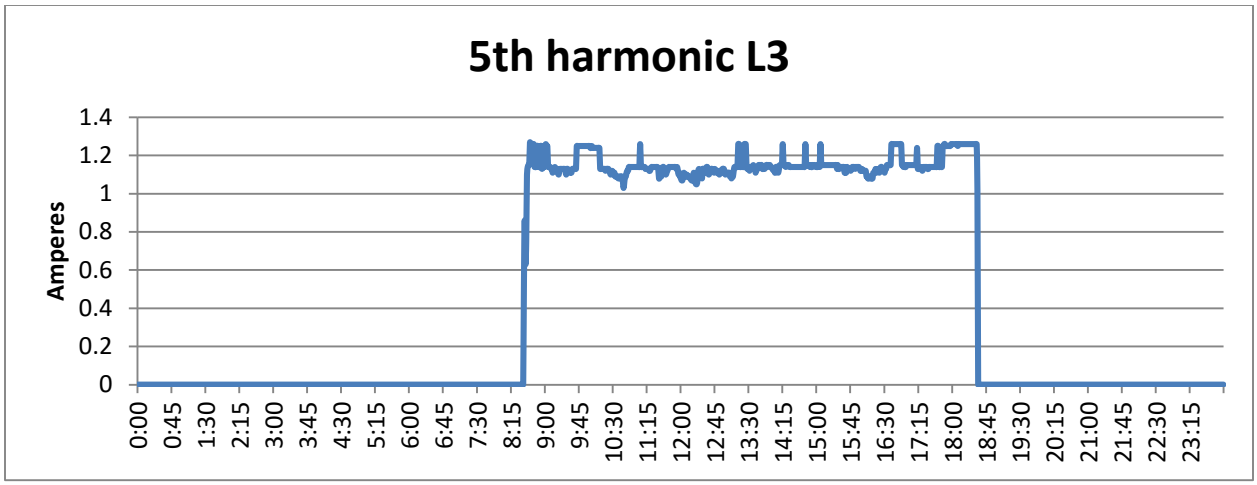

Figure 56. 5th harmonic RMS in Amperes for 4 HPS lamps in L3.

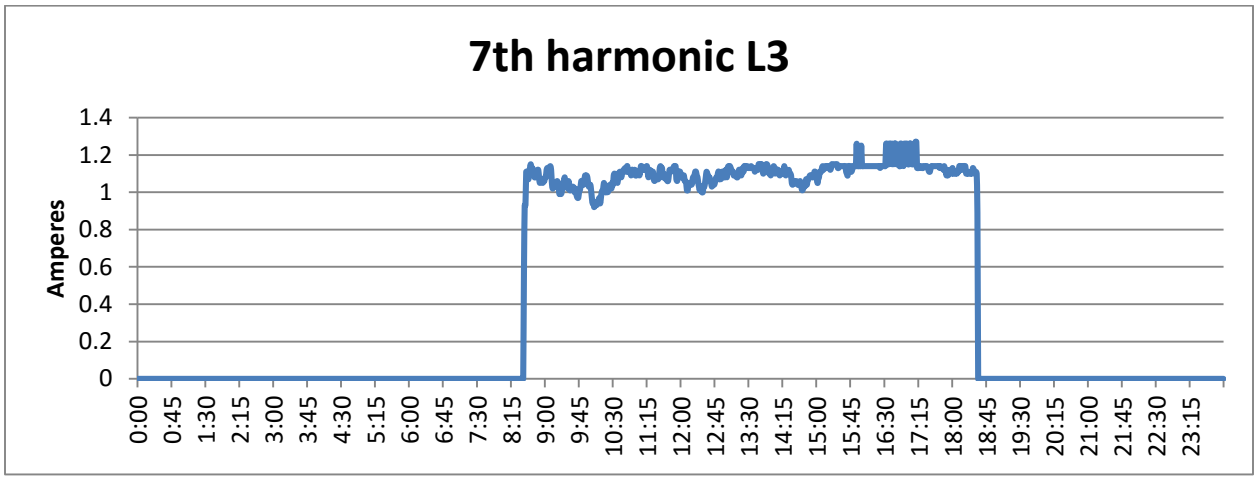

Figure 57. 7th harmonic RMS in Amperes for 4 HPS lamps in L3.

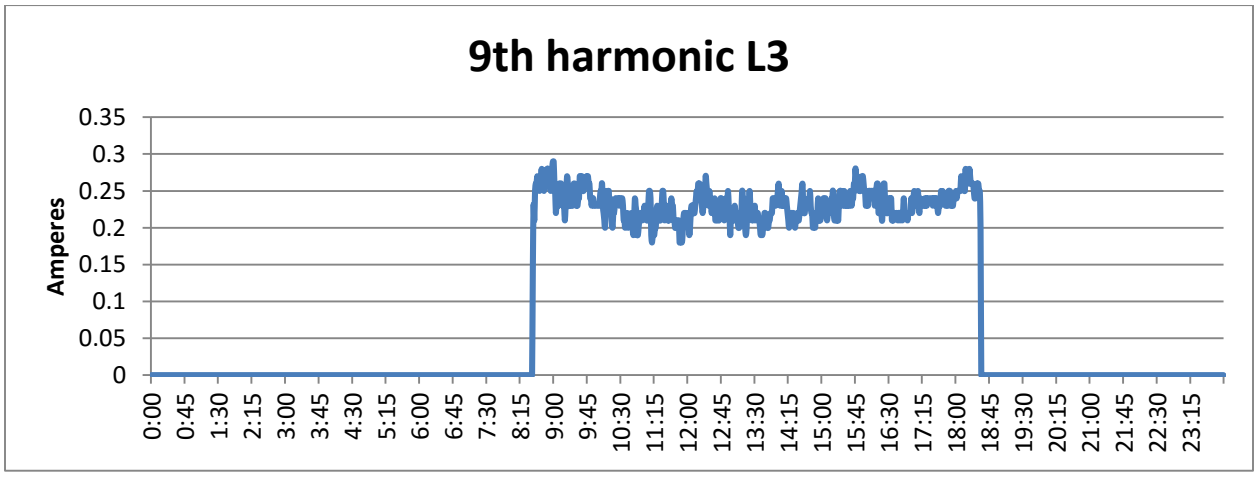

Figure 58. 9th harmonic RMS in Amperes for 4 HPS lamps in L3.

The most important periods of time during the duty cycle of the HPS lamps for the detection is the change of state, or in other words the switching On/Off periods. As it was stated in chapter 2 "Laboratory measurements of the lamps" and as it can be observed in Figure 9, Figure 17, Figure 25 and Figure 54, at the warming stage of the HPS lamps (few minutes after being switched on), the lamps have a very low PF which reflects as spikes in VAR versus time plots. Additionally, it is shown that the harmonics magnitudes increase during the warming stage of the HPS lamps until reaching steady state and disappear at the moment of switching Off (due to the fact that the lamp does not draw current at Off state). The repeatability in the timing of the events for each day is also of great value as the lamps should switch On/Off at the same time every day, in other words the sudden change of harmonics and reactive power at the same time of the day for every day means the existence of a periodic load, in this case the HPS lamps. All these characteristics can be used for the disaggregation of the HPS lamps measurements when connected a LV grid with several parallel loads.

In order to see a comparison between using smart meter measurements and the use of more expensive equipment for PQ measurements, the testing consisted in two stages:

- Using PQ measuring devices for the detection.
- Using the smart meter at the transformer for the detection.

PQ Meter test

PQ meters were installed at the substation. By using the reactive power readings in conjunction with the harmonic values, it gives more electrical characteristics to identify the lamps in the aggregated measurements at the substation.

The PQ meters used were Fluke 1745 Three-phase Power Quality Logger. This PQ meters were connected simultaneously, one at the LV side of the transformer and the others at each feeder of the LV circuits, including the one that feeds the HPS lamps, which for simplicity is called "C1". This was done to observe the influence of the parallel loads to the measured aggregated data at the transformer level and at the circuit level. The PQ meters were programmed to save the data in averages of 1 minute.

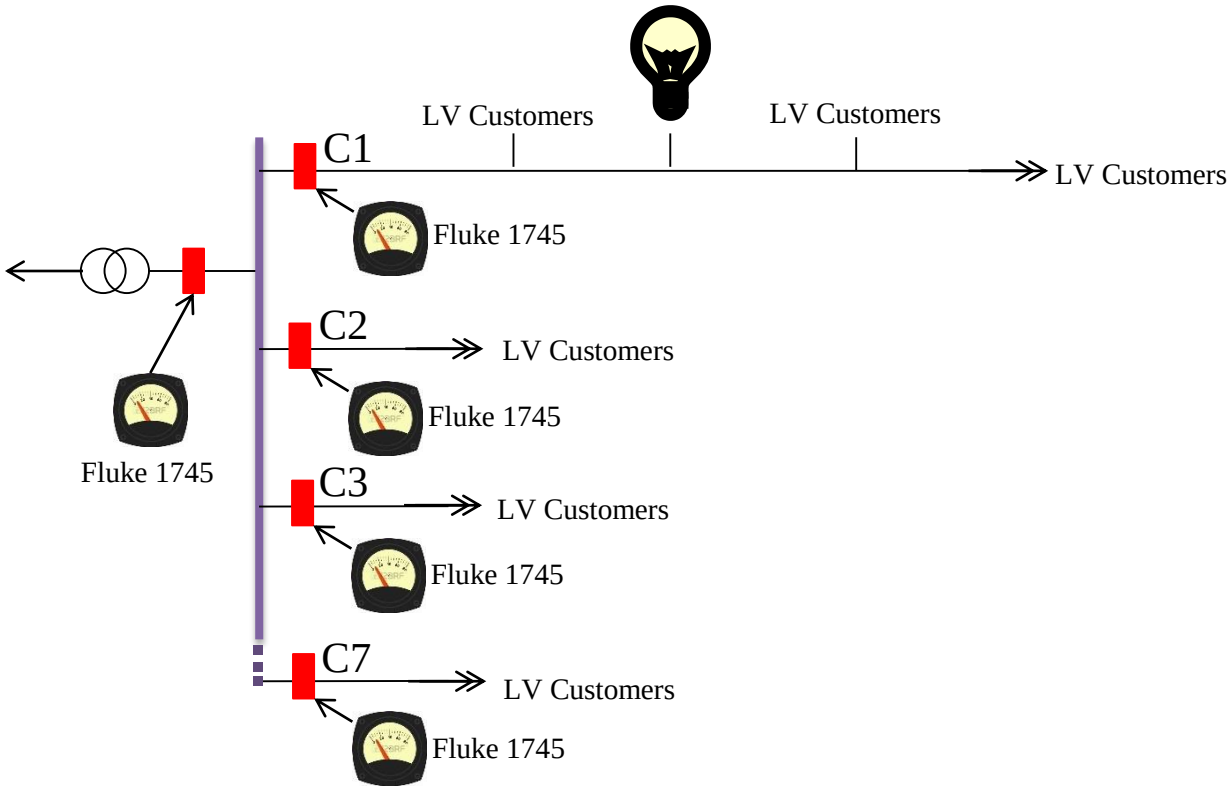

Figure 59. Location of the PQ meter.

The PQ meters collected data for a period of 1 week with the lamps working in the duty cycle of 10 hours On and 14 hours Off, as previously mentioned. Afterwards the data was downloaded and processed.

PQ measurements at C1

Figure 60 to Figure 64 shows the measurements from the C1 circuit, where the characteristics of the HPS lamps are clearly observable. Figure 60 illustrates the flow of reactive power to the circuit. The lamps were switched on between 8:06 and 8:07. As mentioned before, one of the electrical characteristics of the HPS lamp is their low power factor during the first minutes till the lamp reaches certain temperature. This is represented as a reactive power spike in a VAR vs time plot. As the lamps have a high power factor at steady state, the “switching Off” timing cannot be distinguished from the reactive power graphs. Figure 56 represents the same graph as Figure 60, with a zoom at the “switching On” instant were the timing of the VAR spike can be better appreciated.

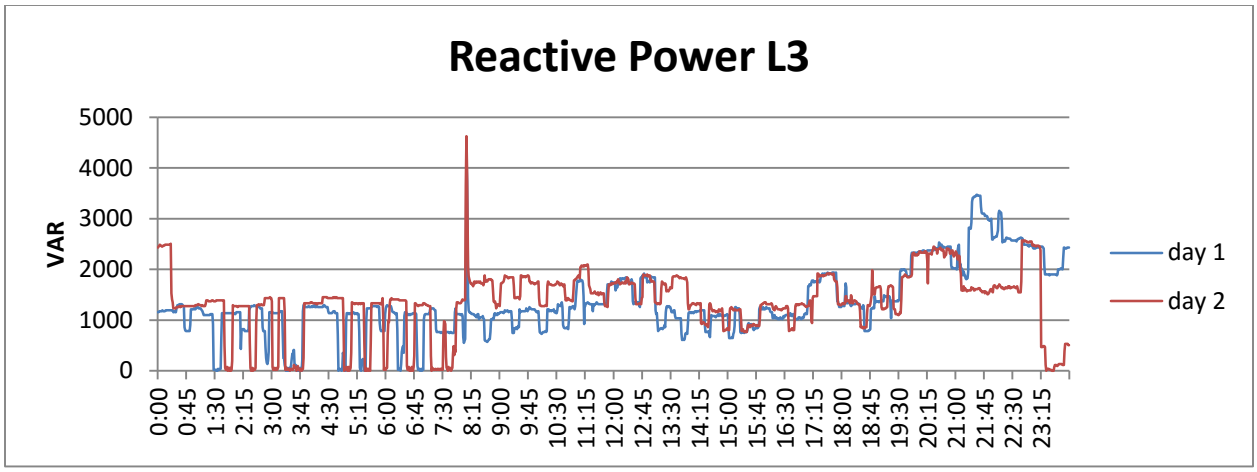

Figure 60. Reactive Power in VAR measured at the feeder C1 for phase L3.

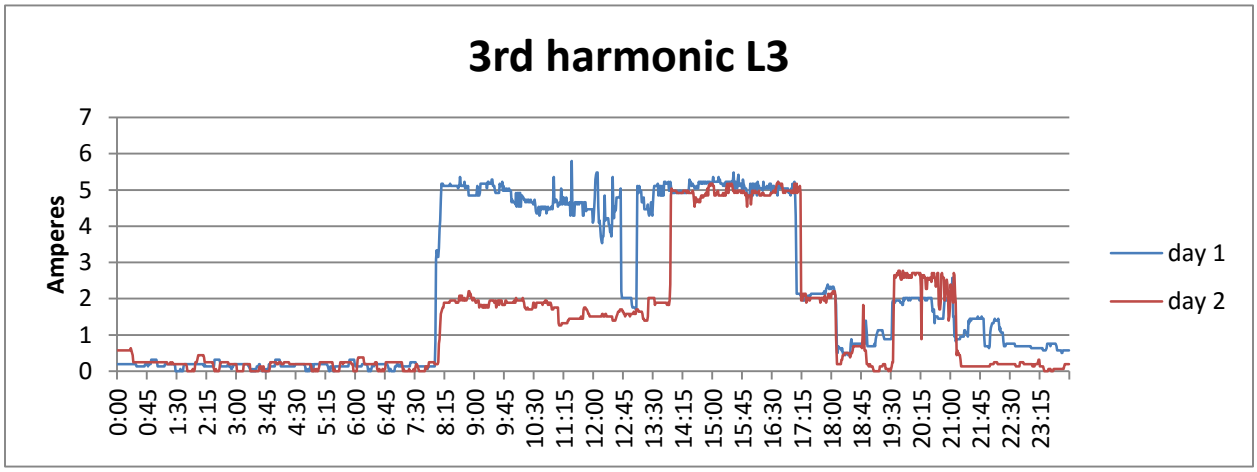

Figure 61. 3rd harmonic RMS in Amperes measured at the feeder C1 for phase L3.

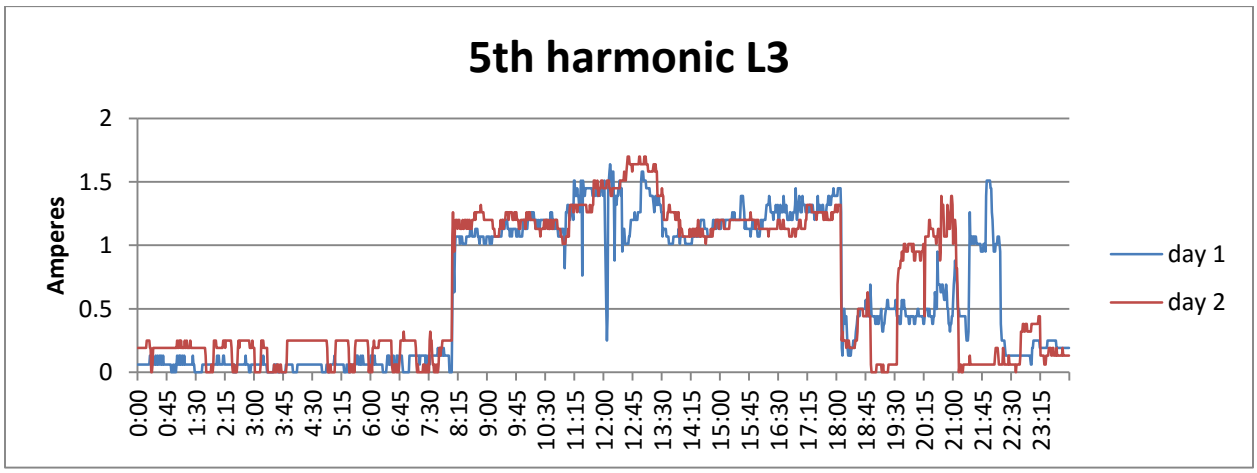

Figure 62. 5th harmonic RMS in Amperes measured at the feeder C1 for phase L3.

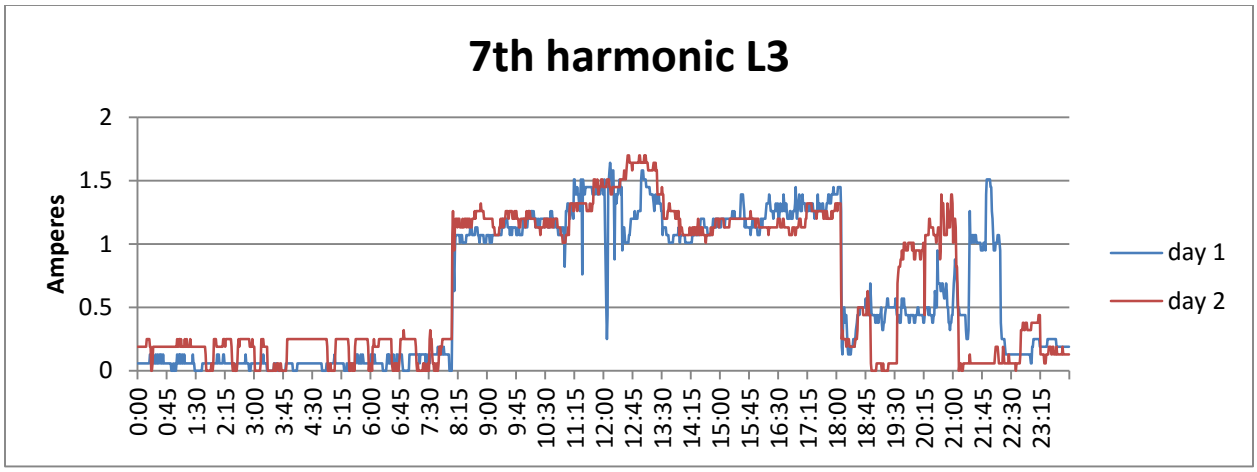

Figure 63. 7th harmonic RMS in Amperes measured at the feeder C1 for phase L3.

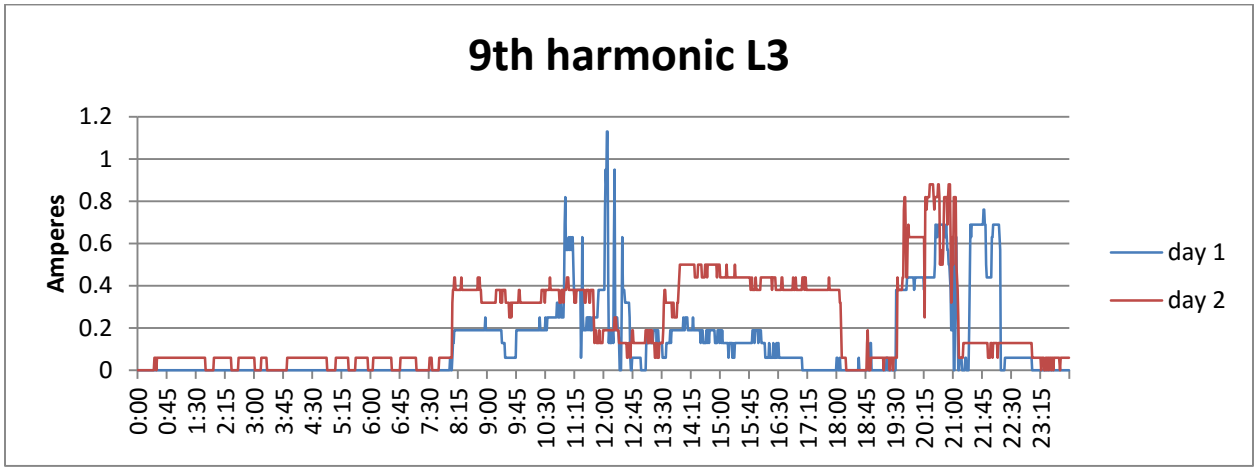

Figure 64. 9th harmonic RMS in Amperes measured at the feeder C1 for phase L3.

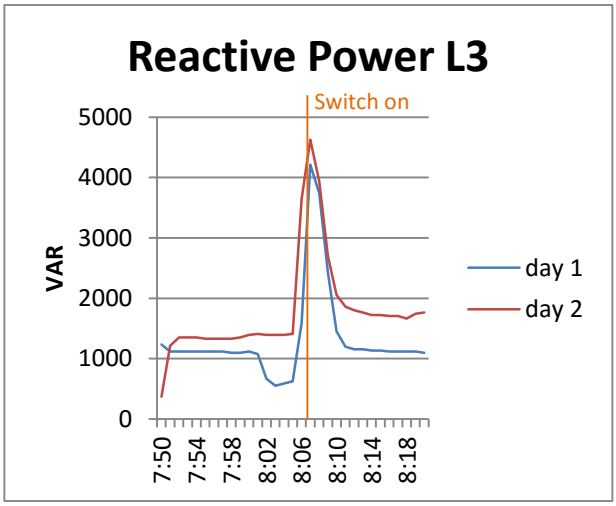

Figure 65. VAR measured at C1 for phase L3 (zoom at the moment the lamps are switched on). Using PQ meter data

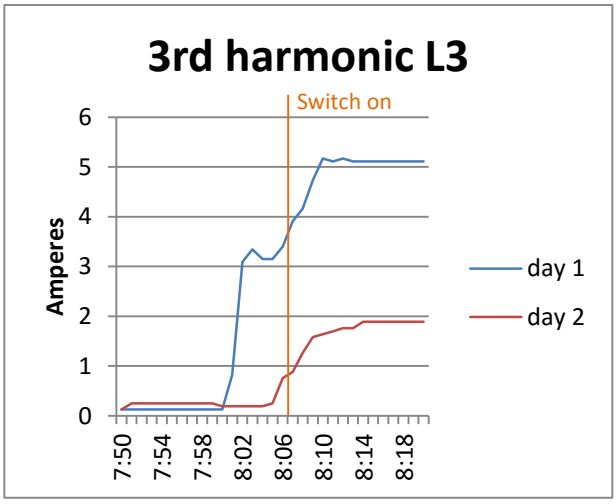

Figure 66. 3rd harmonic RMS in Amperes at C1 for phase L3 (zoom at the moment the lamps are switched on). Using PQ meted data

From Figure 61 to Figure 64 we can observe the odd harmonics from 3rd to 9th in the C1 circuit. As mentioned in Chapter 3 “Laboratory measurements of the HPS lamps” and from Figure 66, we can observe that the harmonics does not have an abrupt change such as the VAR, but rather a progressive increase. This behavior does not produce the spikes as the reactive power when plotted vs time. However, with the almost steady value during the whole working time of the lamps (Figure 60 to Figure 64), it is capable of giving insight in the duration of the duty cycle (the time the HPS lamps are on). At the moment of “switching Off”, the lamp harmonics does disappear in an abrupt form.

The characteristics of the HPS lamps are clearly observable. In Figure 60, it can be seen the flow of reactive power to the circuit. The lamps were switched on between 8:06 and 8:07. As mentioned before, one of the electric characteristics of the HPS lamp is their low power factor during the first minutes until the lamp reaches certain temperature. This is represented as a reactive power spike in a VAR vs time plot. As the lamps have a very high power factor at steady state, the “switching Off” timing cannot be distinguished from the reactive power

PQ measurements at the LV side of the transformer

These were performed in order to observe and discuss if the electrical characteristics of the lamps can be recognized from the aggregated data of the loads in the 7 circuits that are fed by the transformer.

From Figure 67 to Figure 71, the data from 2 different days is presented. The electrical characteristics from the HPS lamps (which were still recognizable at the PQ measurements in C1) cannot be seen at first sight. The parallel loads of all the LV consumers connected to this transformer have significant harmonic currents and reactive power which add to the ones flowing to the lamps. In Figure 74 the reactive power flowing to the circuit C2 during 2 days is presented as an example. The negative values in this graph tell us that reactive power is coming from this circuit, or in other words it is consuming capacitive reactive power. This is of interest because having generation of VAR in another circuit means that not all the VAR consumed by the lamps go through the transformer, therefore through the PQ meter.

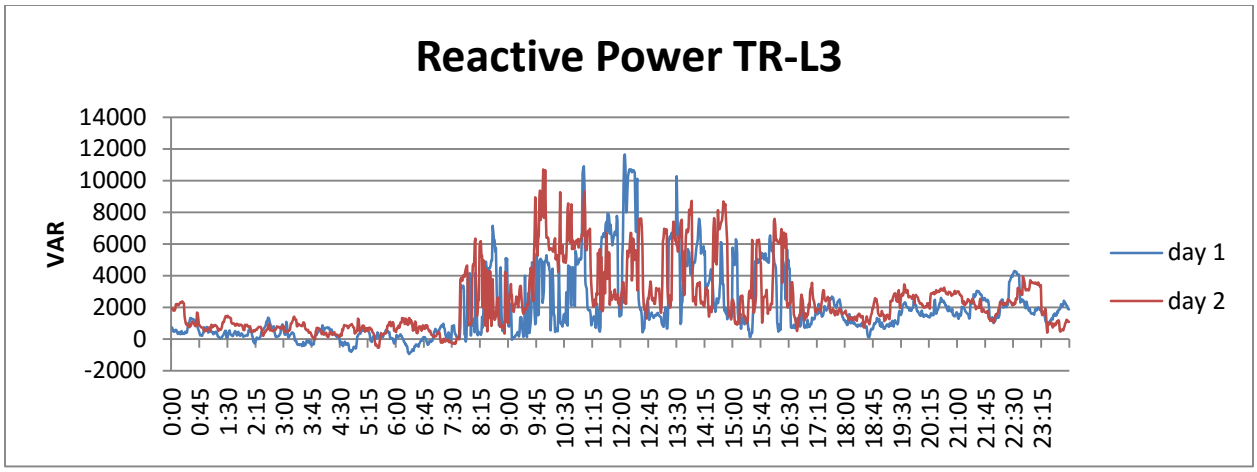

Figure 67. Reactive Power in VAR measured at the transformer for phase L3 (PQ meter data).

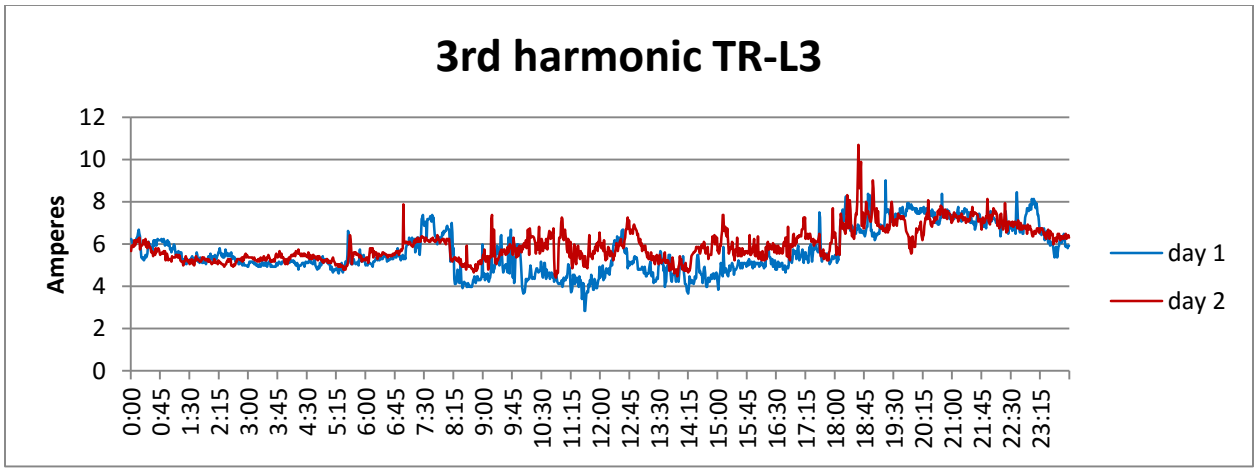

Figure 68. 3rd harmonic RMS in Amperes measured at the transformer for phase L3 (PQ meter data).

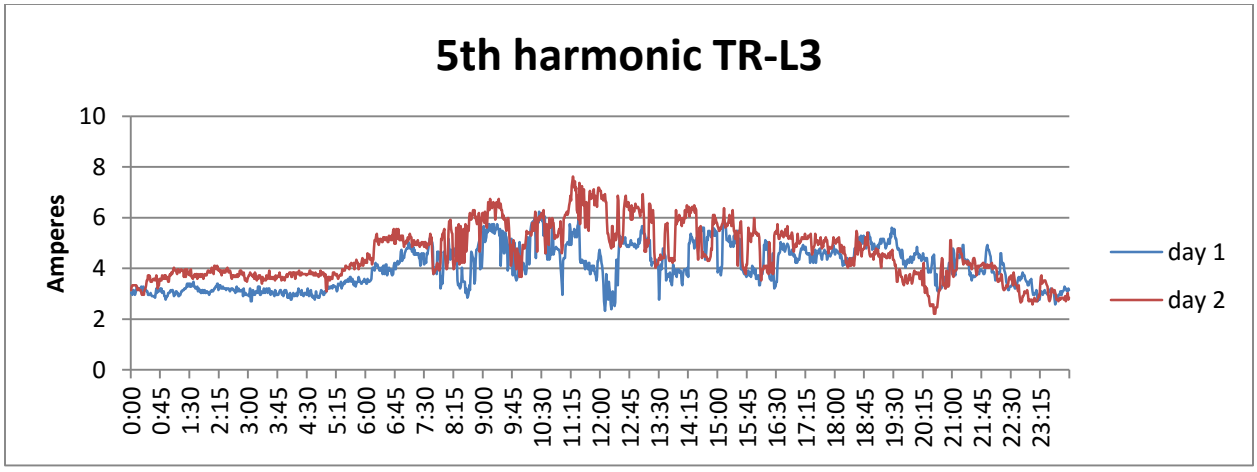

Figure 69. 5th harmonic RMS in Amperes measured at the transformer for phase L3 (PQ meter data).

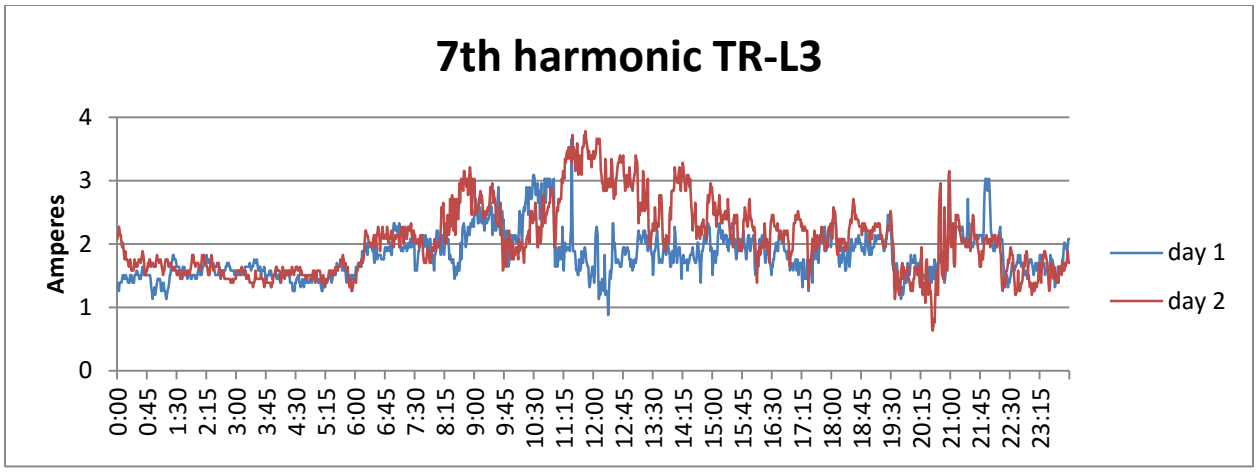

Figure 70. 7th harmonic RMS in Amperes measured at the transformer for phase L3 (PQ meter data).

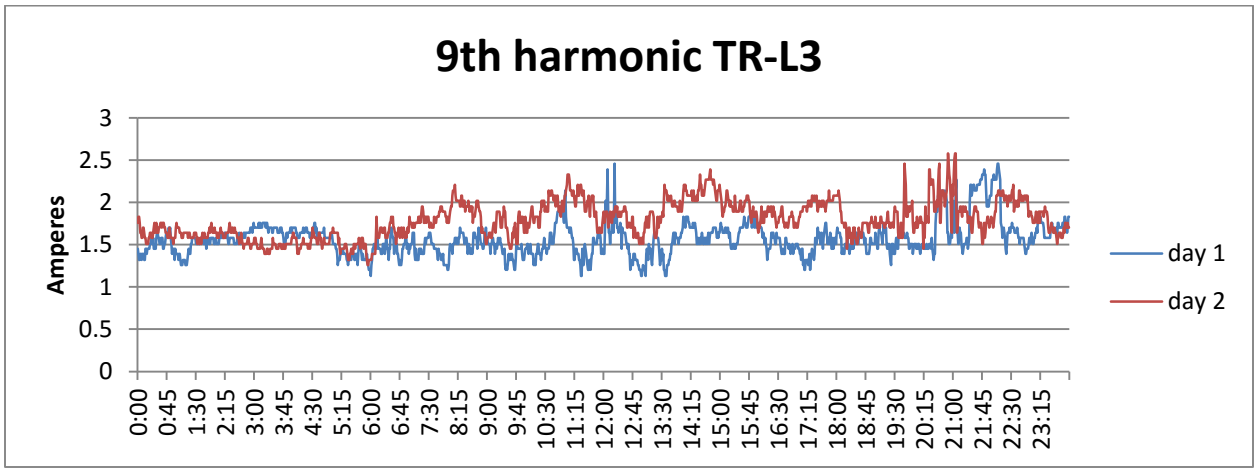

Figure 71. 9th harmonic RMS in Amperes measured at the transformer for phase L3 (PQ meter data).

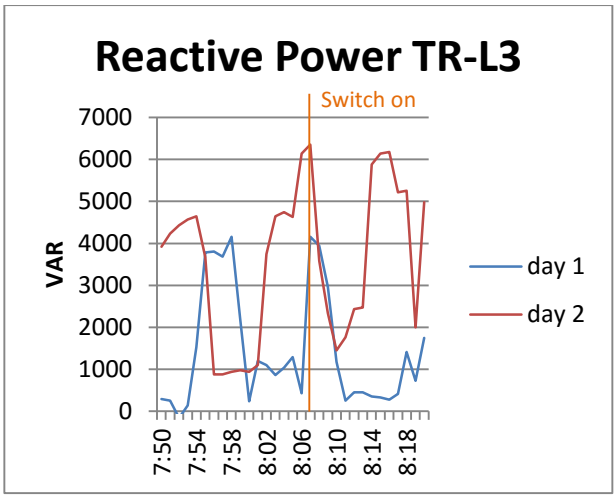

Figure 72. VAR measured at the transformer for phase L3 (zoom at the moment the lamps are switched on). Using PQ meter data

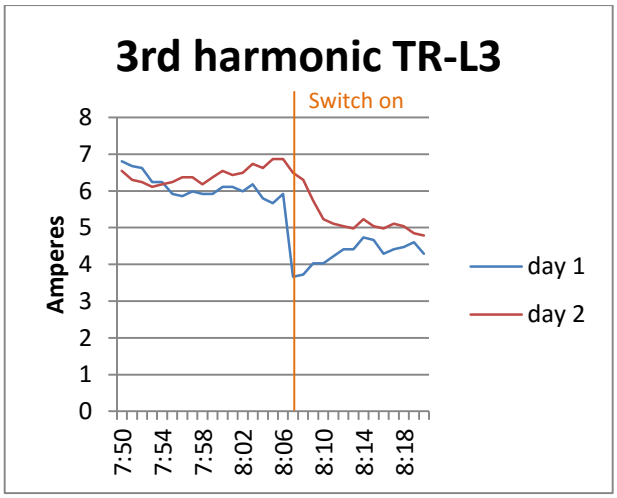

Figure 73. 3rd harmonic RMS in Amperes at C1 for phase L3 (zoom at the moment the lamps are switched on). Using PQ meter data

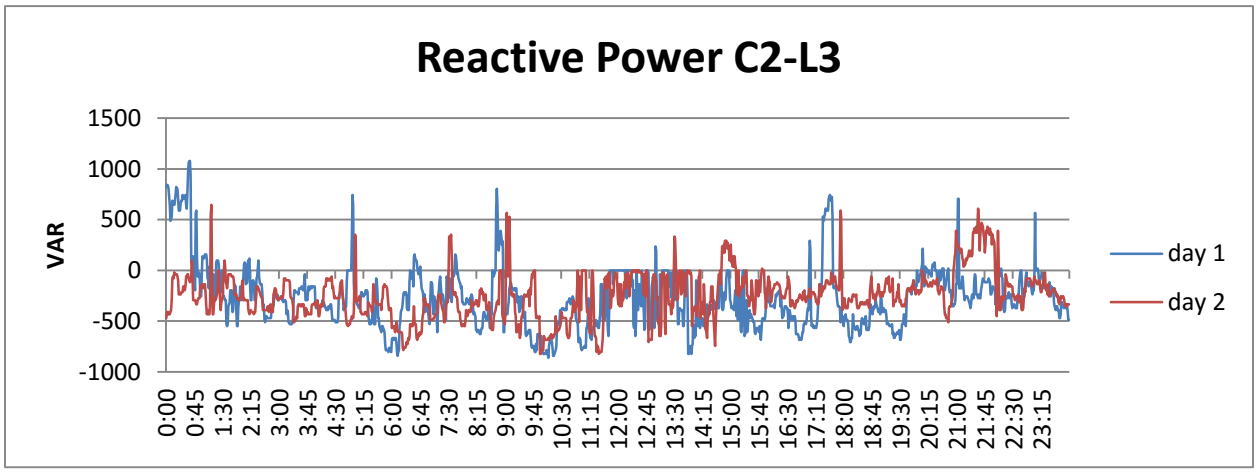

Figure 74. Reactive Power in VAR measured at the feeder C2 for phase L3 (PQ meter data).

Another remark can be slightly observed from Figure 68 to Figure 71. Some harmonics have a reduction of magnitude when the lamps are working even though the lamps produce current harmonics. This reduction can be more easily observed in Figure 73, which is because the harmonics are vectors and not scalars in the summation of the harmonics produced by all the LV loads. This means that the existence of lamps can be recognized not only with the increase of harmonics but with the reduction.

Enhancing the characteristics of the HPS lamps in the aggregated data

Taking into account that the HPS lamps of interest always work at a fixed duty cycle every day. The data of several days can be used to magnify certain events if they happen every day around the same time. There is a sudden increase of reactive power every time the lamps are turned on; this means a high dQ/dt.

We can use the dQ/dt to enhance the spike of the reactive power in the transformer measurements using the data of several days. In Figure 75, the summation of the rate of change of the reactive power for the 6 days of measurements is shown in the graph. The procedure to obtain the values are shown below:

For each day, the rate of change was calculated for every minute of the 24 hours using the reactive power measurements.

$$\left.\frac{dQ}{dt}\right|_t = \frac{Q(t) - Q(t-1)}{t - (t-1)}$$

$\left.\frac{dQ}{dt}\right\|_t$	The rate of change of the reactive power at a specific time of the day.
Q	Reactive Power
t	Time

Each rate of change at a specific time was added to its homologous of the other days.

$$y_Q(t) = \sum_{i=1}^{n} \left.\frac{dQ}{dt}\right|_{t_n}$$

$y_Q(t)$	Vertical axis of graph in Figure 75. Represents the summation of several days' reactive power rate of change at a specific time of the day.
n	Number of days (6 for this case)

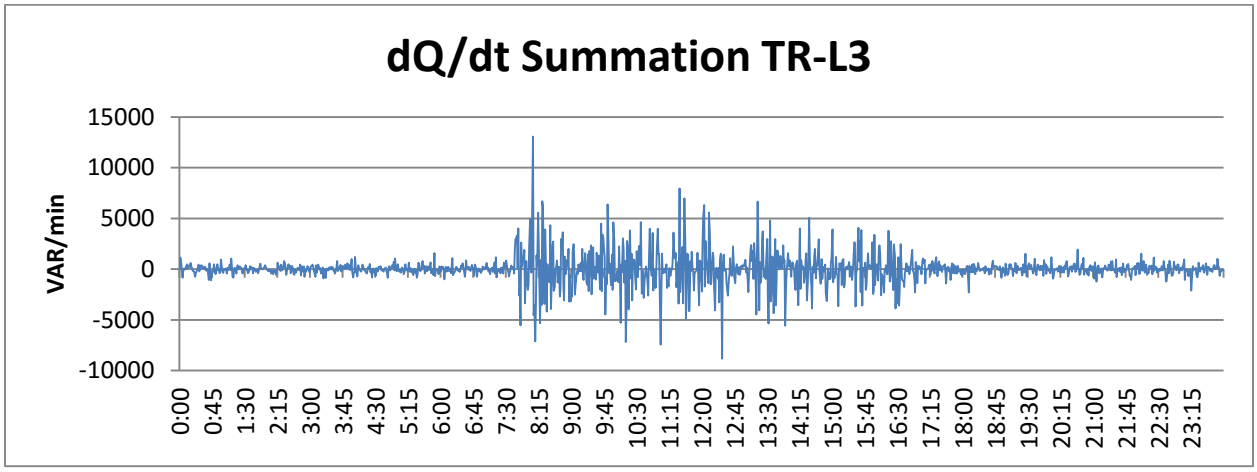

Figure 75. Summation of 6 days' dQ/dt in VAR/min, calculated for the transformer for phase L3 (PQ meter data).

As it can be observed in Figure 75 and Figure 67, in the first one, the switch on instant around 8:06 hours is far more noticeable with the spike. Using the reactive power rate of change summation of several days, enhance the repetitive events compared to the other more random parallel loads of the LV customers, which are also measured at the aggregated data. If more days were used, at the end the only spike visible would be the one at the switch on of the HPS lamps.

The same was done for the rate of change of the harmonics:

$$\left.\frac{dI_h}{dt}\right|_t = \frac{I_h(t) - I_h(t-1)}{t - (t-1)}$$

$$y_h(t) = \sum_{i=1}^{n} \left.\frac{dI_h}{dt}\right|_{t_n}$$

Where:

$\left.\frac{dI_h}{dt}\right\|_t$	The rate of change of the harmonic current at a specific time of the day.
I_h	Current of the h[th] harmonic.
h	Harmonic order.
$y_h(t)$	Summation of several days' h[th] harmonic current rate of change at a specific time of the day.

We can see the rate of change of the 3[rd] harmonic in the graph of Figure 76. As mentioned before in chapter 3 and in the PQ measurements at C1, the harmonics in the HPS lamp does not have a sudden increase at the switch on instant, but is rather periodic. This means that at the switch on instant, it will not be a spike as severe as in the reactive power. On the other hand, at the moment the HPS lamps turn off there is a sudden drop of the harmonics produced by the lamp. This is clearly appreciated in Figure 76 at the 18:06 hours, the time the HPS lamps switch off. The spike is positive because the sum of the third current harmonic vector of the HPS lamps are not in phase with the rest of the LV loads' third harmonic, reducing the total third harmonic in the transformer (in other cases it can be increased), meaning the time the lamps switch off the third harmonic increases.

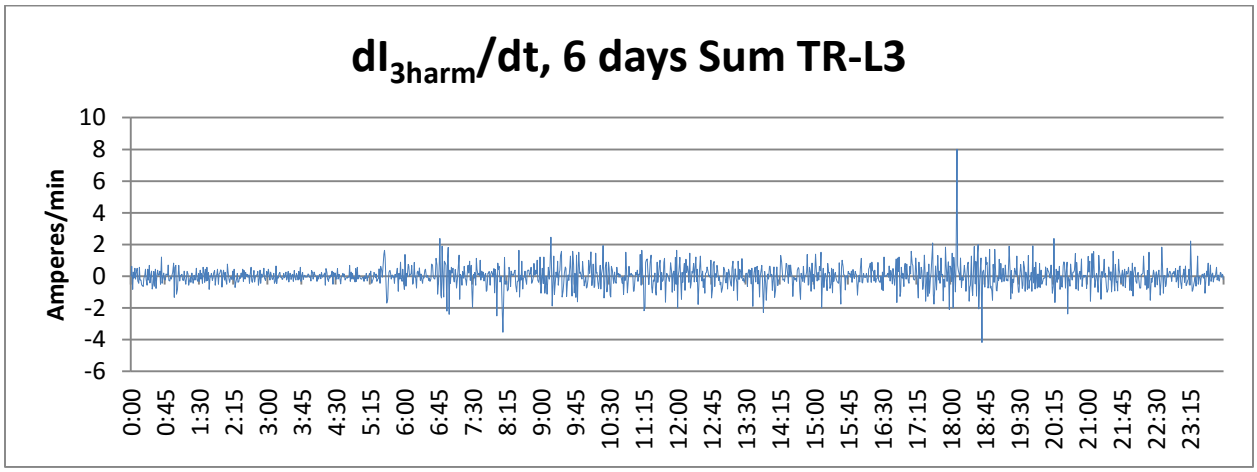

Figure 76. Summation of 6 days' dI_{3harm}/dt in Amperes/min, calculated for the transformer at phase L3 (PQ meter data).

The harmonic current summation for several days can also be used to identify the existence of the HPS lamps and their duty cycle. Following the formula:

$$y2_h(t) = \sum_{i=1}^{n} I_{h_n}$$

$y2_h(t)$ Summation of several days' h[th] harmonic current at a specific time of the day.

In Figure 77, it can observed that adding the harmonic current of several days makes more and more distinguishable the harmonic influence of the HPS lamps. Thus, the strength of disaggregation for the detection of the lamps relies in the use of several days of measurements and in the fixed cycles of the HPS lamps.

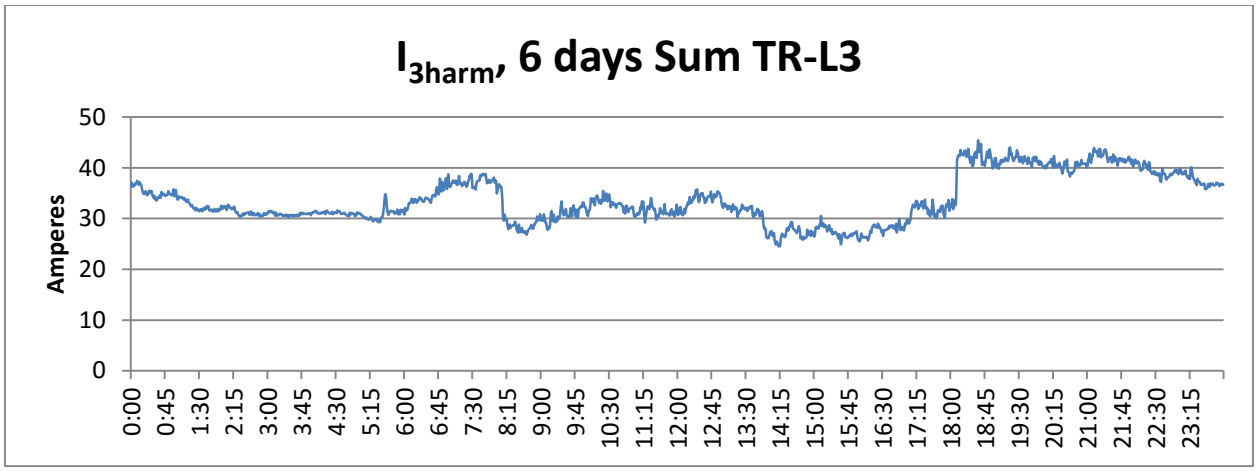

Figure 77. Summation of 6 days' I_{3harm} in Amperes, calculated for the transformer at phase L3 (PQ meter data).

Smart meter test

The reasons for testing the detection capability of the smart meter are the reduced price in comparison with a PQ equipment. Also there is already smart meters in several substations which is an advantage of the implementation compared to PQ meters.

The smart meter at the substation is a Landis+Gyr S650 Smart Grid Terminal. It is connected at the low voltage side of the transformer. This device is able to measure the current, voltage, active and

reactive power and saves the data in averages of 5 minutes. The smart meter collected data for several days with the lamps working in the duty cycle of 10 hours On and 14 hours Off as previously mentioned. Afterwards the data was downloaded and processed.

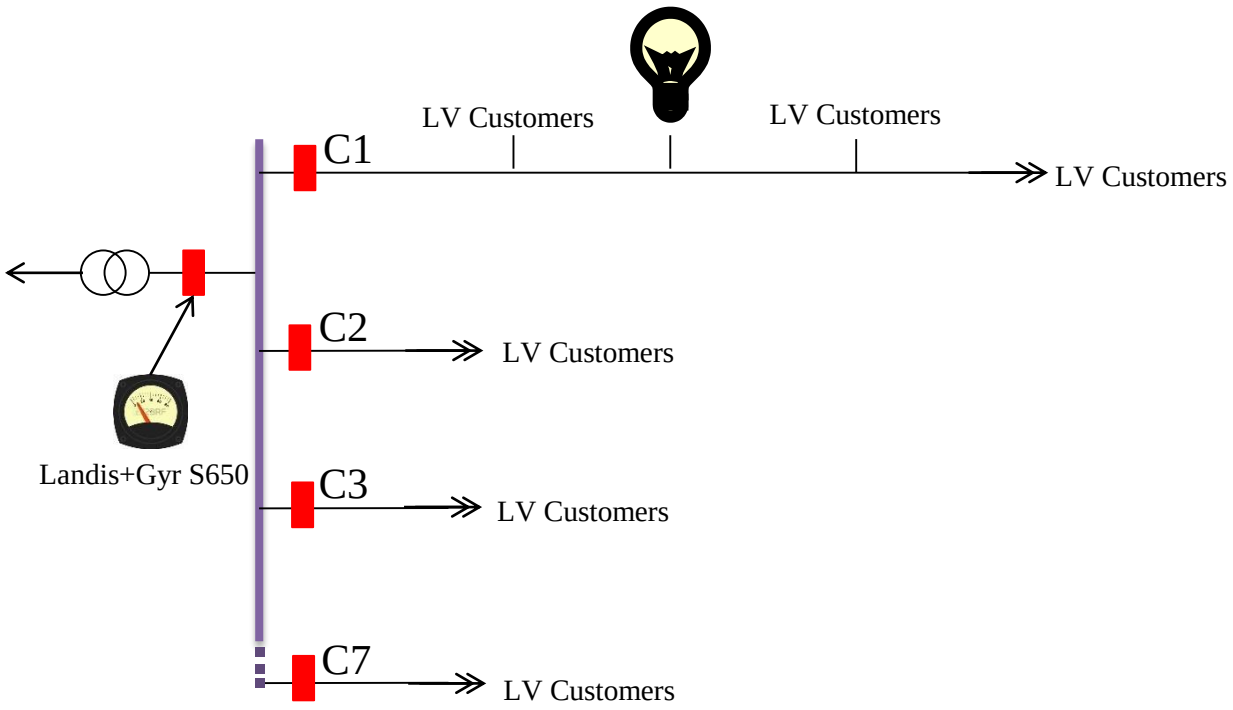

Figure 78. Location of the smart meter.

In Figure 79, the VAR measured at phase L3 by the smart meter are shown. Only 2 different days are plotted to make the graphs less saturate and clearer. From the figures we can observe that the sudden rise of VAR at the switch on instant of the HPS lamps (which were visible as spikes in Figure 54) are no longer visible. The parallel loads of all the LV consumers connected to this transformer have significant reactive power that the reactive power of the lamps is not visible at first sight. To enhance the visibility of the VAR flowing to the lamps, it was applied the same technique as in the PQ meter at the transformer. The difference is that in this case the time steps are taken every five minutes:

$$\left.\frac{dQ}{dt}\right|_t = \frac{Q(t) - Q(t-5)}{t-(t-5)}$$

$$y_Q(t) = \sum_{i=1}^{n} \left.\frac{dQ}{dt}\right|_{t_n}$$

The graph with the values of y_Q for the smart meter are at Figure 80.

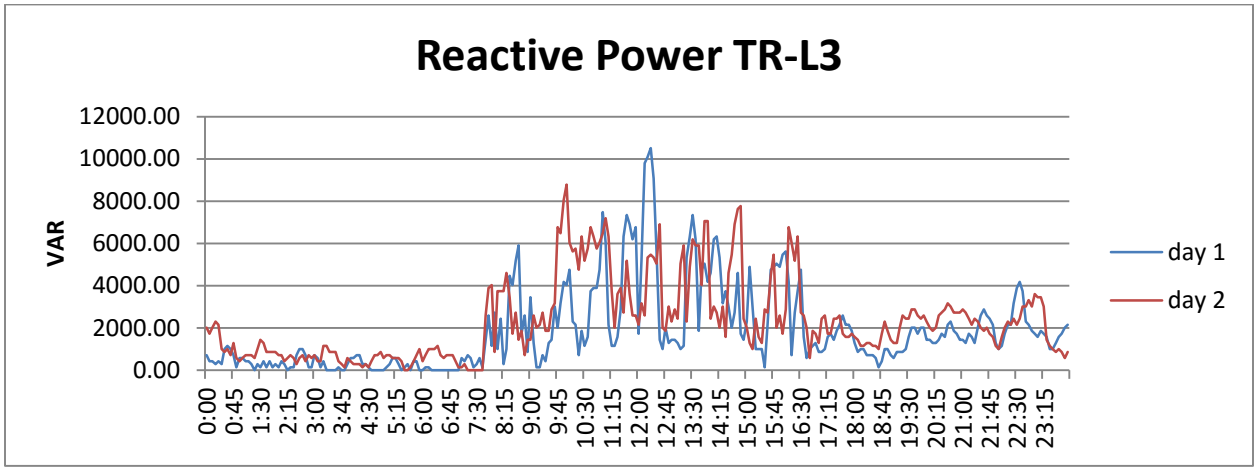

Figure 79. Reactive Power in VAR measured at the substation in L3 (smart meter data).

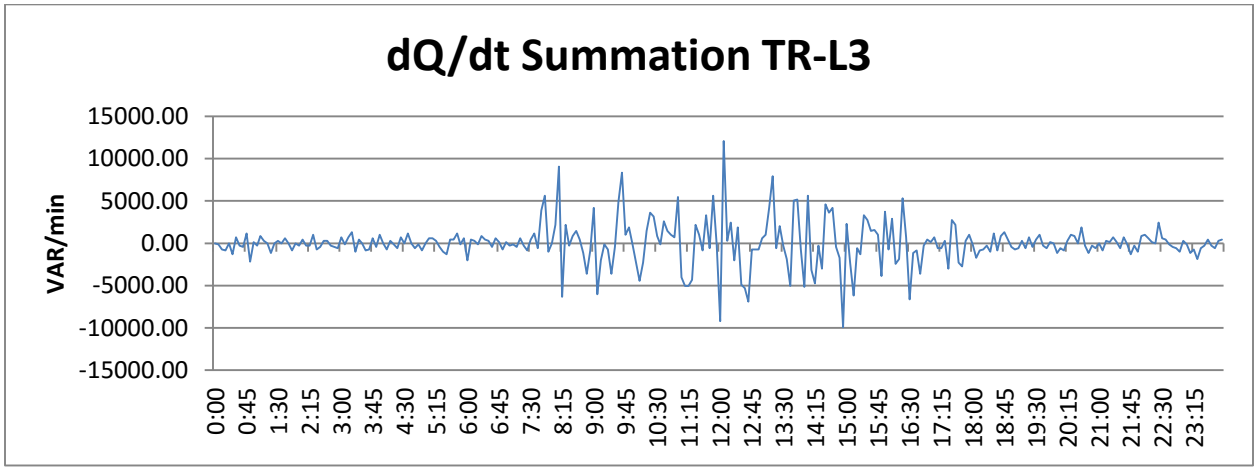

Figure 80. Summation of 6 days' dQ/dt in VAR/min, calculated for the transformer for phase L3 (smart meter data)

As it can be observed in Figure 80, the switching on instant of the HPS lamps at 8:06 using the mart meter data is not as distinguishable as using the data extracted from the PQ meter (Figure 75). The reason for this, is that the smart meter is programmed to save the data of VAR in averages of 5 minutes period in contrast with the 1 minute period used at the smart meter. Having a higher period reduces the amount of data that the meter have to process and save in the memory, but increases the number of events occurring during that lapse of time. This reduces the possibility of detecting individual loads.

Chapter 7

7. Discussion and Conclusions

The goal of this research was to analyze the possibility of detecting the existence of HPS lamps with electromagnetic ballast by means of power quality measurements. The electrical characteristics of the lamps that were taken into account were the reactive power, real power, harmonic currents and time behavior. In addition, the daily repetition of duty cycles when using this type of lamp were used to reinforce the detection.

In chapter 3, the electrical characteristics of several HPS lamps were measured. We were able to see their harmonic components, and the displacement power factor. One important characteristics is that these electrical values have a transition from the moment the lamps are switched on, until they reach steady state values. This knowledge can be used to detect the time instants in which the lamps are turned on and off at a centralized meter location, were the data is a combination of several loads.

In Chapter 4 calculations were made to predict how the combination of HPS lamps and households loads would be seen in a centralized meter located at the substation. The calculations were made using the lamps characteristics measured at the laboratory. As it can be observed from Figure 31 to Figure 44, the switching on/off of the lamps can be distinguished by the use of the spikes of the reactive power at the instant of switching on, as well as the changes in the harmonics. In these calculations, the HPS lamp's waveform were considered undistorted from the waveform measured at chapter 3. In chapter 5 we can see that the harmonics values does change across the LV grid before reaching the centralized measuring point. Nevertheless even though the simulated grid was considerable bigger than the average LV grids, the damping of the lower harmonics did not reached significant values.

In chapter 6, field tests were performed to prove the results of the calculations in chapter 4. By the comparison between the results of the smart meter and the PQ meter, we can see the importance in the time intervals in which the meter saves the data. In the 5 minutes interval, the spikes of reactive power at the instant the lamps switch on are remarkably less evident compared to the 1 minute interval. This is because having a longer time, and with the VAR spike being of short duration, the calculated average results in a lower spike magnitude. Other important reason is that by increasing the time interval,

increases the possibility of having other appliances switching on/off inside this time interval. This means that the smaller the time interval, the more resolution for identification. Still, these time interval cannot be reduced indefinitely because the amount of data becomes too big to handle.

Other important remark is the lack of PQ capabilities in the smart meter. The capacity for measuring harmonics is not possible in the nowadays standardized smart meters. As mentioned in chapter 6, the use of the harmonics for a higher discrimination in crowded networks is a necessity.

As can be seen in the results of chapter 6, the strength of data disaggregation at very loaded circuits relies in the use of several days of measurements and in the fixed cycles of the HPS lamps. By the use of this daily repetitive events, the electrical characteristics of the lamps can be enhanced in order to detect them.

One of the limitations of this work, is that the project focus on HPS lamps with electromagnetic ballast and not in the electronic ones. Other limitation is that the calculations and field tests were done for a specific LV network, using data from specific dates. This is of relevance because the user behavior may differ between different LV networks, as well as at different times of the year. Also every LV network topology is different. This influence the load composition for the aggregated data and might make the results change between different LV grids.

As a conclusion, and answering the research question proposed at the introduction, the HPS lamps can be detected by means of their specific electrical characteristics.

A proposition for future work is to explore different machine learning methods using as first steps the results from this work. By the actual extension of the grid, machine learning methods would save many man-hours of work by automatically detecting possible existence of this lamps in different point in the network. This is a futuristic view, aiming to a future with a whole or at least greatly spread of PQ meters in the network.

Bibliography

[1] Stedin, "http://www.stedin.net/," [Online]. Available: http://www.stedin.net/over-stedin/wat-doet-stedin. [Accessed September 2014].

[2] Siemens, "Harmonics in power systems. Causes, effects and control.," 2013.

[3] E. Csanyi, "Electrical Engineering Portal," 17 September 2012. [Online]. Available: http://electrical-engineering-portal.com/definition-of-harmonics-and-their-origin. [Accessed 2 February 2015].

[4] I. S. C57.110-1998, "IEEE Recommended Practice for Establishing Transformer Capability When Supplying Non-sinusoidal Load Currents," 1998.

[5] J. Das, Power System Harmonics and Passive Filter Designs, Wiley-IEEE Press, 2015.

[6] D. Said and K. Nor, "Effects of Harmonics on Distribution Transformers," in *Australasian Universities Power Engineering Conference (AUPEC'08)*, 2008.

[7] C. Sankaran, "Electrical Construction and Maintenance," 1 October 1999. [Online]. Available: http://ecmweb.com/power-quality/effects-harmonics-power-systems. [Accessed 30 July 2015].

[8] A. Zoha, A. Gluhak, M. A. Imran and S. Rajasegarar, "Non-Intrusive Load Monitoring Approaches for Disaggregated Energy Sensing: A Survey," *Sensors,* pp. 16838-16866, 2012.

[9] L. K. Norford and S. B. Leeb, "Non-intrusive electrical load monitoring in commercial buildings based on steady-state and transient load-detection algorithms," *Energy and Buildings,* pp. 51-64, 1996.

[10] K. L. R. C. S. S. S. L. L. N. a. a. p. A. C. Laughman, "Power Signature Analysis," *IEEE power & energy magazine,* pp. 56-63, 2003.

[11] L. Farinaccio and R. Zmeureanu, "Using a pattern recognition approach to disaggregate the total electricity consumption in a house into the major end-uses," *Energy and Buildings,* pp. 245-259, 1999.

[12] A. Cole and A. Albicki, "Nonintrusive Identification of Electrical Loads in a Three-phase Environment Based on Harmonic Content," in *Proceedings of the 17th IEEE Instrumentation and Measurement Technology Conference* , 2000.

[13] V. Ćuk, "Low-Frequency Distortion in Distribution," Eindhoven, 2013.

[14] V. Cuk, J. F. G. Cobben, W. Kling and P. F. Ribeiro, "Considerations on Harmonic Impedance Estimation in Low Voltage Networks," in *IEEE International Conference on Harmonics and Quality of Power (ICHQP)*, Hong Kong, 2012.

[15] "Rijksdienst voor Ondernemend Nederland," Ministry of Economic Affairs, 1 January 2015. [Online]. Available: http://www.rvo.nl/onderwerpen/duurzaam-ondernemen/energie-en-milieu-innovaties/elektrisch-rijden/stand-van-zaken/cijfers. [Accessed 23 January 2014].

[16] Nu.nl, "general news: Nu.nl," 02 february 2015. [Online]. Available: http://www.nu.nl/binnenland/3984196/minder-hennepkwekerijen-tappen-meer-stroom-af-in-2014.html. [Accessed 02 february 2015].

[17] C. Laughman, K. Lee, R. Cox, S. Shaw, S. Leeb, L. Norford and a. p. Armstrong, "Power Signature Analysis," *IEEE power & energy magazine,* pp. 56-63, 2003.

[18] C. Laughman, K. Lee, R. Cox, S. Shaw, S. Leeb, L. Norford and P. Armstrong, "Power Signature Analysis," *IEEE power & energy magazine,* pp. 56-63, 2003.

[19] A. Ruzzelli, C. Nicolas, S. A. and G. O'Hare, "Real-time recognition and profiling of appliances through a single electricity sensor," in *SECON 2010 - 2010 7th Annual IEEE Communications Society Conference on Sensor, Mesh and Ad Hoc Communications and Networks*, Boston, 2010.

Appendix A. Laboratory measurements procedure

In this appendix, the laboratory measurements setup of chapter 3 is explained. The equipment that was used during the measurements are shown at Table 4 and a schematic is shown at Figure 81.

Each lamp was completely rested (no remaining heat from previous use) before testing. The testing procedure was the following: The lamp was switched on, and the initial voltage and current waveforms were saved in the oscilloscope. After one minute, the voltage and current waveforms were saved again; this process was repeated every minute until no relevant changes were visible in the current waveform.

Afterwards, the values of the waveforms were exported to MatLab software environment, and the harmonic spectrum of the current waveforms were calculated with the FFT of the Powergui block of Simulink. The voltage waveform is used to calculate the displacement power factor.

Device	Model
Oscilloscope	Yokogawa, DLM2034 2.5GS/s 350MHz.
Current probe	Yokogawa, Model 701929, DC to 50 MHz, 30 Amperes max.
Voltage probe	Yokogawa, Model 701921, 100 MHz differential probe.

Table 4. Devices used for the laboratory measurements.

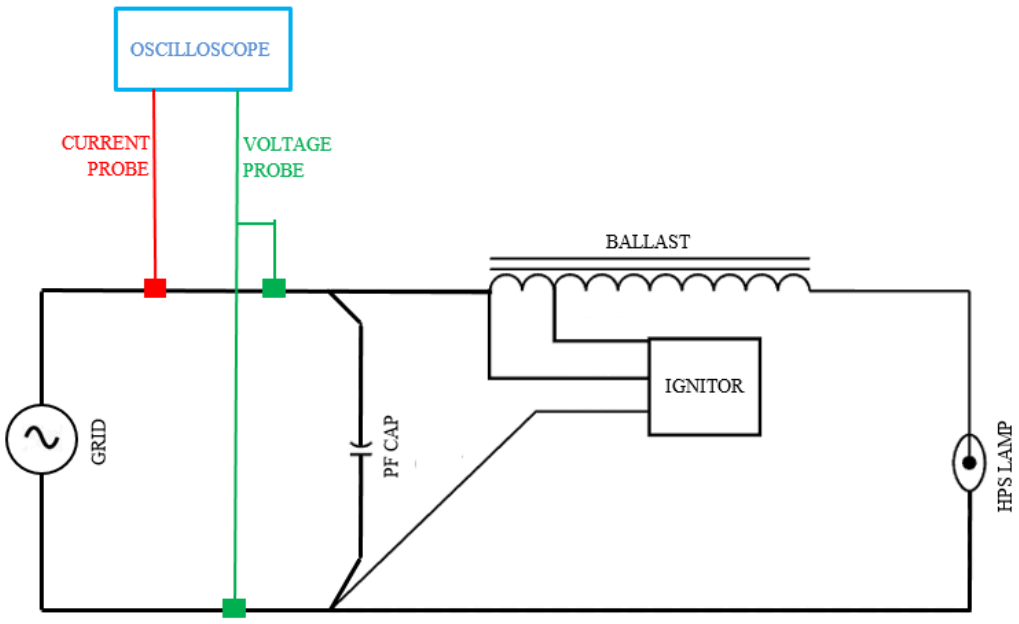

Figure 81. Schematic representation for measurements.

Appendix B. Calculation of aggregated data methodology

The aim of the simulation is to emulate how the current measurements would be seen by a PQ meter in case of lamps existence. For the experiment, real measurements were taken from a LV substation by the use of the Locamation AIM meter, and modified in order to emulate having HPS lamps combined with it. The data was exported and modified in Matlab software environment. Through the rest of this appendix, the unmodified extracted data from the PQ meter (without lamps) would be referred as original circuit or measurements.

From the selected circuit, the measured values of rms current, active power, reactive power, and harmonics magnitude of a 2 days interval were extracted. The Locamation AIM saves to the internal memory an average of the measured discrete values for periods of 5 minutes. For simplicity it would be considered that this value keeps constant during the 5 minutes period.

As mentioned previously, when turned on, the current waveform of the lamp changes with time till it reaches a steady state. The time to reach the steady would be considered to be 6 minutes. The switching-on of the lamps would be considered to be at the second minute of the selected 5 minutes period.

The simulation for every measurement characteristic follow a similar logic. The values of the current measurements from the lamps would be added to the measurements without lamps of the circuit; resembling a connection in parallel of this lamps to the circuit. This would be done for the measurements of the rms current, reactive power, third, fifth and seventh harmonic. For this purpose 3 different values would be created, one corresponding to the first 5 minutes period of the lamps being switch on; the second corresponding to the second 5 minutes period after the lamps are switched on and the third corresponding to the steady state of the lamps being switched on.

Two different scenarios are created. Each configuration has a different scheduling for the switching of the lamps. For the scenario 1, the lamps are switched on for 12 hours (144 periods of 5 minutes) then switched off for 12 hours, afterwards again switched on for 12 hours and so on for a total of 48 hours (see Table 1). For the scenario 2, the lamps turn off and on at the same instant every 12 hours for a total of 48 hours (see Table 2). It has to be taken into account that every time a lamp is turned on, the current characteristics go through a transition till they reach a steady state.

5min period	1 - 107	108 - 109	110 - 252	253 - 395	396 - 397	398 - 540	541 - 576
State	Off	On (transition)	On (steady state)	Off	On (transition)	On (steady state)	Off

Table 5. Scenario 1 schedule.

5min period	1 - 107	108 - 109	110 - 252	253 - 254	255 - 395	396 - 397	398 - 540	541 - 542	543 - 576
State	On (steady state)	Off/On (transition)	On (steady state)	Off/On (transition)	On (steady state)	Off/On (transition)	On (steady state)	Off/On (transition)	On (steady state)

Table 6. Scenario 1 schedule

Rms current, scenario 1

$$I1rms_j = \frac{|Io_j\angle\,\theta_j|+|Io_j\angle\,\theta_j+I_{l0}\angle\emptyset_0|+|Io_j\angle\,\theta_j+I_{l1}\angle\emptyset_1|+|Io_j\angle\,\theta_j+I_{l2}\angle\emptyset_2|+|Io_j\angle\,\theta_j+I_{l3}\angle\emptyset_3|}{5};$$

$$I2rms_j = \frac{|Io_j\angle\,\theta_j+I_{l4}\angle\emptyset_4|+|Io_j\angle\,\theta_j+I_{l5}\angle\emptyset_5|+3*|Io_j\angle\,\theta_j+I_{l6}\angle\emptyset_6|}{5};$$

$$I3rms_j = \left|Io_j\angle\,\theta_j + RMS_6\angle\emptyset_6\right|;$$

$$\left[In_j\right] = \begin{bmatrix} In_1 \\ \vdots \\ In_{107} \\ In_{108} \\ In_{109} \\ In_{110} \\ \vdots \\ In_{252} \\ In_{253} \\ \vdots \\ In_{395} \\ In_{396} \\ In_{397} \\ In_{398} \\ \vdots \\ In_{540} \\ In_{541} \\ \vdots \\ In_{576} \end{bmatrix} = \begin{bmatrix} |Io_1\angle\,\theta_1| \\ \vdots \\ |Io_{107}\angle\,\theta_{107}| \\ I1rms_{108} \\ I2rms_{109} \\ I3rms_{110} \\ \vdots \\ I3rms_{252} \\ |Io_{253}\angle\,\theta_{253}| \\ \vdots \\ |Io_{395}\angle\,\theta_{395}| \\ I1rms_{396} \\ I2rms_{397} \\ I3rms_{398} \\ \vdots \\ I3rms_{540} \\ |Io_{541}\angle\,\theta_{541}| \\ \vdots \\ |Io_{576}\angle\,\theta_{576}| \end{bmatrix};$$

Where:

$I1rms_j$ Rms current of the original circuit with the rms current of the initial 4 minutes of the lamps when they turn on, for the j[th] 5 minutes period.

$I2rms_j$ Rms current of the original circuit with the rms current of the lamps from 5 to 9 minutes of being turn on, for the j[th] 5 minutes period.

$I3rms_j$ Rms current of the original circuit with the rms current of the lamps when they reach steady state, for the j[th] 5 minutes period.

Io_j Rms current magnitude (without lamps) for the j[th] 5 minutes period, which is extracted from the Locamation AIM memory.

θ_j Rms current angle (without lamps) with the voltage as reference for the j[th] 5 minutes period, which is extracted from the Locamation AIM memory.

$I_{l0} \dots I_{l6}$ Rms current of the lamps at 0 to 6 minutes of being switched on.

$\emptyset_0 \dots \emptyset_6$ Rms current angle of the lamps at 0 to 6 minutes of being switched on.

In_j Calculated rms current magnitudes (original circuit + lamps) for the j[th] 5 minutes period.

j Represents the 5 minutes period which goes from 1 to 576 (48 hours). $\boldsymbol{In_j}$ values are plotted and used for analysis. Results of the analysis are showed in the report.

Reactive Power, scenario 1

$$Q1_j = Qo_j + \frac{Q_{l0}+Q_{l1}+Q_{l2}+Q_{l3}}{5};$$

$$Q2_j = Qo_j + \frac{Q_{l4}+Q_{l5}+3*Q_{l6}}{5};$$

$$Q3_j = Qo_j + Q_{l6};$$

$$[Qn_j] = \begin{bmatrix} Qn_1 \\ \vdots \\ Qn_{107} \\ Qn_{108} \\ Qn_{109} \\ Qn_{110} \\ \vdots \\ Qn_{252} \\ Qn_{253} \\ \vdots \\ Qn_{395} \\ Qn_{396} \\ Qn_{397} \\ Qn_{398} \\ \vdots \\ Qn_{540} \\ Qn_{541} \\ \vdots \\ Qn_{576} \end{bmatrix} = \begin{bmatrix} Qo_1 \\ \vdots \\ Qo_{107} \\ Q1_{108} \\ Q2_{109} \\ Q3_{110} \\ \vdots \\ Q3_{252} \\ Qo_{253} \\ \vdots \\ Qo_{395} \\ Q1_{396} \\ Q2_{397} \\ Q3_{398} \\ \vdots \\ Q3_{540} \\ Qo_{541} \\ \vdots \\ Qo_{576} \end{bmatrix};$$

Where:

$Q1_j$ Reactive power of the original circuit with the reactive power of the initial 4 minutes of the lamps when they turn on, for the j[th] 5 minutes period.

$Q2_j$ Reactive power of the original circuit with the reactive power of the lamps from 5 to 9 minutes of being turn on, for the j[th] 5 minutes period.

$Q3_j$ Reactive power of the original circuit with the reactive power of the lamps when they reach steady state, for the j[th] 5 minutes period.

Qo_j Reactive power (without lamps) for the j[th] 5 minutes period, which is extracted from the Locamation AIM memory.

$Q_{l0} \dots Q_{l6}$ Reactive power of the lamps at 0 to 6 minutes of being switched on.

Qn_j Calculated reactive power (original circuit + lamps) for the j[th] 5 minutes period.

j Represents the 5 minutes period which goes from 1 to 576 (48 hours). $\boldsymbol{Qn_j}$ values are plotted and used for analysis. Results of the analysis are showed in the report.

Harmonics, scenario 1

$$H1_{j,h} = \frac{|Ho_{j,h}\angle\theta_j|+|Ho_{j,h}\angle\theta_j+H_{l0,h}\angle(\emptyset_0*h+\alpha_{l0,h})|+\cdots+|Ho_{j,h}\angle\theta_j+H_{l3,h}\angle(\emptyset_3*h+\alpha_{l3,h})|}{5};$$

$$H2_{j,h} = \frac{|Ho_{j,h}\angle\theta_j+H_{l4,h}\angle(\emptyset_4*h+\alpha_{l4,h})|+|Ho_{j,h}\angle\theta_j+H_{l5,h}\angle(\emptyset_5*h+\alpha_{l5,h})|+3*|Ho_{j,h}\angle\theta_j+H_{l6,h}\angle(\emptyset_6*h+\alpha_{l6,h})|}{5};$$

$$H3_{j,h}=|Ho_{j,h}\angle\theta_j + H_{l6,h}\angle(\emptyset_6 * h + \alpha_{l6,h})|;$$

$$[Hn_{j,h}] = \begin{bmatrix} Hn_{1,3} & Hn_{1,5} & Hn_{1,7} \\ \vdots & \vdots & \vdots \\ Hn_{107,3} & Hn_{107,5} & Hn_{107,7} \\ Hn_{108,3} & Hn_{108,5} & Hn_{108,7} \\ Hn_{109,3} & Hn_{109,5} & Hn_{109,7} \\ Hn_{110,3} & Hn_{110,5} & Hn_{110,7} \\ \vdots & \vdots & \vdots \\ Hn_{252,3} & Hn_{252,5} & Hn_{252,7} \\ Hn_{253,3} & Hn_{253,5} & Hn_{253,7} \\ \vdots & \vdots & \vdots \\ Hn_{395,3} & Hn_{395,5} & Hn_{395,7} \\ Hn_{396,3} & Hn_{396,5} & Hn_{396,7} \\ Hn_{397,3} & Hn_{397,5} & Hn_{397,7} \\ Hn_{398,3} & Hn_{398,5} & Hn_{398,7} \\ \vdots & \vdots & \vdots \\ Hn_{540,3} & Hn_{540,5} & Hn_{540,7} \\ Hn_{541,3} & Hn_{541,5} & Hn_{541,7} \\ \vdots & \vdots & \vdots \\ Hn_{576,3} & Hn_{576,5} & Hn_{576,7} \end{bmatrix} = \begin{bmatrix} Ho_{1,3} & Ho_{1,5} & Ho_{1,7} \\ \vdots & \vdots & \vdots \\ Ho_{107,3} & Ho_{107,5} & Ho_{107,7} \\ H1_{108,3} & H1_{108,5} & H1_{108,7} \\ H2_{109,3} & H2_{109,5} & H2_{109,7} \\ H3_{110,3} & H3_{110,5} & H3_{110,7} \\ \vdots & \vdots & \vdots \\ H3_{252,3} & H3_{252,5} & H3_{252,7} \\ Ho_{253,3} & Ho_{253,5} & Ho_{253,7} \\ \vdots & \vdots & \vdots \\ Ho_{395,3} & Ho_{395,5} & Ho_{395,7} \\ H1_{396,3} & H1_{396,5} & H1_{396,7} \\ H2_{397,3} & H2_{397,5} & H2_{397,7} \\ H3_{398,3} & H3_{398,5} & H3_{398,7} \\ \vdots & \vdots & \vdots \\ H3_{540,3} & H3_{540,5} & H3_{540,7} \\ Qo_{541,3} & Qo_{541,5} & Qo_{541,7} \\ \vdots & \vdots & \vdots \\ Qo_{576,3} & Qo_{576,5} & Qo_{576,7} \end{bmatrix};$$

Where:

$H1_{j,h}$ Harmonic magnitude in amperes of the original circuit and the initial 4 minutes of the lamps when they turn on, for the jth 5 minutes period and the hth harmonic.

$H2_{j,h}$ Harmonic magnitude in amperes of the original circuit and the lamps from 5 to 9 minutes of being turn on, for the jth 5 minutes period and the hth harmonic.

$H3_{j,h}$ Harmonic magnitude in amperes of the original circuit and the lamps when they reach steady state, for the jth 5 minutes period and the hth harmonic.

$Ho_{j,h}$ Harmonic magnitude in amperes of the original circuit (without lamps) for the jth 5 minutes period and the hth harmonic, which is extracted from the Locamation AIM memory.

h Harmonic value in multiples of the fundamental.

$H_{l0,h} \dots H_{l6,h}$ Harmonic magnitude in amperes of the lamps at 0 to 6 minutes of being switched on, for the hth harmonic.

$\alpha_{l0,h} \dots \alpha_{l6,h}$ Harmonic angle of the lamps at 0 to 6 minutes of being switched on, with the fundamental as reference and for the hth harmonic.

$Hn_{j,h}$ Calculated harmonic magnitude in amperes (original circuit + lamps) for the jth 5 minutes period and the hth harmonic.

The angle between the harmonics and the fundamental in the original circuit (without lamps) is considered to be 0.

Rms current, scenario 2

$$I1rms_j = \frac{\left|Io_j\angle\,\theta_j + I_{l6}\angle\emptyset_6\right| + \left|Io_j\angle\,\theta_j + I_{l0}\angle\emptyset_0\right| + \left|Io_j\angle\,\theta_j + I_{l1}\angle\emptyset_1\right| + \left|Io_j\angle\,\theta_j + I_{l2}\angle\emptyset_2\right| + \left|Io_j\angle\,\theta_j + I_{l3}\angle\emptyset_3\right|}{5};$$

$$I2rms_j = \frac{\left|Io_j\angle\,\theta_j + I_{l4}\angle\emptyset_4\right| + \left|Io_j\angle\,\theta_j + I_{l5}\angle\emptyset_5\right| + 3*\left|Io_j\angle\,\theta_j + I_{l6}\angle\emptyset_6\right|}{5};$$

$$I3rms_j = \left|Io_j\angle\,\theta_j + RMS_6\angle\emptyset_6\right|;$$

$$\left[In_j\right] = \begin{bmatrix} In_1 \\ \vdots \\ In_{107} \\ In_{108} \\ In_{109} \\ In_{110} \\ \vdots \\ In_{252} \\ In_{253} \\ In_{254} \\ In_{255} \\ \vdots \\ In_{395} \\ In_{396} \\ In_{397} \\ In_{398} \\ \vdots \\ In_{540} \\ In_{541} \\ In_{542} \\ In_{543} \\ \vdots \\ In_{576} \end{bmatrix} = \begin{bmatrix} I3rms_1 \\ \vdots \\ I3rms_{107} \\ I1rms_{108} \\ I2rms_{109} \\ I3rms_{110} \\ \vdots \\ I3rms_{252} \\ I1rms_{253} \\ I2rms_{254} \\ I3rms_{255} \\ \vdots \\ I3rms_{395} \\ I1rms_{396} \\ I2rms_{397} \\ I3rms_{398} \\ \vdots \\ I3rms_{540} \\ I1rms_{541} \\ I2rms_{542} \\ I3rms_{543} \\ \vdots \\ I3rms_{576} \end{bmatrix};$$

Where:

$I1rms_j$ Rms current of the original circuit with the rms current of the initial 4 minutes of the lamps when they turn on, for the j[th] 5 minutes period.

$I2rms_j$ Rms current of the original circuit with the rms current of the lamps from 5 to 9 minutes of being turn on, for the j[th] 5 minutes period.

$I3rms_j$ Rms current of the original circuit with the rms current of the lamps when they reach steady state, for the j[th] 5 minutes period.

Io_j Rms current magnitude (without lamps) for the j[th] 5 minutes period, which is extracted from the Locamation AIM memory.

θ_j Rms current angle (without lamps) with the voltage as reference for the j[th] 5 minutes period, which is extracted from the Locamation AIM memory.

$I_{l0} \dots I_{l6}$ Rms current of the lamps at 0 to 6 minutes of being switched on.

$\emptyset_0 \dots \emptyset_6$ Rms current angle of the lamps at 0 to 6 minutes of being switched on.

In_j Calculated rms current magnitudes (original circuit + lamps) for the j[th] 5 minutes period.

j Represents the 5 minutes period which goes from 1 to 576 (48 hours). $\boldsymbol{In_j}$ values are plotted and used for analysis. Results of the analysis are showed in the report.

Reactive Power, scenario 2

$$Q1_j = Qo_j + \frac{Q_{l6}+Q_{l0}+Q_{l1}+Q_{l2}+Q_{l3}}{5};$$

$$Q2_j = Qo_j + \frac{Q_{l4}+Q_{l5}+3*Q_{l6}}{5};$$

$$Q3_j = Qo_j + Q_{l6};$$

$$[Qn_j] = \begin{bmatrix} Qn_1 \\ \vdots \\ Qn_{107} \\ Qn_{108} \\ Qn_{109} \\ Qn_{110} \\ \vdots \\ Qn_{252} \\ Qn_{253} \\ Qn_{254} \\ Qn_{255} \\ \vdots \\ Qn_{395} \\ Qn_{396} \\ Qn_{397} \\ Qn_{398} \\ \vdots \\ Qn_{540} \\ Qn_{541} \\ Qn_{542} \\ Qn_{543} \\ \vdots \\ Qn_{576} \end{bmatrix} = \begin{bmatrix} Q3_1 \\ \vdots \\ Q3_{107} \\ Q1_{108} \\ Q2_{109} \\ Q3_{110} \\ \vdots \\ Q3_{252} \\ Q1_{253} \\ Q2_{254} \\ Q3_{255} \\ \vdots \\ Q3_{395} \\ Q1_{396} \\ Q2_{397} \\ Q3_{398} \\ \vdots \\ Q3_{540} \\ Q1_{541} \\ Q2_{542} \\ Q3_{543} \\ \vdots \\ Q3_{576} \end{bmatrix};$$

Where:

$Q1_j$ Reactive power of the original circuit with the reactive power of the initial 4 minutes of the lamps when they turn on, for the j[th] 5 minutes period.

$Q2_j$ Reactive power of the original circuit with the reactive power of the lamps from 5 to 9 minutes of being turn on, for the j[th] 5 minutes period.

$Q3_j$ Reactive power of the original circuit with the reactive power of the lamps when they reach steady state, for the j[th] 5 minutes period.

Qo_j Reactive power (without lamps) for the j[th] 5 minutes period, which is extracted from the Locamation AIM memory.

$Q_{l0} \ldots Q_{l6}$ Reactive power of the lamps at 0 to 6 minutes of being switched on.

Qn_j Calculated reactive power (original circuit + lamps) for the j[th] 5 minutes period.

j Represents the 5 minutes period which goes from 1 to 576 (48 hours). $\boldsymbol{Qn_j}$ values are plotted and used for analysis. Results of the analysis are showed in the report.

Harmonics, scenario 2

$$H1_{j,h} = \frac{|Ho_{j,h}\angle\,\theta_j + H_{l6,h}\angle(\emptyset_6 * h + \alpha_{l6,h})| + |Ho_{j,h}\angle\,\theta_j + H_{l0,h}\angle(\emptyset_0 * h + \alpha_{l0,h})| + \cdots + |Ho_{j,h}\angle\,\theta_j + H_{l3,h}\angle(\emptyset_3 * h + \alpha_{l3,h})|}{5};$$

$$H2_{j,h} = \frac{|Ho_{j,h}\angle\,\theta_j + H_{l4,h}\angle(\emptyset_4 * h + \alpha_{l4,h})| + |Ho_{j,h}\angle\,\theta_j + H_{l5,h}\angle(\emptyset_5 * h + \alpha_{l5,h})| + 3*|Ho_{j,h}\angle\,\theta_j + H_{l6,h}\angle(\emptyset_6 * h + \alpha_{l6,h})|}{5};$$

$$H3_{j,h} = |Ho_{j,h}\angle\,\theta_j + H_{l6,h}\angle(\emptyset_6 * h + \alpha_{l6,h})|;$$

$$[Hn_{j,h}] = \begin{bmatrix} Hn_{1,3} & Hn_{1,5} & Hn_{1,7} \\ \vdots & \vdots & \vdots \\ Hn_{107,3} & Hn_{107,5} & Hn_{107,7} \\ Hn_{108,3} & Hn_{108,5} & Hn_{108,7} \\ Hn_{109,3} & Hn_{109,5} & Hn_{109,7} \\ Hn_{110,3} & Hn_{110,5} & Hn_{110,7} \\ \vdots & \vdots & \vdots \\ Hn_{252,3} & Hn_{252,5} & Hn_{252,7} \\ Hn_{253,3} & Hn_{253,5} & Hn_{253,7} \\ Hn_{254,3} & Hn_{254,5} & Hn_{254,7} \\ Hn_{255,3} & Hn_{255,5} & Hn_{255,7} \\ \vdots & \vdots & \vdots \\ Hn_{395,3} & Hn_{395,5} & Hn_{395,7} \\ Hn_{396,3} & Hn_{396,5} & Hn_{396,7} \\ Hn_{397,3} & Hn_{397,5} & Hn_{397,7} \\ Hn_{398,3} & Hn_{398,5} & Hn_{398,7} \\ \vdots & \vdots & \vdots \\ Hn_{540,3} & Hn_{540,5} & Hn_{540,7} \\ Hn_{541,3} & Hn_{541,5} & Hn_{541,7} \\ Hn_{542,3} & Hn_{542,5} & Hn_{542,7} \\ Hn_{543,3} & Hn_{543,5} & Hn_{543,7} \\ \vdots & \vdots & \vdots \\ Hn_{576,3} & Hn_{576,5} & Hn_{576,7} \end{bmatrix} = \begin{bmatrix} H3_{1,3} & H3_{1,5} & H3_{1,7} \\ \vdots & \vdots & \vdots \\ H3_{107,3} & H3_{107,5} & H3_{107,5} \\ H1_{108,3} & H1_{108,5} & H1_{108,7} \\ H2_{109,3} & H2_{109,5} & H2_{109,7} \\ H3_{110,3} & H3_{110,5} & H3_{110,7} \\ \vdots & \vdots & \vdots \\ H3_{252,3} & H3_{252,5} & H3_{252,7} \\ H1_{253,3} & H1_{253,5} & H1_{253,7} \\ H2_{254,3} & H2_{254,5} & H2_{254,7} \\ H3_{255,3} & H3_{255,5} & H3_{255,7} \\ \vdots & \vdots & \vdots \\ H3_{395,3} & H3_{395,5} & H3_{395,7} \\ H1_{396,3} & H1_{396,5} & H1_{396,7} \\ H2_{397,3} & H2_{397,5} & H2_{397,7} \\ H3_{398,3} & H3_{398,5} & H3_{398,7} \\ \vdots & \vdots & \vdots \\ H3_{540,3} & H3_{540,5} & H3_{540,7} \\ H1_{541,3} & H1_{541,5} & H1_{541,7} \\ H2_{542,3} & H2_{542,5} & H2_{542,7} \\ H3_{543,3} & H3_{543,5} & H3_{543,7} \\ \vdots & \vdots & \vdots \\ H3_{576,3} & H3_{576,5} & H3_{576,7} \end{bmatrix};$$

Where:

$H1_{j,h}$ Harmonic magnitude in amperes of the original circuit and the initial 4 minutes of the lamps when they turn on, for the j[th] 5 minutes period and the h[th] harmonic.

$H2_{j,h}$ Harmonic magnitude in amperes of the original circuit and the lamps from 5 to 9 minutes of being turn on, for the j[th] 5 minutes period and the h[th] harmonic.

$H3_{j,h}$ Harmonic magnitude in amperes of the original circuit and the lamps when they reach steady state, for the j[th] 5 minutes period and the h[th] harmonic.

$Ho_{j,h}$ Harmonic magnitude in amperes of the original circuit (without lamps) for the j[th] 5 minutes period and the h[th] harmonic, which is extracted from the Locamation AIM memory.

h Harmonic value in multiples of the fundamental.

$H_{l0,h} \dots H_{l6,h}$ Harmonic magnitude in amperes of the lamps at 0 to 6 minutes of being switched on, for the h[th] harmonic.

$\alpha_{l0,h} \dots \alpha_{l6,h}$ Harmonic angle of the lamps at 0 to 6 minutes of being switched on, with the fundamental as reference and for the h[th] harmonic.

$Hn_{j,h}$ Calculated harmonic magnitude in amperes (original circuit + lamps) for the j^{th} 5 minutes period and the h^{th} harmonic.

The angle between the harmonics and the fundamental in the original circuit (without lamps) is considered to be 0.